MODELING THE EFFECT OF ELECTROLYTE ON THE LITHIUM SULFUR BATTERY PERFORMANCE

by

Aysun Çeçe

B.S., Chemical Engineering, Boğaziçi University, 2021

Submitted to the Institute for Graduate Studies in

Science and Engineering in partial fulfillment of

the requirements for the degree of
Master of Science

Graduate Program in Chemical Engineering

Boğaziçi University
2024

ACKNOWLEDGEMENTS

I would like to express my sincere gratitude to my thesis advisor Assoc. Prof. Dr. Damla Eroğlu Pala. I am very grateful for being able to work with her and for her support and guidance throughout my research. I would also like to thank my friends from Electrochemical Engineering Research Group. I would like to acknowledge to TÜBİTAK (Project No: 220N164) for the support of this research. Finally, I would like to sincerely thank my dear family and friends, for their support throughout my thesis process.

ABSTRACT

MODELING THE EFFECT OF ELECTROLYTE ON THE LITHIUM SULFUR BATTERY PERFORMANCE

Due to their ability to have a higher cell capacity, lithium-sulfur (Li-S) batteries have recently become more prominent compared to Li-ion batteries. This thesis expands on this premise by presenting the impact of electrolyte amount and properties on the performance and lifespan of Li-S cells. To do so, the 0-dimensional electrochemical model by Marinescu et al. [1] is implemented with a C-rate of 0.5 C. The 0-dimensional model is modified to predict continuous charge and discharge cycles and is simulated by using the Fortran programming language. To determine the effect of the amount of electrolyte on cell performance, the electrolyte-to-sulfur (E/S) ratio is altered by changing the electrolyte volume in the model directly. It is demonstrated that when the E/S ratio increases, the capacity of cell discharge remains unaffected, contrary to expectations. However, the capacity fading over the first two cycles is effectively predicted. The effect of electrolyte type and properties on cell performance is captured implicitly through model parameters and sensitivity analysis is conducted. It is shown that cell capacity is sensitive to changes in the initial voltage (V_0), the high voltage plateau standard potential (E_H^0), and the shuttle constant (k_S), whereas cell voltage output is sensitive to changes in E_H^0, V_0, and high and low voltage plateau reaction exchange current densities ($i_{H,0}$, $i_{L,0}$). The model does not respond accurately to changes in the active area (a_r), precipitation constant (k_p), and C-rate. Furthermore, by adjusting the value of the shuttle constant (k_s), the predicted cycling performance can align with experimental data for different E/S ratios and electrolyte types.

ÖZET

ELEKTROLİT ÖZELLİKLERİNİN VE MİKTARININ LİTYUM-KÜKÜRT BATARYA PERFORMANSI ÜZERİNDEKİ ETKİSİNİN MODELLENMESİ

Son dönemde, lityum-kükürt bataryaları, yüksek kapasiteli olmaları nedeniyle lityum-iyon bataryalarından daha fazla ilgi görmektedir. Bu tezde, elektrolit miktarının ve özelliklerinin lityum-kükürt hücrelerinin performansı ve ömrü üzerindeki etkisi incelenmiştir. Marinescu et al. [1] tarafından geliştirilen 0-boyutlu elektrokimyasal model temel alınmıştır. Birbirini takip eden deşarj ve şarj prosesleri, yani döngüler, Fortran programlama kullanılarak simüle edilmiştir. Elektrolit miktarının hücre performansı üzerindeki etkisini belirlemek için, elektrolit hacmi doğrudan değiştirilerek elektrolit-kükürt (E/S) oranı değiştirilmiştir. E/S oranı arttığında, beklentilerin aksine hücre deşarj kapasitesinin etkilenmediği gösterilmiştir. Ancak, döngüler boyunca kapasite azalması etkili bir şekilde tahmin edilmiştir. Elektrolit tipi ve özelliklerinin hücre performansı üzerindeki etkisi, mekanik bir yaklaşımla model parametreleri aracılığıyla dolaylı olarak öngörülmüş ve hassasiyet analizleri yapılmıştır. Hücre kapasitesinin, başlangıç voltajı (V_0), yüksek voltaj platosu standart potansiyeli (E_H^0) ve mekik sabitindeki (k_S) değişimlere duyarlı olduğu, hücre voltajının ise E_H^0, V_0, yüksek ve düşük voltaj platosu değişim akım yoğunluklarındaki ($i_{H,0}$, $i_{L,0}$) değişimlere duyarlı olduğu gösterilmiştir. Model, aktif alan (a_r), çökelme sabiti (k_p) ve C-oranındaki değişimlere doğru bir şekilde yanıt verememektedir. Ek olarak, mekik sabiti (k_s) değeri değiştirilerek deneysel sonuçlara uygun deşarj prosesleri ve kapasiteleri, farklı E/S oranları ve elektrolit tipleri için elde edilmiştir. Bu analizlerin sonucunda, elektrolit tipi ve özelliklerinin etkisinin, modelin duyarlı olduğu parametreler aracılığıyla dolaylı olarak gösterilebileceği çıkarımına varılmıştır.

TABLE OF CONTENTS

LIST OF FIGURES

LIST OF TABLES

LIST OF SYMBOLS

a_r	Active reaction area per cell, m^2
E_H	Equilibrium potential for high voltage plateau, V
E_L	Equilibrium potential for low voltage plateau, V
E_H^0	Standard potential for high voltage plateau, V
E_L^0	Standard potential for low voltage plateau, V
F	Faraday's Constant, C mol^{-1}
f_H	Dimensionality factor *H*, g L mol^{-1}
f_L	Dimensionality factor *L*, g^2 L^2 mol^{-1}
I	External current, A
i_H	Current contribution for high voltage plateau, A
i_L	Current contribution for low voltage plateau, A
$i_{H,0}$	Exchange current density for high voltage plateau, A m^{-2}
$i_{L,0}$	Exchange current density for low voltage plateau, A m^{-2}
k_p	Precipitation rate constant, s^{-1}
k_S	Shuttle constant, s^{-1}
m_S	Mass of active sulfur per cell, g
M_{S_8}	Molar mass of S_8, g mol^{-1}
N_A	Avogadro number, 1 mol^{-1}
n_e	Electron number per reaction, -
n_i	Number of sulfur atoms in polysulfide *i*, -
R	Gas constant, J K^{-1} mol^{-1}
S_*^{2-}	Saturation mass of S^{2-}, g
S_p	Mass of precipitated S^{2-}, g
T	Temperature, K
t	Time, s
V	Cell voltage, V
v	Electrolyte volume per cell, L

V_0	Initial cell voltage, V
η_H	Overpotential for high voltage plateau, V
η_L	Overpotential for low voltage plateau, V
ρ_S	Density of precipitated sulfur g L^{-1}

LIST OF ABBREVIATIONS

C-rate	Current rate
C/S	Carbon-to-sulfur ratio
E/S	Electrolyte-to-sulfur ratio
FORTRAN	Formula Translating System

1. INTRODUCTION

The importance of energy systems, especially batteries, has increased exponentially as electronic devices increase in complexity. Lithium-ion batteries are the most widely used kind of batteries, and with modern technology, they have the highest capacity for energy storage [2]. Heavy metals, such as nickel (Ni) and cobalt (Co), are used in lithium-ion batteries [3]. While these metals are excellent for delivering energy, they are also known to cause tremendous environmental and humanitarian risks [4]. Equivalent energy storage systems are still being researched to overcome the disadvantages of lithium-ion batteries. A newly emerging equivalent energy system is the lithium-sulfur batteries, which could turn out to be a potential replacement for Li-ion batteries [5]. Lithium-sulfur batteries are fundamentally different from lithium-ion batteries and have several advantages in comparison [6].

As mentioned, battery systems, especially in terms of capacity, must keep up with the swiftly developing technologies that, for example, combat global warming through electric vehicles. This is a common demand since zero-carbon emission projects are becoming more and more widespread to prevent global warming [7]. In the coming years, thanks to government policies in various countries [5], the usage of fossil fuel-powered cars will inevitably decrease. The shrinkage of the market for fossil fuel cars will allow electric cars to fill that gap and become more common, as they are seen as the biggest competitor to fossil fuel cars. One of the biggest hurdles for electric cars to become dominant in daily life is the inability of electric cars to travel long distances due to the low capacities of lightweight battery systems. In addition, electric cars need to become cheaper for these and similar technologies to become widespread.

Lithium-sulfur batteries, which offer a potential solution to the shortcomings of Li-ion batteries, have a high theoretical specific energy, 2600 Wh/kg, to be exact [8]. The theoretical specific energy of Li-S batteries is greater than the theoretical specific energy of Li-ion batteries, which is between 500-600 Wh/kg [8]. Lithium-sulfur batteries are composed of electrochemical

cells and oxidation and reduction reactions occur through charge and discharge, namely cycling. In a Li-S cell, there exists a lithium anode, commonly an organic electrolyte, and cathode, which is a composite of sulfur and carbon [9]. Representation of a Li-S cell is shown in the Figure 1.1.

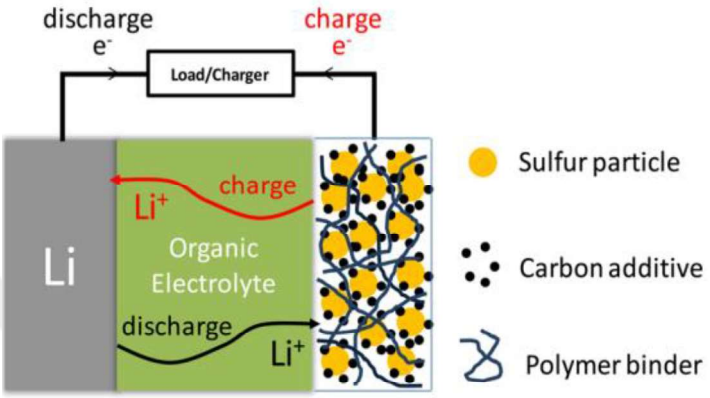

Figure 1.1. Representation of a Li-S with cell reactions [9].

The equation representing the whole redox electrochemical reaction in the Li-S cell is provided as [10]

$$16Li + S_8 \rightarrow 8Li_2S\,. \tag{1.1}$$

The lithium metal is oxidized at the anode and transferred through the cathode, where free electrons are transported with an external circuit, which leads to electricity production. The cathode reaction happens subsequently, and with this reaction, sulfur is reduced to Li_2S. Then, the charging process takes place with the opposite of these reactions. In addition to this, intermediate lithium polysulfides and their dissolution in the electrolyte can be seen during these processes, which initiates the polysulfide shuttle mechanism. Moreover, it poses a great challenge since sulfur and Li_2S are both insulators. Therefore, supporting salts are added to the electrolyte or conductive materials such as carbon are added to the electrode [9,11].

The oxidation process of the lithium anode is as follows

$$Li \leftrightarrow Li^+ + e^-. \tag{1.2}$$

Following the dissolution of $S_{8(s)}$ to the electrolyte, the reduction reactions to polysulfides and the subsequent precipitation and dissolution processes can be written as

$$\frac{1}{2}S_{8(l)} + e^- \leftrightarrow \frac{1}{2}S_8^{2-}, \tag{1.3}$$

$$\frac{3}{2}S_8^{2-} + e^- \leftrightarrow 2S_6^{2-}, \tag{1.4}$$

$$S_6^{2-} + e^- \leftrightarrow \frac{3}{2}S_4^{2-}, \tag{1.5}$$

$$\frac{1}{2}S_4^{2-} + e^- \leftrightarrow S_2^{2-}, \tag{1.6}$$

$$\frac{1}{2}S_2^{2-} + e^- \leftrightarrow S^{2-}, \tag{1.7}$$

$$2Li^+ + S_8^{2-} \leftrightarrow Li_2S_{(s)}, \tag{1.8}$$

$$2Li^+ + S_4^{2-} \leftrightarrow Li_2S_{4(s)}, \tag{1.9}$$

$$2Li^+ + S_2^{2-} \leftrightarrow Li_2S_{2(s)}, \tag{1.10}$$

$$2Li^+ + S^{2-} \leftrightarrow Li_2S_{(s)}. \tag{1.11}$$

The electrochemical processes that take place during discharge are shown in Equations (1.2)-(1.11) [10]. Also, lithium-sulfur battery systems rely on sulfur, which is abundant in nature, incredibly cheap, and non-toxic [12], which makes Li-S batteries excellent for storing energy cheaply [10].

Despite their good properties and advantages, there are some fundamental issues that need to be resolved for Li-S batteries to be successful. The challenges are mainly the polysulfide shuttle mechanism, short cycle life, low utilization of sulfur, self-discharge, and irreversible capacity loss [1,11].

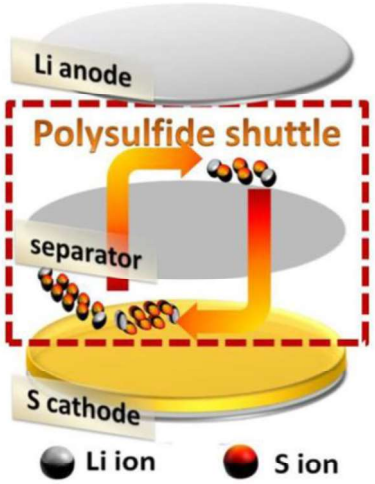

Figure 1.2. Representation of shuttle mechanism in Li-S cell [9]

The polysulfide shuttle mechanism poses a significant challenge in the advancement of Li-S batteries. Typically, in an electrochemical cell, lithium ions (Li^+) move from the anode to the cathode via the electrolyte during discharge. This movement of ions generates electrical energy that is transferred to an external circuit through the flow of electrons [13] Li-S cell also works with this principle, but during discharge, sulfur ($S_{8(s)}$) in the cathode dissolves in electrolyte and reacts with Li+ ions to form lithium polysulfides (Li_2S_x) [9]. The lithium polysulfides generated move in the opposite way through the electrolyte when the cell is being discharged and eventually reach the lithium anode. At the anode, the compounds are reduced to Li_2S and Li_2S_2, causing them to lose solubility in the electrolyte [9]. Furthermore, they can react with chemicals present in the electrolyte, leading to the breakdown of the electrolyte. Polysulfides are responsible for the self-discharge of the lithium-sulfur cell, depletion of active material inside the cell, and the gradual decline in capacity over cycles [9]. Li-S cell polysulfide shuttle mechanism is shown in the Figure 1.2.

There are efforts made to overcome these obstacles, which can be grouped into several main topics. The first one is using electrolyte additives like $LiNO_3$ to protect the anode surface by forming a passivation layer [14]. Another one is to encapsulate polysulfides at the cathode, i.e., by using carbon nanostructures [15]. Also, interlayers of specialized materials may be used to slow down the diffusion of the polysulfides and selectively pass only the lithium ions [16,17].

Suppressing the polysulfide shuttle mechanism is the main purpose of these efforts since the polysulfide shuttle mechanism leads to self-discharge and poor charging efficiency as well as to an irreversible capacity loss [11]. Hence, the design of the Li-S cell has an important role in determining the battery performance.

It is expected that the practical energy density of a battery is less than its theoretical value. However, in Li-S battery systems, this value is much less than it should be in practice, so Li-S batteries are not able to realize their full potential. The practical specific energy is lower, which is between 200 to 400 Wh/kg [18], whereas, for Li-ion batteries, the practical energy density is around 250 Wh/kg [19]. This shows that Li-S batteries have the potential to improve to overcome the problems that are caused by the lack of an advanced battery system. There are many parameters that affect battery performance in lithium-sulfur batteries like electrolyte material, electrolyte-to-sulfur (E/S) ratio, carbon-to-sulfur (C/S) ratios and composite cathode design [20–22]. These are the key parameters in the development of Li-S battery systems. By optimizing these parameters, it can be possible to achieve energy densities closer to the theoretical energy density level.

Among these parameters, the optimum level of the E/S ratio is important for Li-S cell design because electrolyte occupies a large space in the cell and plays a crucial role in the reactions. As the electrolyte volume increases, the energy density of the battery decreases and a high electrolyte volume can cause the electrolyte material to interact with polysulfides more, increasing the shuttle mechanism [23]. Conversely, a low E/S ratio might impair the reaction kinetics by diminishing ion transport inside the cell and decrease cell capacity by limiting the use of active materials [23]. The overpotential is diminished and the conductivity of the cell is enhanced using an adequate quantity of electrolyte.

Moreover, the correct selection of the electrolyte type is crucial since it has a direct impact on the performance of the Li-S cell. Electrolyte properties such as ionic conductivity and viscosity directly affect the reaction kinetics, internal resistance and overpotential in the Li-S cell [24]. While it is important for the electrolyte to have a low viscosity to facilitate the fast transportation of ions, it is also important for it to have a high viscosity to slow down the

polysulfide shuttle mechanism. In addition, it is important that the substances in the electrolyte do not interact with the polysulfides and thus the electrolyte does not degrade [24]. Overall, it is crucial to consider all these factors during cell design and to optimize the E/S ratio to enhance cell performance when selecting the appropriate electrolyte type.

1.1. Scope of the Current Work

As mentioned before, Li-S batteries have challenges that must be overcome, which are caused by complex electrochemical processes during charge and discharge of the battery. As a result of the formation of soluble polysulfide intermediates, electrolyte design is crucial for defining the reaction kinetics and the polysulfide shuttle mechanism. Both the amount and the properties of the electrolyte are key parameters in overcoming these issues, and the design of the electrolyte requires an integrated investigation of materials chemistry, mechanisms, and rates at the cathode level and electrochemical performance at the cell level.

The aim of this thesis is to investigate the effect of the electrolyte properties and amount (or the electrolyte-to-sulfur (E/S) ratio, in other words) on the lithium-sulfur battery performance by developing an electrochemical model predicting the cycling of a cell at a constant current density.

A 0-dimensional model is developed for the charge and discharge, namely cycling, of a Li-S cell where the impact of electrolyte amount and properties on the Li-S battery performance is investigated by examining mechanisms and rates of reactions during cycling. The electrolyte-to-sulfur ratio is directly defined by adjusting the volume of the electrolyte in the model. However, it is not feasible to directly modify the type and properties of the electrolyte in the model. Therefore, the impact of the electrolyte type and properties on both discharge and charge performance is implicitly evaluated through model parameters.

The parameters that are investigated to determine the effect of electrolyte type and properties on the Li-S battery performance are active reaction area (a_r), initial cell voltage (V_0), shuttle constant (k_s), high and low voltage plateau standard potentials $(E_H^0,\ E_L^0)$, high and low voltage plateau electrochemical reaction exchange current densities $\left(i_{H,0}, i_{L,0}\right)$, and precipitation rate constant $\left(k_p\right)$. By conducting a sensitivity analysis through alteration of these parameters, the implicit impact of electrolyte type and properties on cell capacity, voltage output, and reaction kinetics is determined. Due to its concentration independence, the 0-dimensional model has fewer assumed parameters, resulting in increased computational effectiveness. The model is solved numerically using computational methods and the Fortran programming language.

The 0-dimensional model proposed by Marinescu et al. is used for this study, and the cell design parameters from this publication are taken [1]. In the "2. Literature Review" part, several electrochemical models studied in the literature and research for Li-S cells, along with the key parameters that are modified to enhance the performance of Li-S cells are presented. This part also covers studies that investigated the impact of different electrolyte types and the electrolyte-to-sulfur (E/S) ratio on cell performance.

The details of the model simulating the continuous discharge and charge processes and the electrochemical and precipitation/dissolution reactions are explained in "3. Model Development" part. In addition, the initial conditions and model parameters, along with a detailed explanation of the linearization procedure for the model equations are included in the same chapter.

In the "4. Results and Discussions" part, an explanation of the cycle simulation graphs and sensitivity analysis of the model according to the changing model parameters are provided. Discharge and charge processes are examined separately, and two cycle results are given for all to prevent repetition. Voltage outputs and capacity changes are examined in detail, whereas the effect of electrolyte type and properties on cell performance is investigated implicitly through model parameters; model parameters reflecting electrolyte properties are determined. The impact of the electrolyte-to-sulfur (E/S) ratio on cell performance is also thoroughly analyzed

in the same chapter. A comprehensive conclusion of the study and the results are provided in “5. Conclusion” part.

2. LITERATURE REVIEW

In this part of the thesis, previous studies on the effect of electrolyte amount and properties on the Li-S battery performance are summarized.

Electrolyte amount and properties influence battery performance by affecting the depth of sulfur reduction and the cycle life. This is because of the development of solvate complexes of lithium polysulfides during charge and discharge processes, and electrolytes carry ions between the anode and the cathode. Solvate complexes of Li_2S_m and their structures necessitate a sufficient level of electrolyte contents and additives since they influence overall charge and discharge processes and the efficiency of the Li-S cell [6]. The experiments carried out by Kolosnitsyn et al. in 2016, which used sulfolane as the electrolyte, examined solvate numbers of Li-ion in lithium polysulfide, and the minimum solvate number is determined as 1 for the Li-ion [6].

In Li-S cells, a mixture of dimethoxyethane (DME) and 1,3 dioxolane (DOL) is used as electrolytes in general, and as the salt, lithium bis-(trifluoromethanesulfonyl)amide (Li[TFSA]) is used [25,26]. $LiNO_3$ is also typically used to increase the performance by suppressing the shuttle mechanism to some extent. However, the dissolution of lithium polysulfides cannot be prevented completely, which is a major problem since it causes low cycle life and rapid fading of capacity as well as low Coulombic efficiency [27–29]. According to a study, an increase in the electrolyte amount increases the cycle life and depth of sulfur reduction, and if the supporting salt is changed, such as lithium perchlorate, the cycle life is not affected, but the capacity is affected [6].

Different electrolyte types, such as polymers and inorganic solid states, are suggested to overcome the shuttle mechanism [30–32]. In addition, the study done by Ueno et al. suggests solvating ionic liquid electrolytes rather than aprotic ionic liquids and lithium salts and examines their anionic effects [33]. For this purpose, different anionic versions of [Li(glyme)]X

electrolytes are used, and it is concluded that [Li(G4)][BETI] and [Li(glyme)][TFSA] are electrochemically stable in the Li–S cell and [Li(G4)][BETI], which is a concentrated electrolyte leads to a low capacity [33].

As investigated by Cheng et al. in 2016, the electrolyte system that achieves a long-lasting battery is a sparingly solvating electrolyte [34]. In this type of an electrolyte, salt dissolves sparingly which provides the control mechanism of the migration of substances in the electrolyte solution.

Another research done by Weller et al. in 2017 presents an electrolyte system that can be applied to large-scale batteries since its volatility is not high, which is a requested property in large-scale applications [35]. The method suggests an intrinsic shuttle suppression with a pouch cell. The study presents an electrolyte, which is a mixture of hydrofluoroether and sulfolane, which is successful in suppressing polysulfide solubility without adding lithium nitrate while providing high discharge capacity and coulombic efficiency (>94%) [35].

In the paper published by Nakanishi et al. to examine the properties of sulfolane-based electrolytes with high and low concentrations, the binary systems of sulfolane and lithium bis(trifluoromethanesulfonyl)amide(LiTFSA) and its diluted version with hydrofluoroether (HFE) is examined along with the tetraglyme(G4)-based electrolytes, which are sparingly solvating [36]. It is concluded that the dilution with HFE leads to a lower viscosity and higher conductivity as expected and in addition, the electrolytes with sulfolane display good mass transfer properties [36].

In addition to the electrolyte type, the effect of the electrolyte-to-sulfur (E/S) ratio has also been widely investigated since this ratio also influences the Li-S battery performance. The analysis done by Kilic et al. indicates that low E/S ratios and high sulfur loadings are required for high energy densities [37]. In addition, material design, including the design of the encapsulation of cathodes and electrolyte contents, is key for the future of lithium-sulfur battery systems [37]. Another research, which is carried out by Bilal and Eroglu, determines 13 mL/g^{-1} as the best E/S ratio, showing good performance at the cell and system level, and this study

considers discharge capacity, capacity retention, and specific energy metrics while carrying out the analysis for the E/S ratio [21].

In a study by Mikhaylik et al. [11], the effect of the shuttle mechanism on the discharge and charge performance in a Li-S cell is modeled. For this purpose, a shuttle equation is introduced to the model and a shuttle constant is included in the calculations. Two distinct reactions in the two discharge plateaus are considered for the sulfur reduction.

The model proposed by Kumaresan et al. [10] is a comprehensive electrochemical model of a Li-S cell, which is then used by various studies. The model can predict two discharge voltage plateaus and the dip between them in the discharge process. In addition, the anode and cathode reactions and mass transport of various species within the cell are well defined in this model. There are six electrochemical and five dissolution and precipitation reactions in the model, which enables the model to predict concentrations of species with respect to time and space. Consequently, the model is a one-dimensional model, as it is concentration and time dependent. Ghaznavi et al. [38] conducted a sensitivity analysis using the mathematical model presented by Kumaresan et al. [10] The study is conducted based on variations in the C-rate and cathode conductivity, and shortcomings in the model are determined.

3. MODEL DEVELOPMENT

The zero-dimensional discharge and charge electrochemical models proposed by Marinescu et al. are applied to model the cycling of a Li-S cell within the scope of this thesis [1]. Continuous discharge and charge profiles are obtained by performing cycles where discharge and charge are carried out consecutively. FORTRAN (f90) is used to code and execute these theoretical models. The model is time-dependent, and the changes in variables are observed over time. On the contrary, the model is concentration-invariant, indicating mass transport phenomena are not considered.

The cycles are executed at 0.5 C-rate, which indicates that the discharge/charge would take 2 hours theoretically for 1.675 A per gram of sulfur. A delta time of 0.1 is applied to get more precise outcomes. For instance, the initial investigation at a 0.5 C-rate takes 72000 steps to complete to achieve a delta time of 0.1. Different cycling (continuous discharge and charge processes) simulations at various C-rates are also performed for comparison.

This model is zero-dimensional; thus, some assumptions must be made to see the time-dependent changes. To begin with, the sulfur is in the S_8^0 form and initially dissolved completely. There are two stages of discharge: the low plateau and the high plateau. One electrochemical reaction is dominant at every stage, giving a total of two electrochemical reactions. Given that the overpotentials at the anode and the separator are insignificant, the overpotentials at the anode and the separator are ignored. The precipitation of Li_2S is considered in the model through the k_p constant. The symmetry factor is taken as 0.5 in the Butler-Volmer equations since reactions are assumed to be symmetrical. In the model, the shuttle mechanism is represented by including the k_s constant. Current is positive during discharge and negative during charge, and it is constant during both processes. The governing and electrochemical reactions are the same for charge and discharge but are carried out in opposite directions. The model neglects the double-layer effect that happens at the electrolyte-electrode interface.

As mentioned above, discharge occurs in two stages, and for every stage, a distinct electrochemical reaction is valid. The equation suitable for the initial plateau of discharge is assumed to be the following equation as

$$S_8^0 + 4e^- \rightarrow 2S_4^{2-}. \tag{3.1}$$

At the beginning of the discharge, it is assumed that all the sulfur is present in the dissolved S_8^0 form. The equation that applies to the second plateau of discharge is assumed as follows

$$S_4^2 + 4e^- \rightarrow 2S^{2-} \downarrow + S_2^{2-}. \tag{3.2}$$

It is assumed that the discharge and charge electrochemical equations are identical but in the reverse directions. For the discharge part, governing equations in this zero-dimensional model are taken from Marinescu et al. [1]. The first governing equations are Nernst equations for high and low potentials at equilibrium which are shown as

$$E_H = E_H^0 + \frac{RT}{4F} ln\left(f_H \frac{S_8^0}{(S_4^{2-})^2} \right), \tag{3.3}$$

$$E_L = E_L^0 + \frac{RT}{4F} ln\left(f_L \frac{S_4^{2-}}{(S^{2-})^2\, S_2^{2-}} \right), \tag{3.4}$$

E_H^0 and E_L^0 are standard potentials for the high and low plateau, respectively. The f_H and f_L are defined to obtain masses of sulfur species in grams. They are calculated as

$$f_H = \frac{n_{S_4}^2 M_{S_8} v}{n_{S_8}}, \tag{3.5}$$

$$f_H = \frac{n_S^2\, n_{S_2} M_{S_8}^2 v^2}{n_{S_4}}, \tag{3.6}$$

v is electrolyte volume of the cell, M_{S_8} is the molar mass of sulfur and n represents the number of polysulfides in the subscripts. For the reaction kinetics, Butler-Volmer approximations are used for the high and low voltage plateaus, which are estimated from the equations shown as

$$i_H = 2\, i_{H,0}\, a_R\, sinh\frac{n_e F \eta_H}{2RT}\ , \tag{3.7}$$

$$i_L = 2\, i_{L,0}\, a_R\, sinh\frac{n_e F \eta_L}{2RT}\ , \tag{3.8}$$

$i_{H,0}$ and $i_{L,0}$ are exchange current densities for high and low plateau reactions subsequently. a_r is the active reaction area of the cell. n_e is the electron number per reaction, which is 4. η_H and $\eta_L$are the overpotentials for the first and the second electrochemical reaction, which are calculated as

$$\eta_H = V - E_H\ , \tag{3.9}$$

$$\eta_L = V - E_L\ . \tag{3.10}$$

The following formulae are used to determine the concentration evolution of the five species in this model over time:

$$\frac{dS_8^0}{dt} = -\frac{n_{S_8} M_{S_8}}{n_e F}\, i_H - k_s S_8^0\ , \tag{3.11}$$

$$\frac{dS_4^{2-}}{dt} = \frac{n_{S_8} M_{S_8}}{n_e F}\, i_H + k_s S_8^0 - \frac{n_{S_4} M_{S_8}}{n_e F}\, i_L\ , \tag{3.12}$$

$$\frac{dS_2^{2-}}{dt} = \frac{n_{S_2} M_{S_8}}{n_e F}\, i_L\ , \tag{3.13}$$

$$\frac{dS^{2-}}{dt} = \frac{2 n_S M_{S_8}}{n_e F}\, i_L - \frac{1}{v\rho_S} k_p S_p (S^{2-} - S_*^{2-})\ , \tag{3.14}$$

$$\frac{dS_p}{dt} = \frac{1}{v\rho_S} k_p S_p (S^{2-} - S_*^{2-})\ , \tag{3.15}$$

k_s is the shuttle constant. Since the shuttle effect is considered in this model, it is indicated through a shuttle constant. In the model, precipitation effects are included. The precipitation rate is represented through k_p in the formula, and ρ_S is density of precipitated sulfur. S_*^{2-} is the saturation mass of S^{2-}.

Given that the charge is preserved, cell current is calculated using the following equation which is expressed as

$$I = i_H + i_L \, . \tag{3.16}$$

The applied current is calculated through considering the C-rate and mass of active sulfur (m_S) for 1.675 A per gram of sulfur, by using the equation which is expressed as

$$I_{applied} = m_S * \ 1.675 * c_{rate} \, . \tag{3.17}$$

The value of cell current applied ($I_{applied}$) is taken as positive during discharge and the same but opposite sign, negative during charging. There are 12 variables in the model. S_8°, S_4^{2-}, S_2^{2-}, S^{2-}, S_p are the mass of species in grams. i_H, i_L are current contributions from the two (high and low voltage plateau) electrochemical reactions in A/m^2. η_H, η_L are overpotentials for the high and low voltage plateau reactions, respectively, in V. E_H, E_L are Nernst potentials for the high and low voltage plateau reactions, and V is the cell voltage, all in V.

3.1. Initial Conditions

Initial conditions of each parameter for the first discharge are determined by using the values in Marinescu et al. [1] which is expressed as

$$S_8^0 = \ ms * 0.99 \, , \tag{3.18}$$

$$S_p = \ ms * 10^{-6} \, , \tag{3.19}$$

$$i_H = I \, , \tag{3.20}$$

$$i_L = I - I_H \ or \ i_L = 0 \, , \tag{3.21}$$

$$V = 2.4 \ , \tag{3.22}$$

$$\eta_H = \frac{sinh\left(-\frac{i_H}{2\, i_{H,0} a_r}\right)}{8FRT}\ , \tag{3.23}$$

$$\eta_L = \frac{sinh\left(-\frac{i_L}{2\, i_{L,0} a_r}\right)}{8FRT}\ , \tag{3.24}$$

$$E_H = V - \eta_H\ , \tag{3.25}$$

$$S_4^{2-} = \sqrt{\frac{f_H\, S_8^0}{exp\left(\frac{E_H - E_H^0}{4RTF}\right)}}\ , \tag{3.26}$$

$$E_L = V - \eta_L\ , \tag{3.27}$$

$$S^{2-} = 10^{-8}. \tag{3.28}$$

S_2^{2-} cannot be calculated directly, so it is calculated in the Fortran code by doing 100000 iterations, satisfying both equations which are

$$S^{2-} = \left(\frac{f_L * S_4^{2-}}{exp\left((E_L - E_L^0) * \frac{4F}{RT}\right)} * S_2^{2-}\right)^{1/2}\ , \tag{3.29}$$

$$S_2^{2-} = S^{2-} + S_p\ . \tag{3.30}$$

The initial values of the first charge and the following charges are the variable values at the end of the previous discharge. Similarly, the variable values of the previous charge are taken as the initial condition for the 2nd discharge and the following discharges.

3.2. Parameters in the Model

The parameters in the model are shown in the Table 3.1. The values are taken from the zero-dimensional model by Marinescu et al. [1]

Table 3.1. Parameters in the zero-dimensional model [1].

Notation	Name	Units	Value
F	Faraday's Constant	C mol^{-1}	9.649 x 10^4
R	Gas constant	J K^{-1} mol^{-1}	8.3145
T	Temperature	K	298
M_{S_8}	Molar mass of S_8^0	g mol^{-1}	32
N_A	Avogadro number	1 mol^{-1}	6.0221 x 10^{23}
n_e	Electron number per reaction	-	4
$n_{S_8}, n_{S_4}, n_{S_2}, n_S$	Number of sulfur atoms in polysulfide	-	8,4,2,1
ρ_S	Density of precipitated sulfur	g L^{-1}	2 x 10^3
a_r	Active reaction area per cell	m^2	0.960
f_H	Dimensionality factor H	g L mol^{-1}	0.7296
f_L	Dimensionality factor L	g^2 L^2 mol^{-1}	0.0665
v	Electrolyte volume per cell	L	0.0114
m_S	Mass of active sulfur per cell	g	2.7
E_H^0	Standard potential H	V	2.35
E_L^0	Standard potential L	V	2.195
$i_{H,0}$	Exchange current density H	A m^{-2}	10
$i_{L,0}$	Exchange current density L	A m^{-2}	5

Table 3.1. Parameters in the zero-dimensional model [1]. (cont.)

Notation	Name	Units	Value
S_*^{2-}	S^{2-} saturation mass	g	0.0001
k_p	Precipitation rate constant	s^{-1}	100
k_s	Shuttle constant	s^{-1}	0.0002
I	External current	A	Variable

3.3. Linearization Procedure

The governing equations are linearized, and their coefficients ($b_{i,k}, d_{i,k}$ *and* $g_{i,k}$) are found. These coefficients are then used in the FORTRAN code to solve the equations using the previously reported subroutines [39]. After linearization, they are brought to the following equation form which is expressed as

$$b_{i,k}\,(x)\frac{dC}{dx} + \,d_{i,k}\,(x)\,C = g_{i,k}(x)\,. \tag{3.31}$$

To determine $b_{i,k}\,(x)$, $d_{i,k}\,(x)$ and $g_{i,k}(x)$, the following procedures are applied. For instance, the variable $i_{H,}$ *is replaced by* $i_{H,prev} + \Delta i_H$, and this is done for all variables (step 1). Then, the values in the common factors are placed in parentheses after the nonlinear terms of delta products, if any, are ignored and removed from the equations (step 2). Eventually, coefficients are determined.

For example, for Equation 3.11, the linearization is carried out as

Step 1: $$\frac{\Delta S_8^\circ}{\Delta t} = -\frac{n_{S_8} * M_{S_8}}{n_e * F}\left(i_{H,prev} + \Delta i_H\right) - k_s * (S_{8,prev}^\circ + \Delta S_8^\circ)\,,$$

Step 2: $$\Delta S_8^\circ\left(\frac{1}{\Delta t} + k_s\right) + \frac{n_{S_8} * M_{S_8}}{n_e * F}\,\Delta i_H = -\frac{n_{S_8} * M_{S_8}}{n_e * F} i_{H,prev} - k_s * S_{8,prev}^\circ.$$

Finally, coefficients are determined as

$$d_{1,1} = \frac{1}{\Delta t} + k_s\,,$$

$$d_{1,6} = \frac{n_{S_8} * M_{S_8}}{n_e * F},$$

$$g_1 = -\frac{n_{S_8} * M_{S_8}}{n_e * F} i_{H,prev} - k_s * S^{\circ}_{8,prev}.$$

These coefficients are then used in matrices in Fortran to solve the equations. The Fortran codes generated in this work are presented in the Appendix.

4. RESULTS AND DISCUSSION

The simulations of the cycles, specifically the sequential discharge and charge profiles of the 0-dimensional electrochemical model discussed earlier, were executed using the Fortran programming language, and the results were acquired. In the sensitivity analysis section, the effect of the changes in parameters on the predicted Li-S cell performance was examined. In the next section, Li-S cell performance was investigated as a function of the electrolyte-to-sulfur (E/S) ratio. Following the modifications, graphs illustrating the variations in cell capacity and discharge profiles over cycles were generated. The impact of the electrolyte design on Li-S cell performance was assessed by analyzing these graphs and comparing the results with the existing literature data. Furthermore, the impact of both the amount and the properties of electrolytes on the performance of Li-S cells was examined implicitly through model parameters.

4.1. Sensitivity Analysis

In this part, the simulation of cycles, that is, successive discharge and charge profiles, in the 0-dimensional electrochemical cell was achieved by varying various parameters. The graphs below show the discharge profiles and capacity variations in each cycle based on parameter alterations. The changed parameters are active reaction area (a_r), initial cell voltage (V_0), shuttle constant (k_s), high and low voltage plateau standard potentials $(E_H^0,\ E_L^0)$, high and low voltage plateau electrochemical reaction exchange current densities $\left(i_{H,0}, i_{L,0}\right)$, precipitation rate constant $\left(k_p\right)$, and C-rate. By performing this analysis, the model's sensitivity to variations in several parameters was evaluated.

Initially, one hundred discharge and charge cycles were simulated at a C-rate of 0.5; however, only the discharge capacities and the final variable values of the first and second cycles were different. The capacities were the same in the second cycle of discharge and in subsequent cycles, and the final variable values ended up at the same values as shown in Figure 4.1.

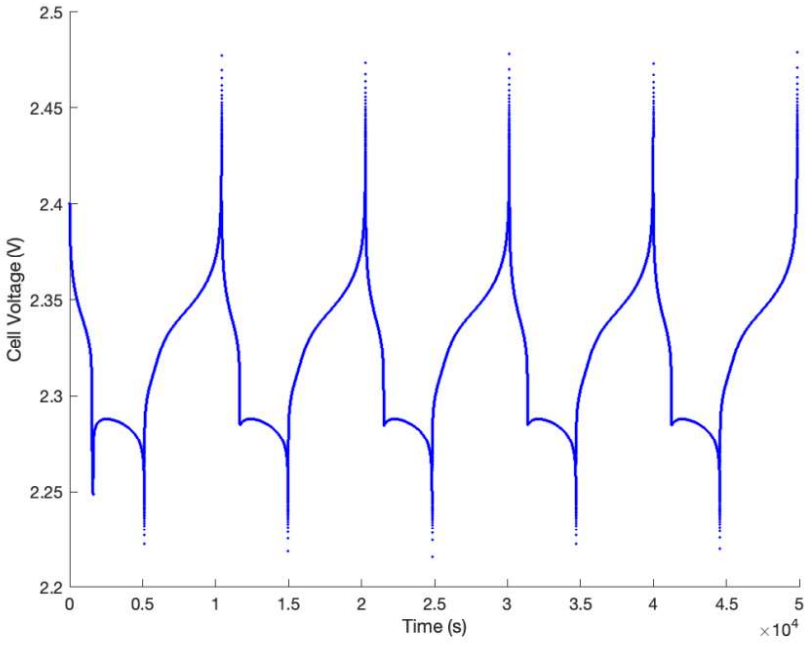

Figure 4.1. Simulated discharge and charge voltages vs. time at a C-rate of 0.5 for 5 cycles.

Therefore, for each simulation, two cycles were run to demonstrate the results and to prevent repetition in each cycle. For the charge, all cycles ended with the same final variables and charge capacities. Therefore, only the first and the second cycle charge voltage vs. capacity graphs were taken. All the graphs obtained from the simulations are shown below.

4.1.1. Active Reaction Area

The first parameter changed was the active reaction area, and discharge profile scenarios were obtained by taking 10 and 1/10 times the baseline active reaction area value as shown in Figure 4.2. The discharge capacity of the lithium-sulfur cell should theoretically increase as the active reaction area increases since a rise in the active area indicates better kinetics, thus more sulfur utilization [40,41].

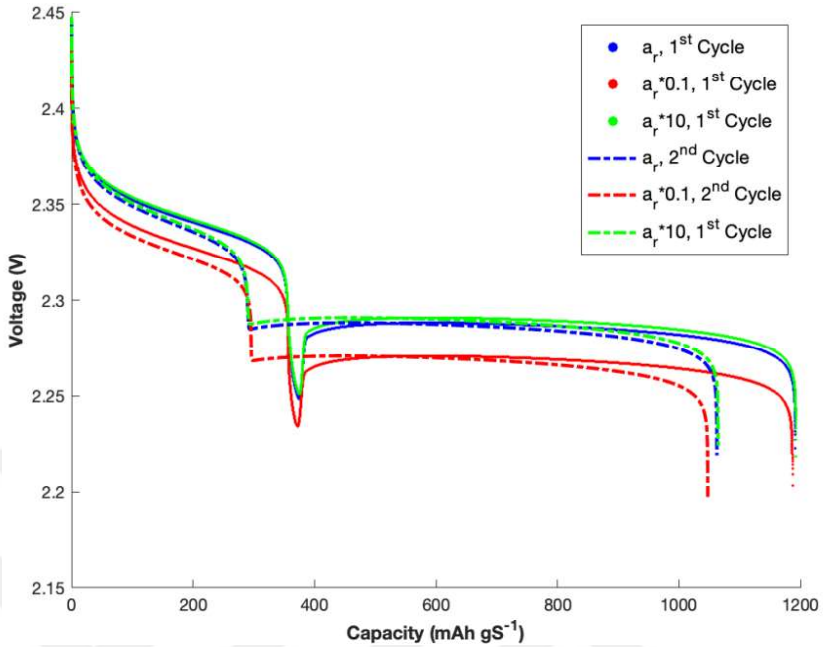

Figure 4.2. Simulated discharge voltages vs. capacities for various active reaction areas (a_r) at a C-rate of 0.5 for 2 cycles.

As the a_r value increases, high and low voltage plateaus, i.e., discharge voltage output values, are higher, as shown in Figure 4.2. These changes in voltage values are more noticeable in $a_r/10$ but are minor in a_r*10. This leads to the conclusion that when the a_r value goes below a specific threshold, it has a detrimental impact on cell voltage. On the other hand, the drop in voltage output as a_r reduces is to be expected since as the active area increases, so does the utilization of lithium and sulfur ions, and the reaction kinetics improve [42]. In general, the results obtained with the change in the active area appear to be analogous with those reported in the literature.

As seen in Figure 4.3, the discharge capacity of the cell increases as the active reaction area (a_r) increases, but very slightly. The decrease in the capacity with a tenfold decrease in the area is slightly more prominent. Figure 4.3 shows that the discharge capacity of the second cycle is lower than the first cycle in all cases, independent of the a_r value. However, as can be seen, this decrease is more noticeable in the case of $a_r/10$. From this, it can be concluded that when the

active area declines, the capacity loss in the second cycle becomes more noticeable. This may be explained by the hindered kinetics at lower values of this parameter.

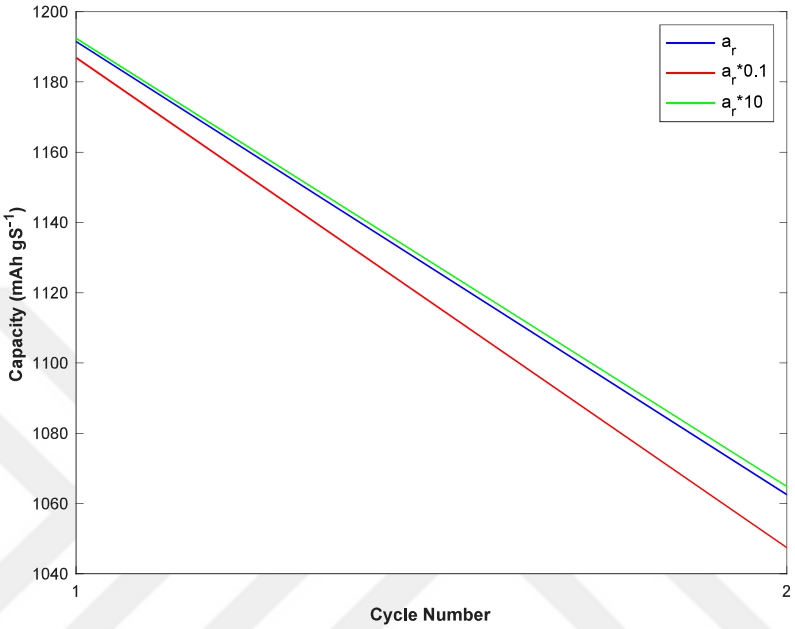

Figure 4.3. Simulated discharge capacities for 2 different cycles for various active reaction areas (a_r) at a C-rate of 0.5.

As previously stated, the charge voltage outputs remain constant for both the first and second cycles despite the alteration of the a_r values. Figure 4.4 illustrates that an increase in a_r leads to an insignificant decrease in charge voltage output values. However, the capacity remains nearly unaltered, similar to the discharge scenario. Unlike during discharge, where there are two distinct voltage plateaus separated by a dip, there is only one plateau during charge.

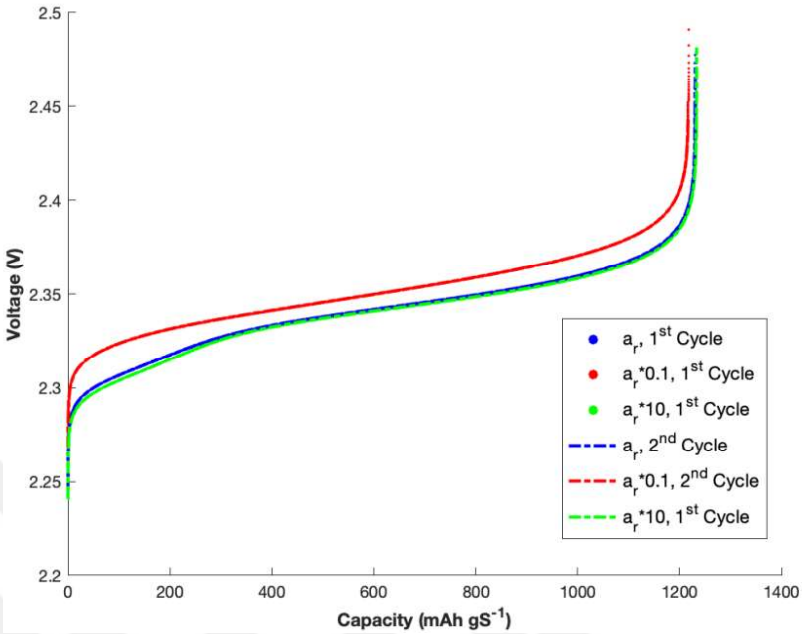

Figure 4.4. Simulated charge voltages vs. capacities for various active reaction areas (a_r) at a C-rate of 0.5 for 2 cycles.

4.1.2. Initial Voltage

Figures 4.5 and 4.6 show the consequences of altering the initial cell voltage value. The largest capacity value is attained when the initial voltage is the lowest, i.e., 2.35 V. As the initial voltage decreases, the cell capacity increases, but the capacity difference between V_0 values of 2.4 V and 2.45 V is not very significant. In all scenarios, the capacity in the 2nd cycle is less than the 1st cycle. The capacity difference between the first and second cycles is roughly the same in all circumstances.

The low voltage plateau values are similar across all situations but lower in the high voltage plateau where V_0 is equal to 2.45. This shows that the initial voltage value decreases the high voltage plateau when it falls below a certain value. According to the literature, high initial voltages can increase sulfur utilization and voltage values, but low voltage plateau may end earlier due to the shuttle effect [43]. On the other hand, the decrease in the initial voltage also decreased the difference between the plateaus, and a more stable discharge plateau was obtained. The first voltage drop occurred almost simultaneously in all three scenarios.

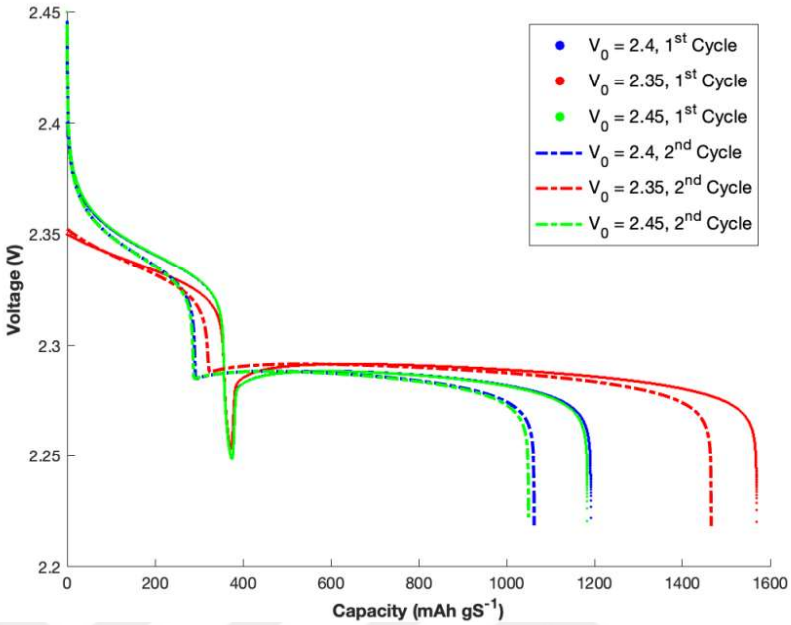

Figure 4.5. Simulated discharge voltages vs. capacities for various initial cell voltages (V_0) at a C-rate of 0.5 for 2 cycles.

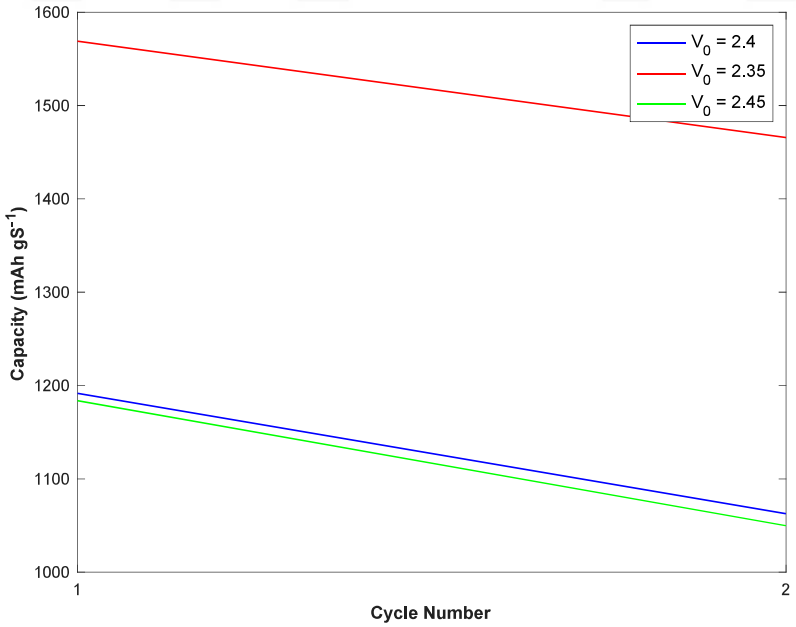

Figure 4.6. Simulated discharge capacities for 2 different cycles for various initial cell voltages (V_0) at a C-rate of 0.5.

According to Figure 4.7, when the initial voltage increases, the charge capacity reduces and the voltage output increases. Capacity change exhibits similarities to changes in discharge.

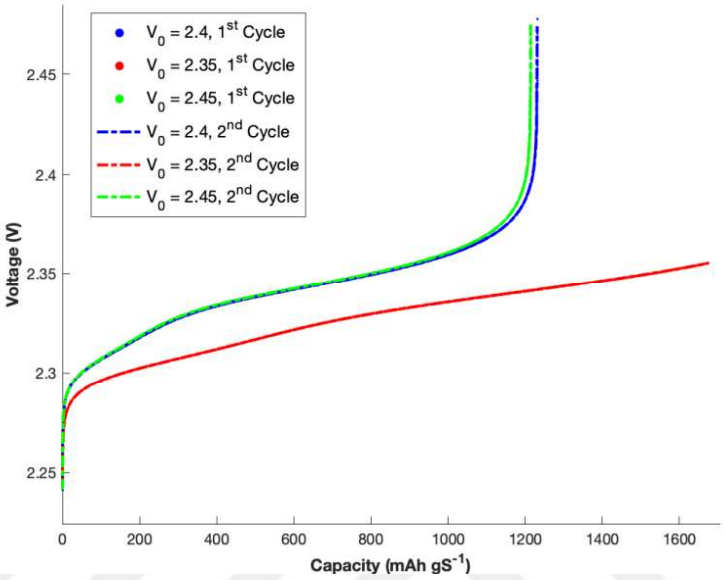

Figure 4.7. Simulated charge voltages vs. capacities for various initial cell voltages (V_0) at a C-rate of 0.5 for 2 cycles.

4.1.3. Shuttle Constant

Increasing the shuttle constant strengthens the shuttle effect in the Li-S cell, lowering the coulombic efficiencies, reducing the first discharge capacity, and causing capacity to drop over time in each cycle [44]. Figures 4.8 and 4.9 illustrate that when the shuttle constant increases, the capacity decreases in the initial discharge. Furthermore, the second discharge capacity is lower than the first, as expected.

As k_s increases, the high voltage plateau values decrease, and the first voltage drop occurs faster. The low voltage plateau values exhibit no substantial change according to shuttle constant changes; however, when k_s increases, the discharge time reduces, which is reasonable.

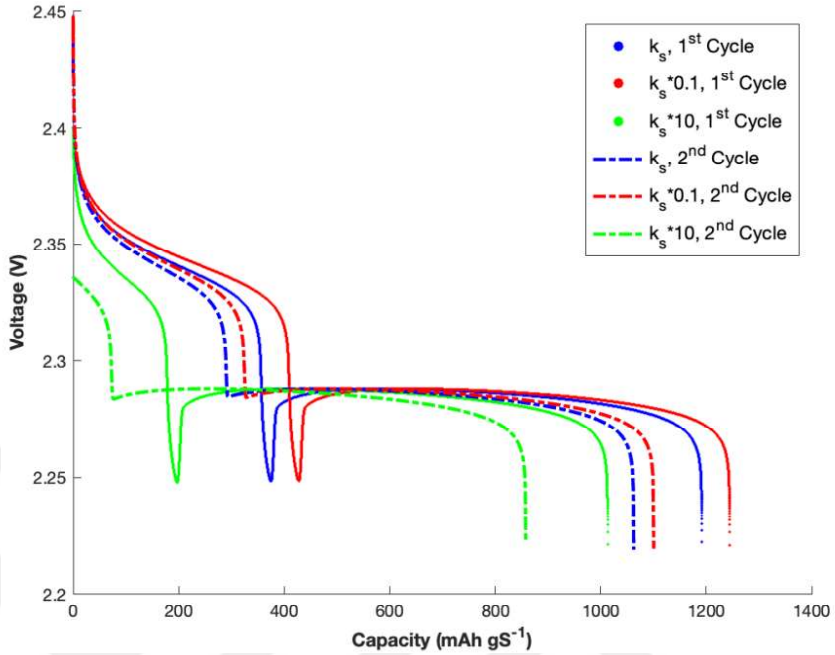

Figure 4.8. Simulated discharge voltages vs. capacities for various shuttle constants (k_s) at a C-rate of 0.5 for 2 cycles.

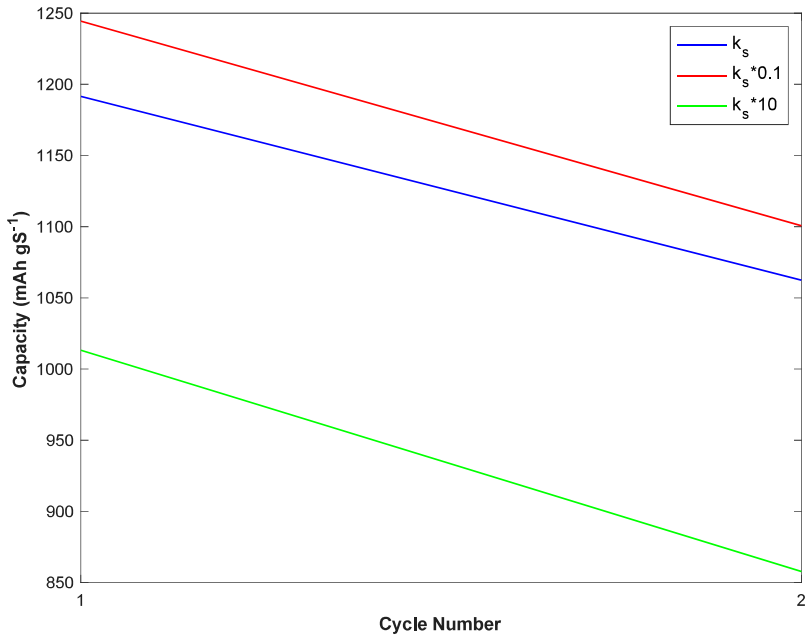

Figure 4.9. Simulated discharge capacities for 2 different cycles for various shuttle constants (k_s) at a C-rate of 0.5.

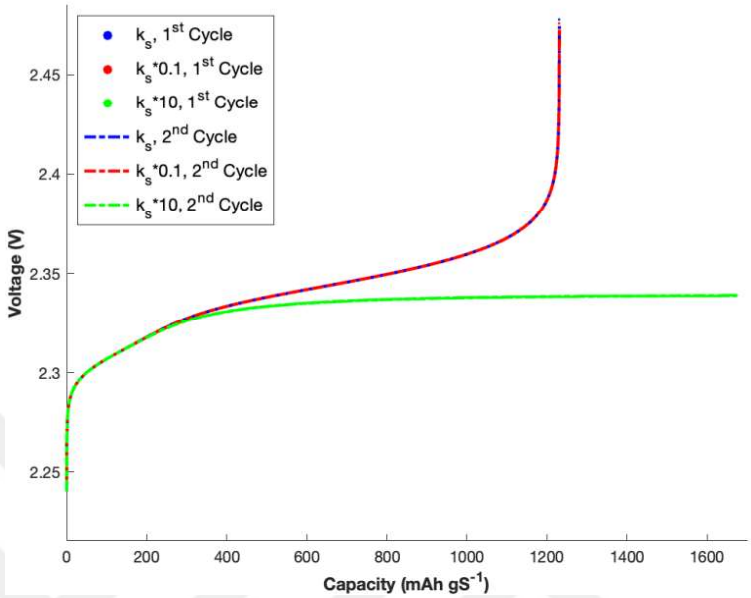

Figure 4.10. Simulated charge voltages vs. capacities for various shuttle constants (k_s) at a C-rate of 0.5 for 2 cycles.

Concerning the charge aspect, as depicted in Figure 4.10, altering the value of k_s results in a modification of the curve's form and an unanticipated rise in capacity. The rise in k_s leads to infinite charging, as expected from the experimental trends.

4.1.4. Precipitation Constant

An increase in the precipitation rate can increase the polysulfide precipitates formed during discharge, resulting in a reduction in the cathode surface, an increase in the shuttle effect, and a decrease in the electrochemical performance of the Li-S battery cell, thus lowering cell capacity and voltage profile stability [45].

Figure 4.11 illustrates that during the first cycle, the voltage profiles overlap and are nearly indistinguishable. In the second cycle, the voltage profile at k_p*3 appears to be the most stable, whereas the one at k_p*0.8 appears to be the least stable, with the high voltage section being nearly a straight line downwards. It seems that k_p has no influence on capacity in the first

cycle, and the capacity difference between the first and second cycles appears to be the least at k_p*3 and the greatest at k_p*0.8, indicating that increasing k_p lessens capacity fading, which is unexpected.

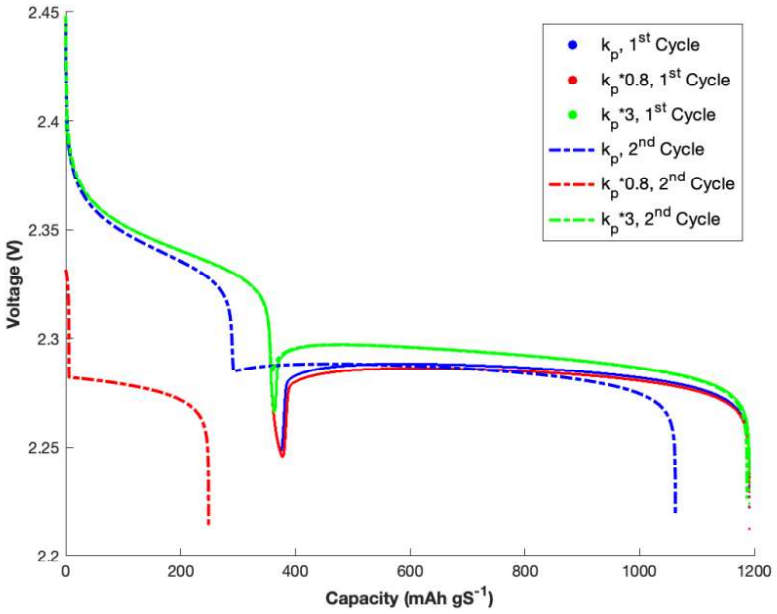

Figure 4.11. Simulated discharge voltages vs. capacities for various precipitation rates (k_p) at a C-rate of 0.5 for 2 cycles.

Based on Figure 4.13, the reduction in k_p has significantly diminished the charge capacity. The decrease in k_p also resulted in a reduction of the discharge capacity during the 2nd cycle. As the value of k_p increased, the charge capacities also increased, resulting in a corresponding increase in duration. The cause of this phenomenon may be attributed to the increased precipitation of Li_2S in the discharge, which consequently necessitates a longer duration for its oxidation back to S_8.

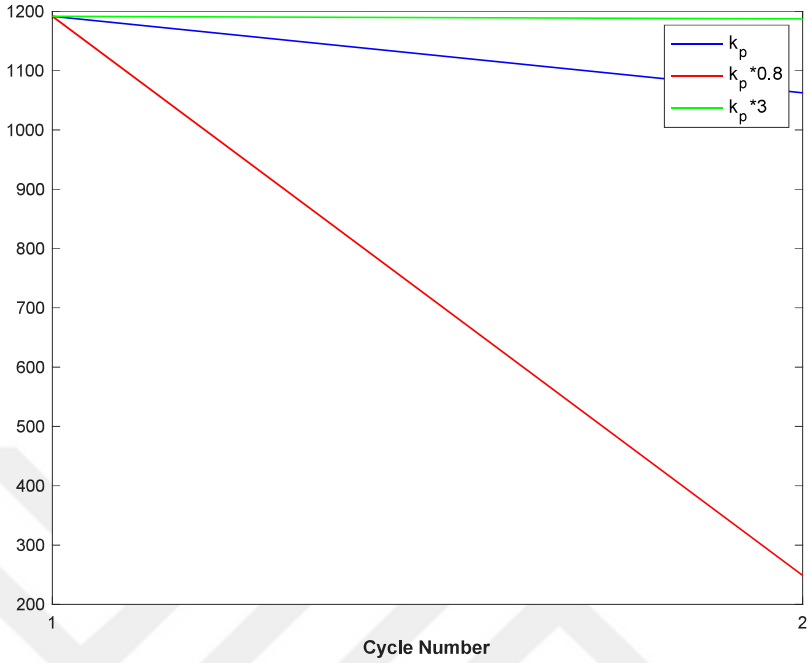

Figure 4.12. Simulated discharge capacities for 2 different cycles for various precipitation rates (k_p) at a C-rate of 0.5.

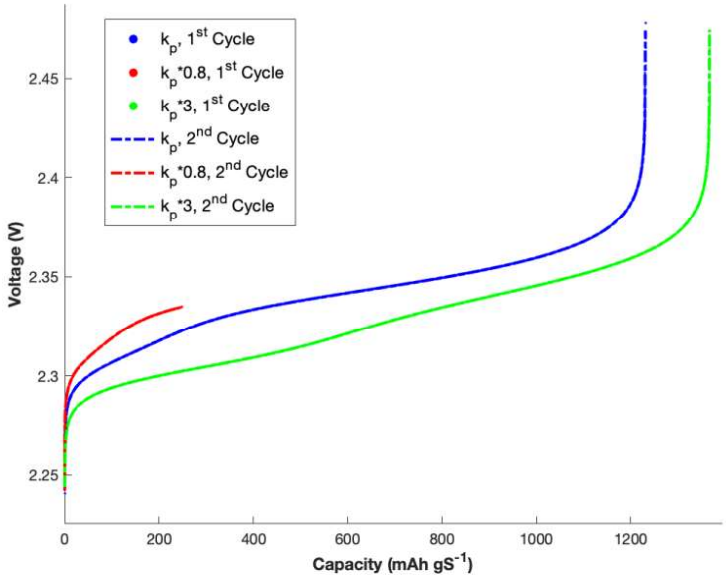

Figure 4.13. Simulated charge voltages vs. capacities for various precipitation rates (k_p) at a C-rate of 0.5 for 2 cycles.

4.1.5. Standard Potential for High Voltage Plateau

Changes in E_H^0 impact the high voltage plateau, whereas changes in E_L^0 affect the low voltage plateau. According to Figure 4.14, as E_H^0 increases, the capacity increases, and, in all scenarios, the capacity in the 2nd cycle is lower than in the 1st cycle. The capacity difference between the 1st and 2nd cycles increases as E_H^0 decreases, which shows that the decrease in E_H^0 increases capacity fading. As expected, there is a significant difference in high-voltage plateaus. As E_H^0 increases, the high voltage plateau becomes higher, and the difference between the high and low voltage plateau also increases. There is also some change in low voltage plateaus, but it is significantly less than the high voltage plateau.

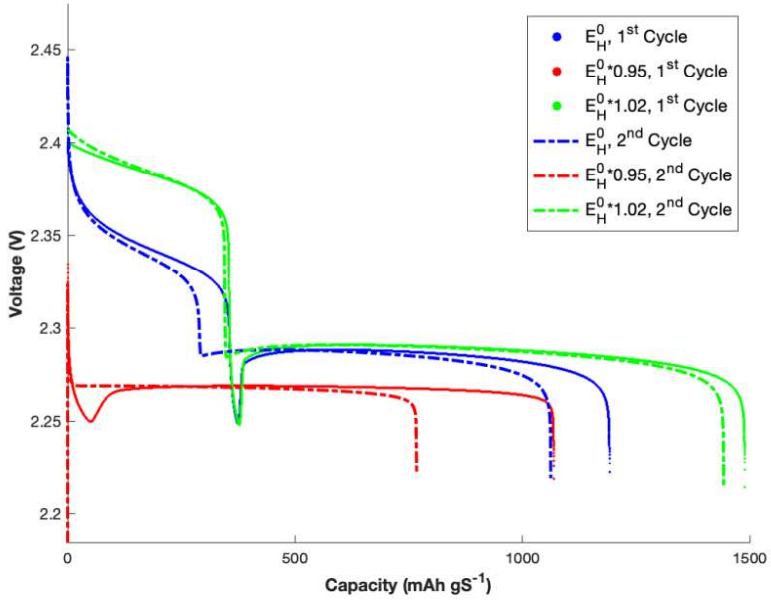

Figure 4.14. Simulated discharge voltages vs. capacities for various high voltage standard potentials (E_H^0) at a C-rate of 0.5 for 2 cycles.

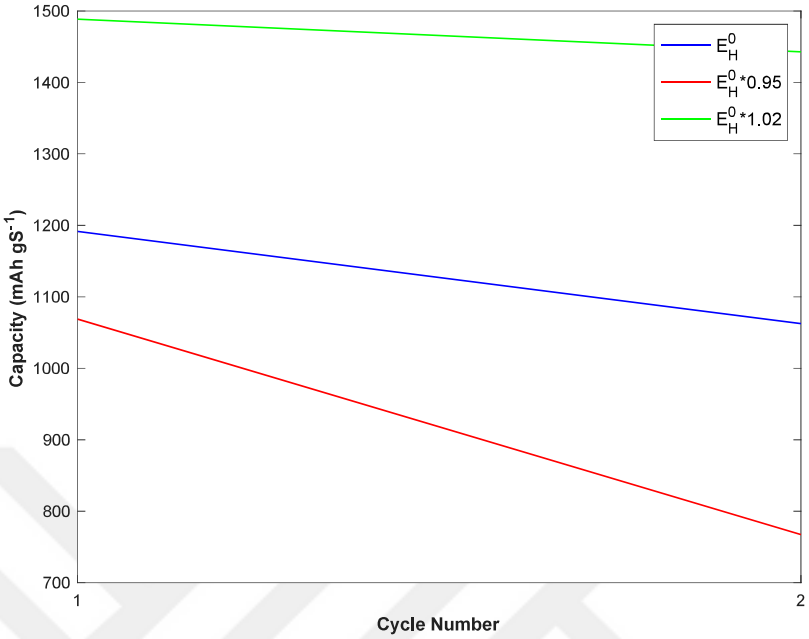

Figure 4.15. Simulated discharge capacities for 2 different cycles for various high voltage standard potentials (E_H^0) at a C-rate of 0.5.

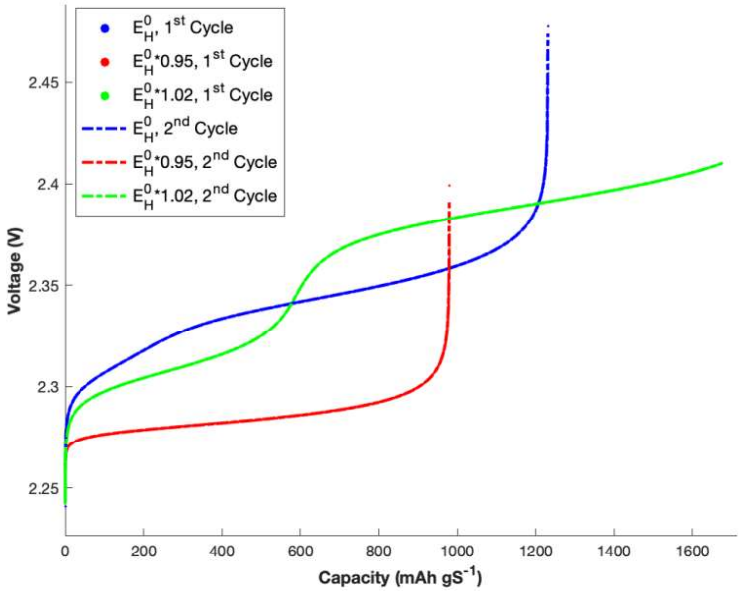

Figure 4.16. Simulated charge voltages vs. capacities for various high voltage standard potentials (E_H^0) at a C-rate of 0.5 for 2 cycles.

Upon analyzing Figure 4.16, it is evident that increasing E_H^0 not only enhances the capacity but also elevates the charge voltage output. Furthermore, for E_H^0*1.02, it becomes apparent that two voltage plateaus start to develop. An increase in E_H^0 can lead to an acceleration in reaction kinetics, resulting in a faster dissolution of the precipitated material.

4.1.6. Standard Potential for Low Voltage Plateau

In Figure 4.17, E_L^0 was increased and decreased by a factor of 1.05 and 0.97, respectively. As E_L^0 increases, capacity reduces, and the time required to reach the first voltage drop point shortens. There is no significant change in high voltage plateaus in all 3 cases, but there is a change in low voltage plateaus, as expected. The low voltage plateau is the highest when E_L^0 is high and the lowest when it is low. As seen in Figure 4.18, the capacity decrease from the first cycle to the second cycle is the highest in the scenario where E_L^0 is the highest, while it is very similar in the other two. Accordingly, it can be predicted that increasing the E_L^0 value increases capacity fading in cycles.

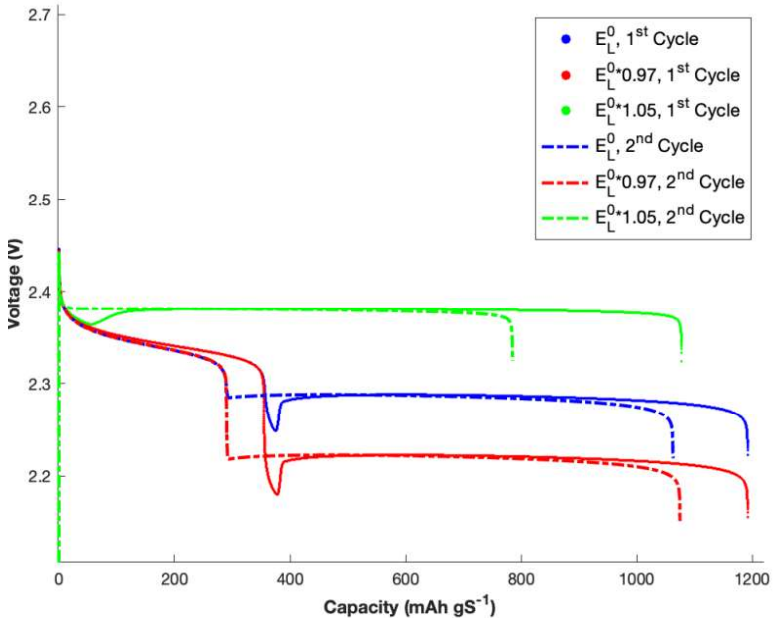

Figure 4. 17. Simulated discharge voltages vs. capacities for various low voltage standard potentials (E_L^0) at a C-rate of 0.5 for 2 cycles.

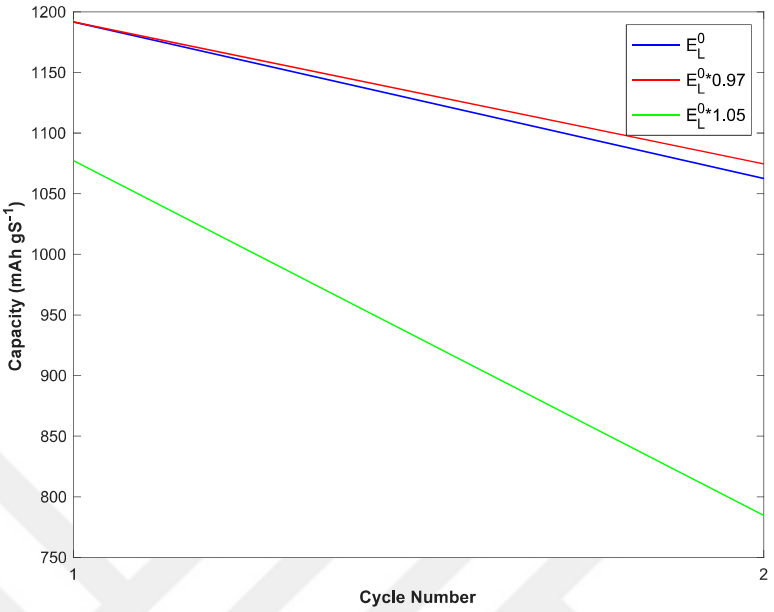

Figure 4.18. Simulated discharge capacities for 2 different cycles for various low voltage standard potentials (E_L^0) at a C-rate of 0.5.

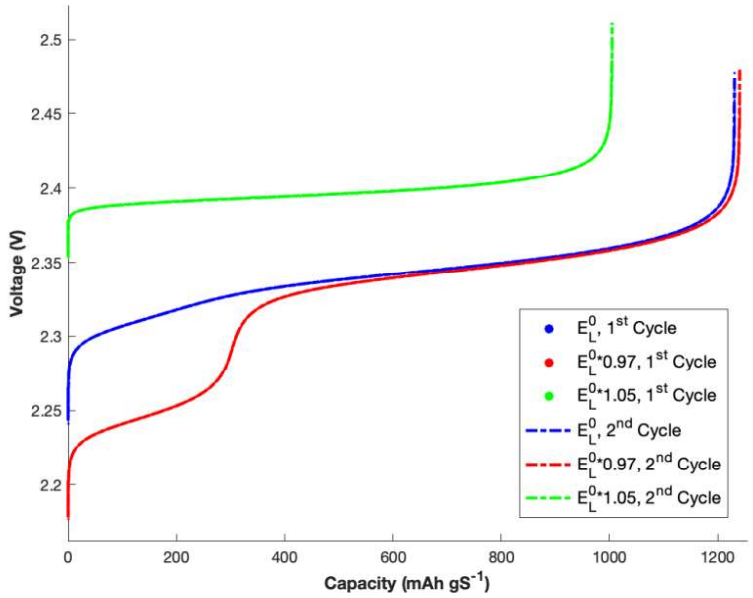

Figure 4.19. Simulated charge voltages vs. capacities for various low voltage standard potentials (E_L^0) at a C-rate of 0.5 for 2 cycles.

Based on Figure 4.19, when E_L^0 increases, the capacity declines while the charge voltage output increases. As the E_L^0 value falls, two distinct charge plateaus become evident, as in the E_H^0*1.02 charge graph.

4.1.7. Exchange Current Density for High Voltage Plateau

As high voltage plateau electrochemical reaction exchange current density increases, capacity is expected to increase, whereas capacity fading diminishes [44]. As opposed to these conclusions, an increase in $i_{H,0}$ does not have a major effect on capacity in all cycles. As observed in Figure 4.20, only iH0/10 has a lower capacity value; however, the difference is minor. Yet, it is apparent in the figure that a decrease in $i_{H,0}$ causes lower first plateau voltages; this is expected as worse kinetics would lead to higher overpotentials. On the other hand, lower voltage plateau is indifferent to this parameter. Cycle 2 has a lower capacity than cycle 1, as expected, but capacity fading has not changed significantly in Figure 4.21.

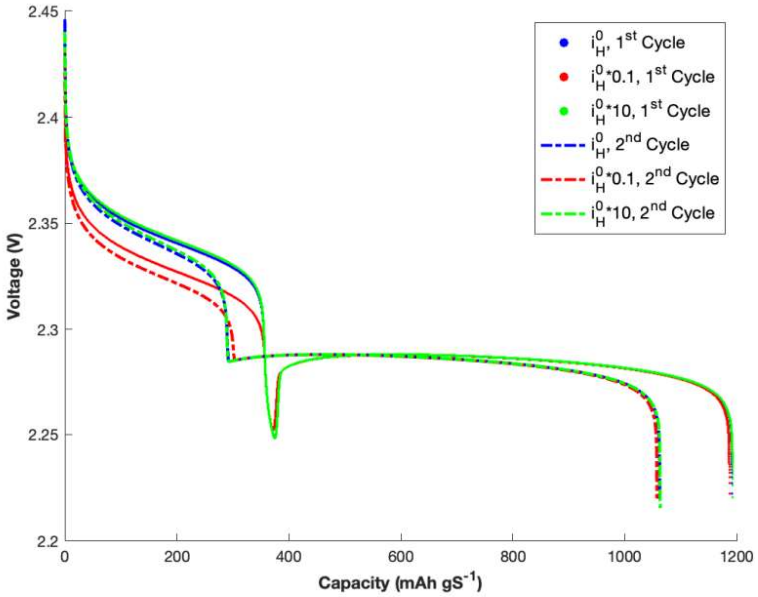

Figure 4.20. Simulated discharge voltages vs. capacities for various high voltage plateau electrochemical reaction exchange current densities $(i_{H,0})$ at a C-rate of 0.5 for 2 cycles.

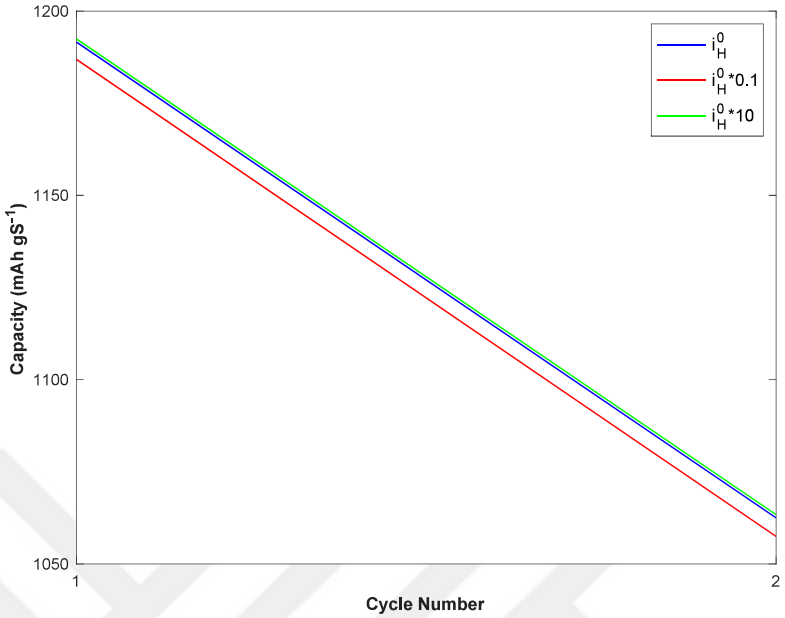

Figure 4.21. Simulated discharge capacities for 2 different cycles for various high voltage plateau electrochemical reaction exchange current densities $(i_{H,0})$ at a C-rate of 0.5.

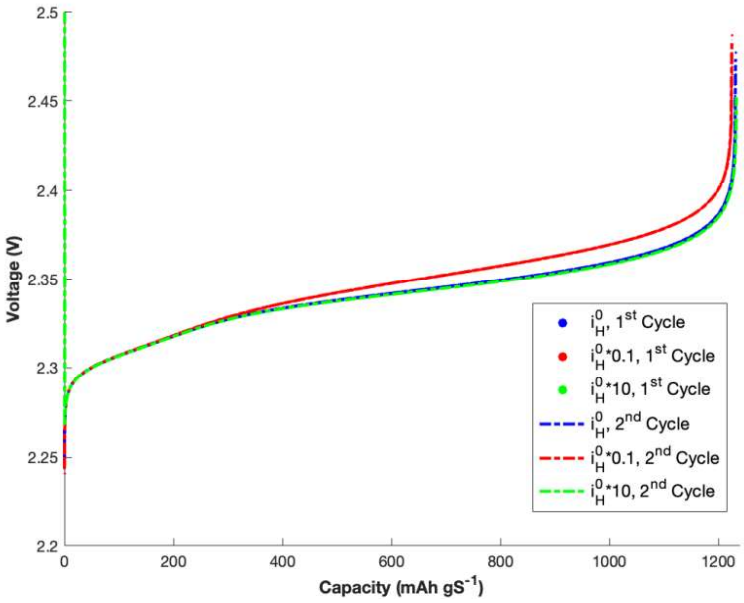

Figure 4.22. Simulated charge voltages vs. capacities for various high voltage plateau electrochemical reaction exchange current densities $(i_{H,0})$ at a C-rate of 0.5 for 2 cycles.

In addition, as demonstrated in Figure 4.22, like the discharge results, the variations in $i_{H,0}$ have no influence on the charge capacities.

4.1.8. Exchange Current Density for Low Voltage Plateau

Figure 4.23 shows that the high voltage plateau is not affected by the changes in the low voltage plateau electrochemical reaction exchange current density, and the high voltage plateaus cannot be distinguished, unlike the changes in the discharge profiles when $i_{H,0}$ was changed.

The low voltage plateau increases as $i_{L,0}$ increases, and for $i_{L,0}/10$, the difference in the low voltage plateau is more apparent. On the other hand, $i_{L,0}$ and $i_{L,0}*10$ low voltage plateau values are close to each other. The change in $i_{L,0}$ does not seem to affect the capacity change at all. However, according to Figure 4.24, the capacity decrease in the 2nd cycle is slightly greater at $i_{L,0}*0.1$.

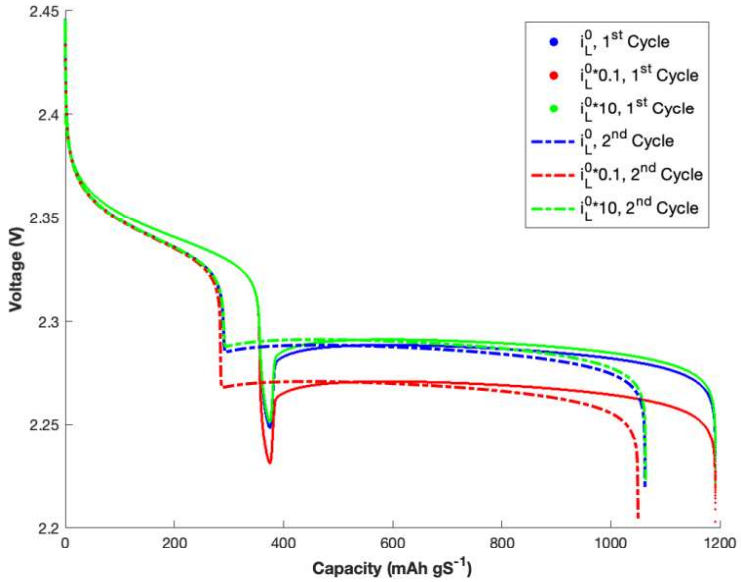

Figure 4.23. Simulated discharge voltages vs. capacities for various low voltage plateau electrochemical reaction exchange current densities $(i_{L,0})$ at a C-rate of 0.5 for 2 cycles.

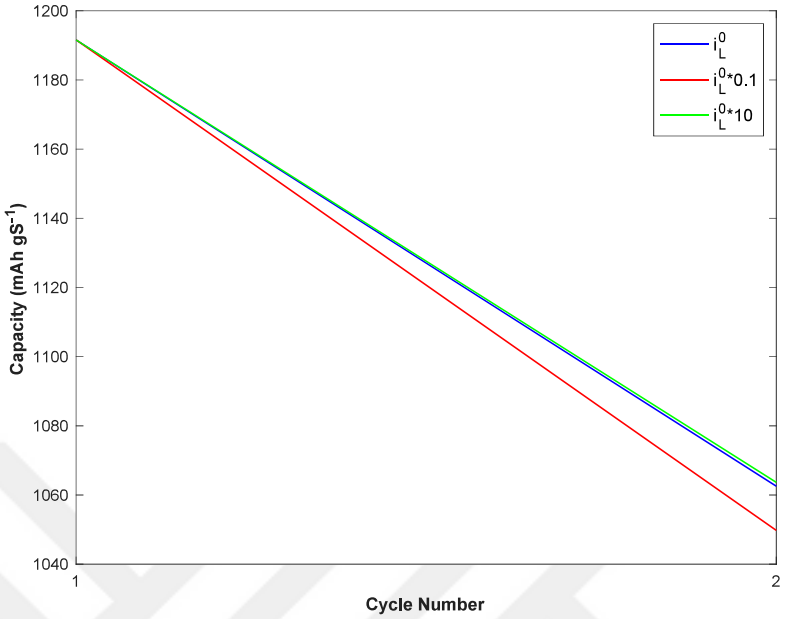

Figure 4.24. Simulated discharge capacities for 2 different cycles for various low voltage exchange current densities $(i_{L,0})$ at a C-rate of 0.5.

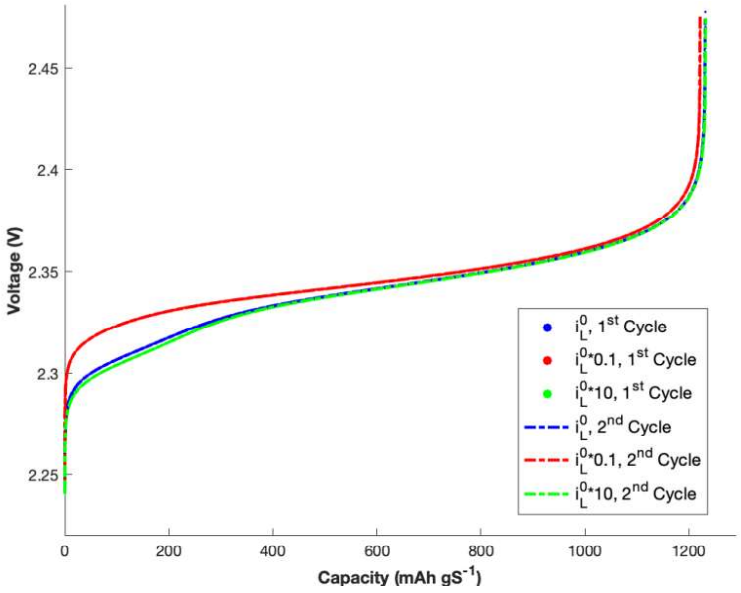

Figure 4.25. Simulated charge voltages vs. capacities for various low voltage plateau electrochemical reaction exchange current densities $(i_{L,0})$ at a C-rate of 0.5 for 2 cycles.

Moreover, as depicted in Figure 4.25, it can be observed that the variation in $i_{L,0}$ has minimal impact on the charge voltage output and capacity. Yet, the initial values of the charge voltage output are slightly greater at $i_{L,0}$*0.1 because of poorer kinetics.

4.1.9. C-rate

The C-rate is the parameter that governs the rate at which the battery can be discharged or charged. A decrease in C-rate signifies an extension of the battery's discharge duration. The simulation of this model was conducted at C-rates of 0.1, 0.5, and 0.7, and the sensitivity to C-rate was evaluated. According to Figures 4.26 and 4.27, when the C-rate increases, it also affects the capacity in the first cycle; the initial discharge capacity increases with increasing C-rate. This predicted trend is not correct, as both the discharge voltage and capacity are expected to decrease at higher current densities. It is known that zero-dimensional models fail to predict the right trend for C-rate as mass transfer phenomena are not included in these models. As the C-rate increases, there is a predicted increase in overpotential, diffusion limitations, and a loss in voltage efficiency. Conversely, as the time needed for reactions reduces, there is a reduce in sulfur and active material utilization [46]. Due to the simplification of the diffusion effects in the 0-dimensional model, the stated effects are not observable.

Yet, the capacity difference between cycle 1 and cycle 2 is the highest at a C-rate of 0.7 and the lowest at a C-rate of 0.1, which shows that capacity fading increases with increasing C-rate, as expected from experimental trends. The voltage profiles indicate that, as the C-rate increases in all cycles, voltage values decrease, but discharge time increases. The lowest difference between high and low-voltage plateaus is at the lowest C-rate of 0.1.

Based on Figure 4.28, the capacity increases, and the voltage output decreases as the C-rate decreases during the charging processes. The voltage output begins to flatten when the C-rate reaches 0.1. The voltage output becomes flattens due to the prolonged charge time at a C-rate of 0.1, which in turn impacts the reaction kinetics.

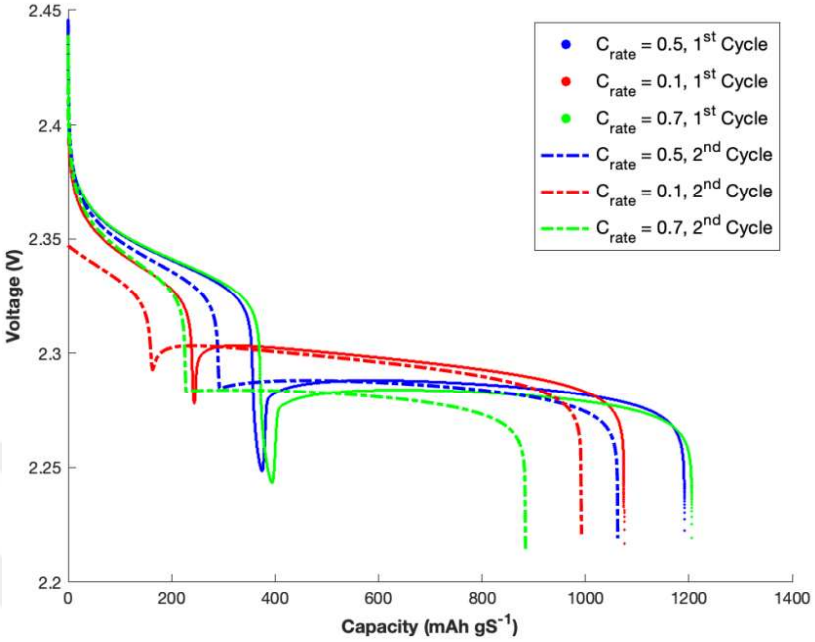

Figure 4.26. Simulated discharge voltages vs. capacities for various C-rates for 2 cycles.

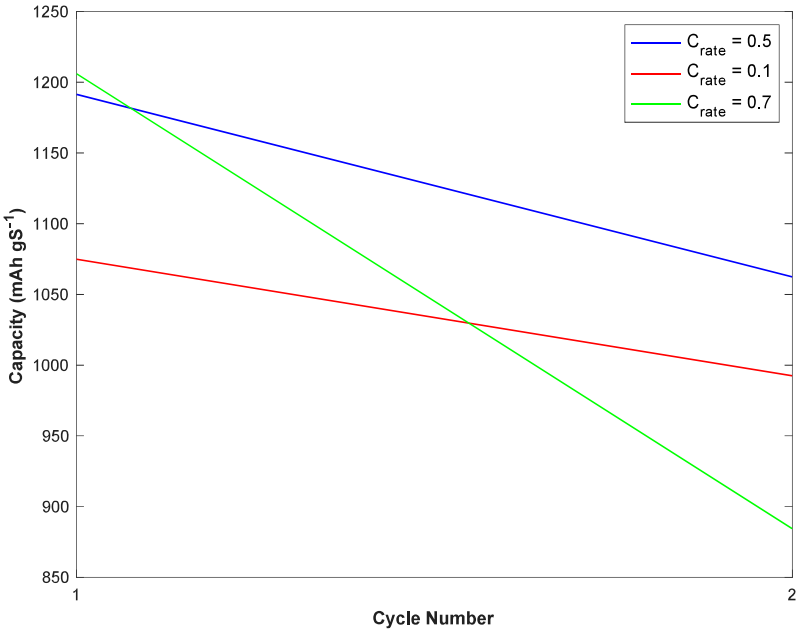

Figure 4.27. Simulated discharge capacities for 2 different cycles for various C-rates.

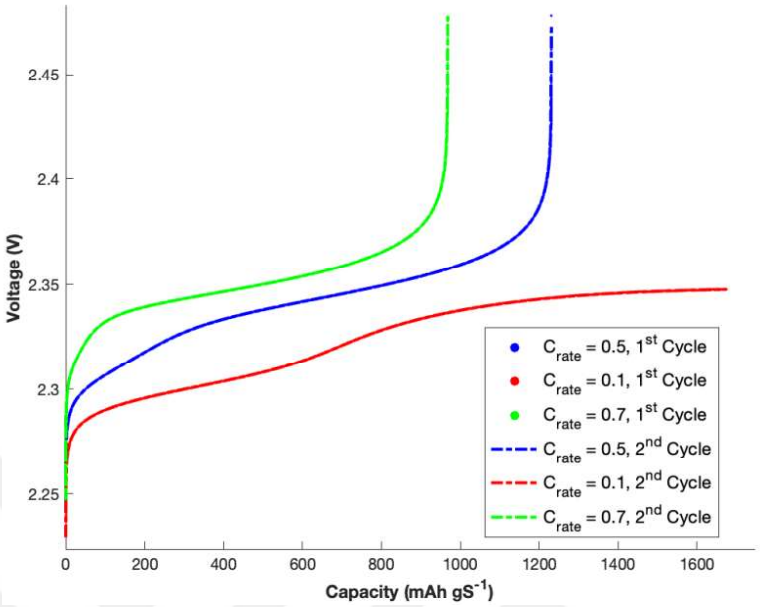

Figure 4.28. Simulated charge voltages vs. capacities for various C-rates for 2 cycles.

4.2. The Effect of Electrolyte-to-Sulfur (E/S) Ratio on Li-S Cell Performance

Electrolyte is one of the main constituents of the Li-S cell, with the greatest weight proportion, additionally performing a crucial role within the cell [47]. The presence of the electrolyte influences the rate at which reactions occur by impacting the shuttle mechanism and enabling polysulfide dissolution and precipitation reactions, as well as the transfer of ions between electrodes. Additionally, electrolyte properties impact the efficiency at which sulfur is utilized in the cathode [24]. This demonstrates that both the amount and the properties of the electrolyte have a direct impact on the performance of a Li-S cell.

The E/S ratio is altered in the model to assess the impact of electrolyte quantity on performance. The impact of the E/S ratio on cell performance is given in the graphs provided and analyzed below. Although the 0-dimensional model does not allow for direct measurement of the impact of electrolyte type and properties on cell capacity and discharge voltage, it can be implicitly measured through model parameters. The effect of electrolyte properties on cell

capacity, cycling performance, and discharge behaviors according to the change of parameters is further examined in the next section.

Based on Figure 4.29, the alteration in the E/S ratio does not have any discernible impact on the discharge capacity, either positive or negative. During the initial discharge, the capacity remains constant, independent of the electrolyte-to-sulfur ratio. Upon analyzing the discharge profile of the initial cycle, it is observed that the alteration in the E/S ratio only influences the voltage profile at the low voltage plateau, with no impact on the high voltage plateau. As the E/S ratio increases, the low voltage output decreases. Consequently, the highest voltage output is observed when the E/S ratio is 2.5 mL/g.

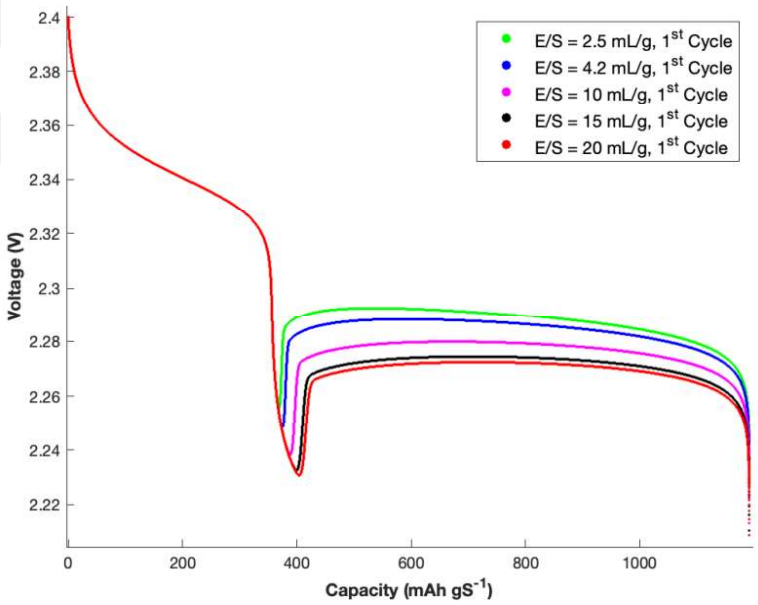

Figure 4.29. Simulated discharge voltages vs. capacities for various E/S ratios for 1st cycles.

The experimental data contradicts the notion that the capacity and high discharge plateau remain unaffected, as investigations have shown that the capacity increases with an increase in the E/S ratio [22,48]. This phenomenon occurs since as the electrolyte volume rises, there is a corresponding increase in the utilization of active materials and ameliorated reaction kinetics. The decrease in the low voltage plateau, resulting from the rise in the E/S ratio, contradicts the

expected low voltage profile. Consequently, this model fails to accurately forecast the impact of the E/S ratio on capacity and voltage profiles of the 1st cycle.

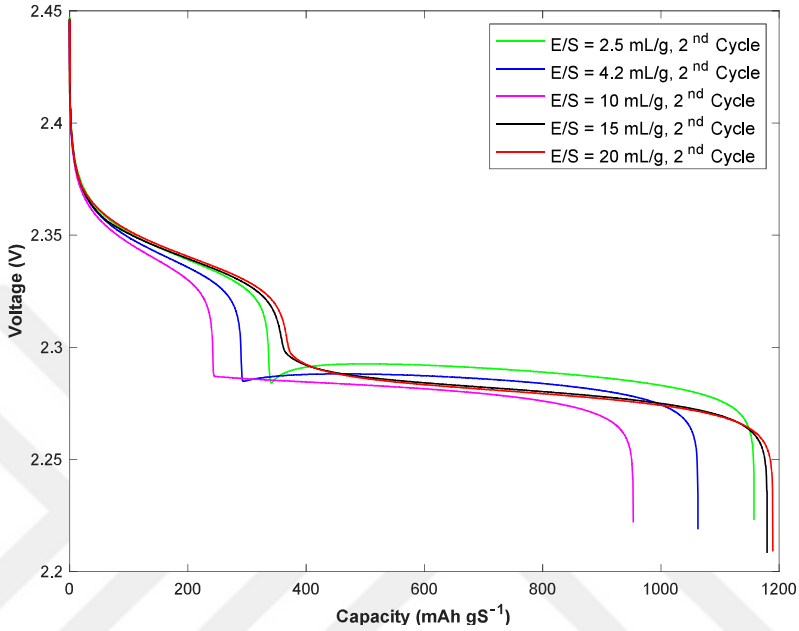

Figure 4.30. Simulated discharge voltages vs. capacities for various E/S ratios for 2nd cycles.

The effect of the change in the electrolyte-to-sulfur ratio on the change in capacity is evident in the discharge profile of the second cycle, as depicted in Figure 4.30. The capacity reaches its maximum when the E/S ratio is 20 mg/L. As the E/S ratio increases from 2.5 mg/L to 10 mg/L, there is a decrease in both cell capacity and voltage output. Nevertheless, when the E/S ratio exceeds 10 mg/L, the capacity of the cell increases in proportion to the increase in the E/S ratio. However, beyond a certain threshold, a further increase in the electrolyte volume do not result in a substantial change in capacity.

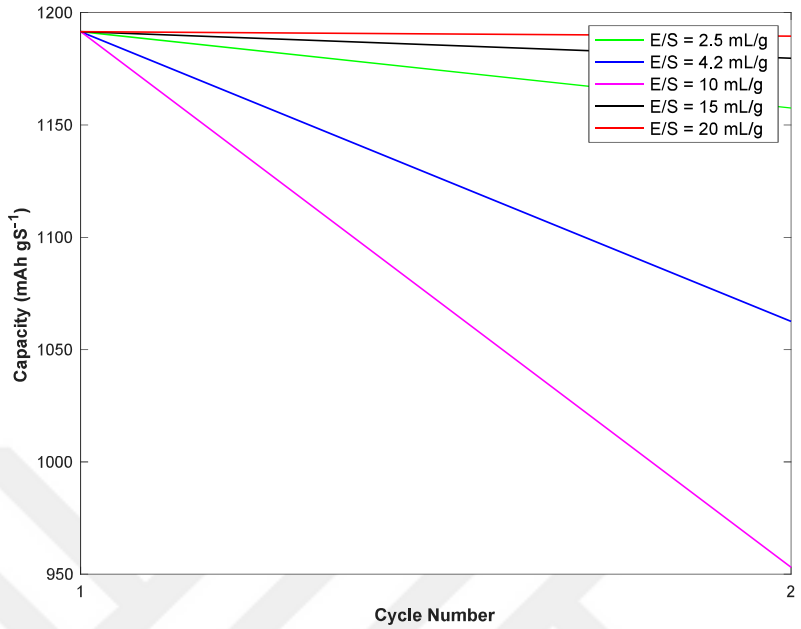

Figure 4.31. Simulated discharge capacities for 2 different cycles for various E/S ratios.

In all E/S ratios, the first discharge capacity remains constant, however it subsequently declines in the second cycle as illustrated in Figure 4.31. Capacity fading increases as the E/S ratio increases from 2.5 mg/L to 10 mg/L, but diminishes as the E/S ratio exceeds 10 mg/L. This demonstrates that as the volume of the electrolyte is increased, the decrease in capacity also increases up to a certain threshold. However, as the concentration exceeds the threshold of 10 mg/L, the capacity fading begins to diminish.

4.3. The Effect of Electrolyte Type and Properties on Li-S Cell Performance

Modifying the E/S ratios in the model clearly does not lead to the experimental trends. Similarly, the effect of electrolyte type and properties cannot be directly modeled using this model. One approach to capture the experimental trends on the effect of the E/S ratio and electrolyte type on the initial discharge capacity and cycling performance of a Li-S cell would be changing model parameters, shown in the previous section to be determinative of the capacity. For instance, an analysis of the initial voltage (V_0), high voltage standard potential

(E_H^0), and shuttle constant (k_S) can determine the implicit relationship between the capacity and the type and properties of the electrolyte. These parameters are included in the model since the electrolyte content affects cell performance by altering these parameters and the cell capacity is sensitive to changes in V_0, E_H^0, and k_S in the first cycle.

As the E_H^0 has a higher value, capacity of the cell and voltage output increases due to enhanced reaction kinetics. This occurs because an elevation in E_H^0 leads to a corresponding rise in the equilibrium potential, thus resulting in an augmentation of the Nernst potentials [1]. This results in a decrease in the surface overpotential, which is the main driving force for electrochemical processes. Considering that the electrolyte has a major effect on the electrochemical reactions and, as a result, the capacity of the cell, we can infer that the changes in E_H^0 implicitly indicate the impact of electrolyte type and properties on the cell performance. On the other hand, E_L^0 can demonstrate electrolyte properties indirectly by causing a gradual increase in the low voltage plateau as its value rises, as predicted.

Figures 4.5 and 4.6 demonstrate that as the initial voltage value decreases, the high voltage plateau decreases, as expected, while the low voltage plateau elongates and the overall cell capacity increases. It is anticipated that increasing the initial voltage will result in higher voltage and capacity of the cell, as it improves the use of active materials. The reduction in capacity can be related to the degradation of the electrolyte and electrode by accelerating the rates of side reactions as initial voltage increases. This degradation can subsequently lead to a drop in capacity during the first and subsequent cycles [46] The sensitivity analysis of the initial voltage parameter may provide information on the characteristics of the electrolyte.

It is anticipated that the capacity will decrease as the shuttle constant increases, since the effect of the shuttle mechanism will be intensified by the increase in the shuttle constant [49]. Similarly, as illustrated in Figure 4.8, an increase in k_s leads to a reduction in the high voltage output. The shuttle effect in Li-S batteries leads to self-discharge, decreased utilization of active material, and anode corrosion, resulting in a reduction in cell performance [50]. The shuttle constant is inversely proportional to the ionic conductivity and the solubility of lithium

polysulfides of electrolyte [51]. Therefore, it can be inferred that the impact of the electrolyte type and properties on cell performance can be indirectly assessed through analysis of the k_s parameter.

On the other hand, an increase in the value of precipitation constant only has a minor effect on the voltage output. Consequently, this shift can be disregarded, and it can be inferred that changing k_p does not accurately represent the effect of properties of the electrolyte.

The cathode area (a_r) is a critical factor that significantly impacts the performance of the cell [52]. In this model, any changes in a_r do not have an observable effect on capacity. Nevertheless, the active area of electrodes is directly related to the wettability of the electrolyte and the electrochemical reaction rate and stability effects of the electrolyte can be shown by changing active area since as a_r increases overall voltage output increases as well. This implicitly demonstrates the impact of electrolyte characteristics on the voltage output.

Moreover, as $i_{H,0}$ increases, the high voltage output also increases, while an increase in $i_{L,0}$ results in an increase in the low voltage output. However, both exchange current densities do not have an impact on the capacity of the cell in the first cycle. However, these factors affect the kinetics of the reaction. These characteristics do not directly indicate the impact of electrolyte properties on cell capacity. Nevertheless, they indirectly reflect this impact by changing the outputs of the high and low voltage plateaus. Overall, due to the limitations of this 0-dimensional model, it is not feasible to directly modify the electrolyte type and properties. Therefore, the cell's performance and voltage output were examined by altering the parameters, a process referred to as sensitivity analysis. This facilitated the identification of parameters that had an implicit impact.

4.4. Capturing the Experimental Trends on the Discharge Performance by Changing the Model Parameters

According to the experimental data obtained by Yuksel and Firtin et al. [52], shown in Tables 4.1, 4.3 and 4.5, the discharge capacity decreases by certain percentages in each cycle from the first to the tenth cycle. The data is obtained from experiments for the two electrolyte types at different electrolyte-to-sulfur ratios: 1 M LiTFSI containing sulfolane electrolyte (SL-LiTFSI) at an E/S ratio of 6 mL/g in Table 4.1., SL-LiTFSI at an E/S ratio of 9 mL/g in Table 4.3, and 1 M LiTF containing triglyme electrolyte (G3-LiTF) at an E/S ratio of 6 mL/g in Table 4.5.

As discussed in the previous sections, the capacity decrease after the second cycle cannot be predicted by this model. In this part, the discharge capacity drop percentage in each cycle calculated from the experimental data is tried to be captured by the model by changing k_s or E_H^0 for each cycle since our previous results indicate that the predicted discharge capacities are highly sensitive to these parameters.

Table 4.1. Experimental Discharge Capacities and Decrease Rates of the 1st, 2nd and 10th Cycles for the SL-LiTFSI Electrolyte at an E/S Ratio of 6 mL/g.

Cycle Number	**Discharge Capacity (mAh gS^{-1})**	**Decrease Rate of Capacity (%)**
1	977.75	-
2	851.026	13.0
10	711.371	16.4

Initially, the discharge capacity decrease percentage of SL-LiTFSI at an E/S ratio of 6 mL/g in Table 4.1 is obtained by simulating the model at a C-rate of 0.5 and the k_s values providing this acquisition are presented in Table 4.2. When the E/S ratio changes, only the electrolyte volume is altered in the model while the mass of the sulfur is kept constant. Then, to be able to predict the capacity decreases in Table 4.3, an E/S ratio of 9 mL/g is used in the simulation and

the shuttle constant values providing the same discharge capacity reduction percentage as the experiments are obtained and presented in Table 4.4.

Table 4.2. Simulated Discharge Capacities, Decrease Rates and Precipitation Constants (k_s) of the 1st, 2nd and 10th Cycles for the Simulation at an E/S Ratio of 6 mL/g.

Cycle Number	Discharge Capacity (mAh gS^{-1})	Decrease Rate of Capacity (%)	Shuttle constant (k_s)
1	1191.58	-	0.000200
2	1037.33	13.0	0.001520
10	866.800	16.4	0.028000

Table 4.3. Experimental Discharge Capacities and Decrease Rates of the 1st, 2nd and 10th Cycles for the SL-LiTFSI Electrolyte at an E/S Ratio of 9 mL/g.

Cycle Number	Discharge Capacity (mAh gS^{-1})	Decrease Rate of Capacity (%)
1	1022.21	-
2	948.981	7.16
10	826.020	13.0

Table 4.4. Simulated Discharge Capacities, Decrease Rates and Precipitation Constants (k_s) of the 1st, 2nd and 10th Cycles for the Simulation at an E/S ratio of 9 mL/g.

Cycle Number	Discharge Capacity (mAh gS^{-1})	Decrease Rate of Capacity (%)	Shuttle constant (k_s)
1	1191.58	-	0.000200
2	1105.96	7.18	0.000700
10	962.420	13.0	0.003790

In the next experiment, which is shown in Table 4.5, the electrolyte is replaced with G3-LiTF and the E/S ratio is set at 6 mL/g. Thus, the E/S value is taken as 6 mL/g in the simulation as well. As the electrolyte type cannot be explicitly modified in the code, one of the factors that influences cell capacity in the sensitivity analysis is selected to demonstrate the implicit effect of changing the electrolyte. For this purpose, E_H^0 parameter is selected, and it is multiplied by 0.95. This implies that a different type of electrolyte is developed implicitly. The k_s values obtained from the simulations are presented in Table 4.6.

Table 4.5. Experimental Discharge Capacities and Decrease Rates of the 1st, 2nd and 10th Cycles for the G3-LiTF Electrolyte at an E/S Ratio of 6 mL/g.

Cycle Number	**Discharge Capacity (mAh gS^{-1})**	**Decrease Rate of Capacity (%)**
1	717.660	-
2	692.746	3.47
10	636.226	8.16

Table 4.6. Simulated Discharge Capacities, Decrease Rates and Precipitation Constants (k_s) of the 1st, 2nd and 10th Cycles for the Simulation at E_H^0*0.95 and an E/S ratio of 6 mL/g.

Cycle Number	**Discharge Capacity (mAh gS^{-1})**	**Decrease Rate of Capacity (%)**	**Shuttle constant (k_s)**
1	1069.79	-	0.0002000
2	1032.85	3.45	0.0002545
10	948.888	8.13	0.0004000

It is evident that in all three simulations, the discharge capacity decrease percentage of the experiments can be obtained by manipulating the shuttle constants in the 2nd and 10th cycles. Therefore, it is obvious that in all three scenarios, the experimental discharge capacity

decrease trend can be approximated by increasing the value of k_s as the number of cycles increases.

5. CONCLUSION

This study presents an electrochemical model of the Li-S cell predicting the impact of electrolyte design on performance using the 0-dimensional model by Marinescu et al. The model is evaluated by solving differential equations and discharge and charge processes were simulated in the Fortran program. In this way, the effect of electrolyte amount and properties on the cycle performance of the Li-S cell was examined individually for discharge and charge. The current was taken as positive for discharge, and it is assumed to be negative for charge process.

Initial conditions are set and solved for the first discharge. Subsequently, the program proceeds with the charge and discharge operations, utilizing its own variable values that change over time as new initial conditions. It is recognized that the initial two cycle behaviors and discharge/charge variables were distinct from each other. For the subsequent cycles, the results were the same with the previous cycles. Therefore, the analyses in the rest of the thesis were simulated only for the two-cycle process, and the effect of electrolyte amount and properties on cell performance could be examined over the first two cycles.

The C-rate was taken as 0.5 C first, but this value was changed to examine the cell behavior as a function of the C-rate. Model predictions demonstrate that the discharge capacity of the battery increases proportionally with increasing C-rate. Nevertheless, this outcome is inaccurate as both the discharge voltage and capacity are anticipated to diminish at elevated current densities. The model cannot predict the effect of the C-rate on the cell capacity.

The model examined the impact of varying E/S ratios on discharge and charge voltage outputs and capacity over cycles by simply altering the electrolyte volume. The E/S ratio has no impact on the capacity during the first discharge. Moreover, increasing the E/S ratio only leads to a reduction in the low voltage output. This indicates that the model is incapable of quantifying the impact of electrolyte volume on discharge capacity and voltage. The rate of capacity loss

over the cycles increases when the E/S ratio increases up to 10 mg/L, but decreases beyond this value, contrary to expectations.

Modifications were made to the model parameters to assess the impact of changes in the electrolyte type and characteristics on the voltage behavior and capacity of the model. The sensitivity analysis allowed for the implicit investigation of the impact of the electrolyte type and characteristics on the cell performance. Based on this investigation, it was concluded that the voltage output and cell capacity were sensitive to variations in the parameters V_0, E_H^0, $i_{H,0}$, $i_{L,0}$, a_r and k_S. As E_H^0 increases and V_0 and k_S diminishes, the capacity of the cell increases. Increasing the values of E_H^0, V_0, and $i_{H,0}$, leads to a rise in the high voltage plateau output. Similarly, increasing $i_{L,0}$ results in an increase in the low voltage plateau output. These outcomes are in line with expectations. As the value of k_s increases, the voltage output decreases, whereas an increase in a_r leads to an overall increase in voltage output, as expected. Nevertheless, the impact of k_p on cell performance and cycles remains undetectable, and the model lacks the ability to determine its effect. Given that these parameters have an impact on variables that can be modified through electrolyte properties, such as reaction kinetics, active material utilization, side reaction rate, anode corrosion, and ionic conductivity, it is feasible to identify the electrolyte properties that enhance cell performance by analyzing model parameters.

To conclude, experimental discharge and charge behaviors cannot be obtained solely by changing the E/S ratio or the electrolyte type and properties in the model. One possible approach to capture the experimental trends on the change of the discharge capacity and voltage with changing E/S ratio and electrolyte characteristics might be varying the k_s values at each cycle. Therefore, to obtain the experimental decrease in the discharge capacity for the 2nd and the 10th cycles, k_s parameter is changed for each cycle in the simulations. Thus, the discharge capacity decrease percentages in the experiments are achieved by increasing the value of k_s parameter in simulations.

In future studies, new methods can be developed to estimate how much the k_s parameter should change for discharge and charge at each cycle and to define the changes in this parameter

depending on the cycle number and the results closer to experimental data can be obtained. For this purpose, machine learning methods can be implemented by using various experimental data. Therefore, a more accurate estimation of cell performance may be achieved by considering the impact of the electrolyte type, properties, and the E/S ratio.

REFERENCES

1. Marinescu, M., T. Zhang, and G.J. Offer, "A Zero Dimensional Model of Lithium-Sulfur Batteries During Charge and Discharge", *Physical Chemistry Chemical Physics*, Vol. 18, No. 1, pp. 584–593, 2016.

2. Liu, Y., Zhang, R., Wang, J., and Wang, Y, "Current and Future Lithium-ion Battery Manufacturing" , *IScience*, Vol. 24, No. 4, 2021.

3. Lupi, C., M. Pasquali, and A. Dell'Era, "Nickel and Cobalt Recycling from Lithium-Ion Batteries by Electrochemical Processes", *Waste Management*, Vol. 25, No. 2, pp. 215–220, 2005.

4. Bozich, J., M. Hang, R. Hamers, and R. Klaper, "Core Chemistry Influences the Toxicity of Multicomponent Metal Oxide Nanomaterials, Lithium Nickel Manganese Cobalt Oxide, and Lithium Cobalt Oxide to Daphnia Magna", *Environmental Toxicology and Chemistry*, Vol. 36, No. 9, pp. 2493–2502, 2017.

5. Li, M., C. Wang, Z. Chen, K. Xu, and J. Lu, "New Concepts in Electrolytes", *Chemical Reviews*, Vol. 120, No. 14, pp. 6783-6819, 2020.

6. Kolosnitsyn, V.S., E. V. Karaseva, E. V. Kuzmina, and A.L. Ivanov, "Reasons for the Effect of the Amount of Electrolyte on the Performance of Lithium–Sulfur Cells", *Russian Journal of Electrochemistry*, Vol. 52, No. 3, pp. 273–282, 2016.

7. Cairns, E.J., and P. Albertus, "Batteries for Electric and Hybrid-Electric Vehicles", *Annual Review of Chemical and Biomolecular Engineering*, Vol. 1, No.1, pp. 299–320, 2010.

8. Hofmann, A.F., D.N. Fronczek, and W.G. Bessler, "Mechanistic Modeling of Polysulfide Shuttle and Capacity Loss in Lithium-Sulfur Batteries", *Journal of Power Sources*, Vol. 259, pp. 300–310, 2014.

9. Manthiram, A., Y. Fu, S.H. Chung, C. Zu, and Y.S. Su, "Rechargeable Lithium-Sulfur Batteries", *Chemical Reviews*, Vol. 114, No. 23, pp. 11751-11787, 2014.

10. Kumaresan, K., Y. Mikhaylik, and R.E. White, "A Mathematical Model for a Lithium–Sulfur Cell", *Journal of the Electrochemical Society*, Vol. 155, No. 8, p. A576, 2008.

11. Mikhaylik, Y.V., and J.R. Akridge, "Polysulfide Shuttle Study in the Li/S Battery System", *Journal of the Electrochemical Society*, Vol. 151, No. 11, p. A1969, 2004.

12. Ren, Y.X., T.S. Zhao, M. Liu, P. Tan, and Y.K. Zeng, "Modeling of Lithium-Sulfur Batteries incorporating the Effect of Li_2S Precipitation", *Journal of Power Sources*, Vol. 336, pp. 115–125, 2016.

13. Chawla, N., N. Bharti, and S. Singh, "Recent Advances in Non-Flammable Electrolytes for Safer Lithium-ion Batteries", *Batteries*, Vol. 5, No. 1, p.19, 2019.

14. Ding, N., L. Zhou, C. Zhou, D. Geng, J. Yang, S.W. Chien, Z. Liu, M.F. Ng, A. Yu, T. S.A. Hor, M.B. Sullivan, and Y. Zong, "Building Better Lithium-Sulfur Batteries: from $LiNO_2$ to Solid Oxide Catalyst", *Scientific Reports*, Vol. 6, No. 1, p. 33154, 2016.

15. Zheng, M., Y. Chi, Q. Hu, H. Tang, X. Jiang, L. Zhang, S. Zhang, H. Pang, and Q. Xu, "Carbon Nanotube-Based Materials for Lithium-Sulfur Batteries", *Journal of Materials Chemistry A*, Vol. 7, No. 29, pp. 17204–17241, 2019.

16. Ghazi, Z.A., X. He, A.M. Khattak, N. A. Khan, B. Liang, A. Iqbal, J. Wang, H. Sin, L. Li, and Z. Tang, "MoS_2/Celgard Separator as Efficient Polysulfide Barrier for Long-Life Lithium–Sulfur Batteries", *Advanced Materials*, Vol. 29, No. 21, 2017.

17. Wang, G., Q. Jiao, Z. Zhang, et al., "Improved Electrochemical Behavior of Li–S Battery with Functional WS_2@PB–PPy–Modified Separator", *Chemical Engineering Journal Advances*, Vol. 8., No. 100145, 2021.

18. Scheers, J., S. Fantini, and P. Johansson, 2014, "A Review of Electrolytes for Lithium-Sulphur Batteries", *Journal of Power sources*, Vol. 255, pp. 204-218, 2014.

19. Eshetu, G.G, H. Zhang, X. Judez, H. Adenusi, M. Armand, S. Passerini, and E. Figgemeier, "Production of High-Energy Li-Ion Batteries Comprising Silicon-Containing Anodes and insertion-Type Cathodes", *Nature Communications*, Vol. 12, No. 1, p. 5459, 2021.

20. Michaelis, C., N. Erisen, D. Eroglu, and G.M. Koenig, "Electrochemical Performance and Modeling of Lithium-Sulfur Batteries with Varying Carbon to Sulfur Ratios", *international Journal of Energy Research*, Vol. 43, No. 2, pp. 874–883, 2019.

21. Bilal, H.M., and D. Eroglu, "Assessment of Li-S Battery Performance as a Function of Electrolyte-to-Sulfur Ratio", *Journal of the Electrochemical Society*, Vol. 168, No. 3, 2021.

22. Emerce, N.B., and D. Eroglu, "Effect of Electrolyte-to-Sulfur Ratio in the Cell on the Li-S Battery Performance", *Journal of the Electrochemical Society*, Vol. 166, No. 8, pp. A1490–A1500, 2019.

23. Evers, S., and L.F. Nazar, "New Approaches for High Energy Density Lithium-Sulfur Battery Cathodes", *Accounts of Chemical Research*, Vol. 46, No. 5, pp. 1135–1143, 2013.

24. Liu, Y., Y. Elias, J. Meng, D. Aurbach, R. Zou, D. Xia, and Q. Pang1, "Electrolyte Solutions Design for Lithium-Sulfur Batteries", *Joule,* Vol. 5, No.9, pp. 2323-2364, 2021.

25. Aurbach, D., E. Pollak, R. Elazari, G. Salitra, C.S. Kelley, and J. Affinito, "On the Surface Chemical Aspects of Very High Energy Density, Rechargeable Li–Sulfur Batteries", *Journal of the Electrochemical Society*, Vol. 156, No. 8, p. A694., 2009.

26. Zhao, X., G. Cheruvally, C. Kim, K.K. Cho, H.J. Ahn, K.W. Kim, and J.H. Ahn, "Lithium/Sulfur Secondary Batteries: A Review", Vol. 7, No. 2, pp. 97-114, 2016.

27. Shim, J., K.A. Striebel, and E.J. Cairns, "The Lithium/Sulfur Rechargeable Cell", *Journal of the Electrochemical Society*, Vol. 149, No. 10, p. A1321, 2002.

28. Choi, J.W., J.K. Kim, G. Cheruvally, J.H. Ahn, H.J. Ahn, and K.W. Kim, "Rechargeable Lithium/Sulfur Battery with Suitable Mixed Liquid Electrolytes", *Electrochimica Acta*, Vol. 52, No. 5, pp. 2075–2082, 2007.

29. Gao, J., M.A. Lowe, Y. Kiya, and H.D. Abruña, "Effects of Liquid Electrolytes on the Charge-Discharge Performance of Rechargeable Lithium/Sulfur Batteries: Electrochemical and in-Situ X-Ray Absorption Spectroscopic Studies", *Journal of Physical Chemistry C*, Vol. 115, No. 50, pp. 25132–25137, 2011.

30. Kobayashi, T., Y. Imade, D. Shishihara, et al., "All Solid-State Battery with Sulfur Electrode and Thio-LISICON Electrolyte", *Journal of Power Sources*, Vol. 182, No. 2, pp. 621–625, 2008.

31. Hayashi, A., T. Ohtomo, F. Mizuno, K. Tadanaga, and M. Tatsumisago, "All-Solid-State Li/S Batteries with Highly Conductive Glass-Ceramic Electrolytes", *Electrochemistry Communications*, Vol. 5, No. 8, pp. 701–705, 2003.

32. Jeong, S.S., Y.T. Lim, Y.J. Choi, et al., "Electrochemical Properties of Lithium Sulfur Cells Using PEO Polymer Electrolytes Prepared Under Three Different Mixing Conditions", *Journal of Power Sources*, Vol. 174, No. 2, pp. 745–750, 2007.

33. Ueno, K., J.W. Park, A. Yamazaki, et al., "Anionic Effects on Solvate Ionic Liquid Electrolytes in Rechargeable Lithium-Sulfur Batteries", *Journal of Physical Chemistry C*, Vol. 117, No. 40, pp. 20509–20516, 2013.

34. Cheng, L., L.A. Curtiss, K.R. Zavadil, A.A. Gewirth, Y. Shao, and K.G. Gallagher, "Sparingly Solvating Electrolytes for High Energy Density Lithium-Sulfur Batteries", *ACS Energy Letters*, Vol. 1, No. 3, pp. 503-509, 2016.

35. Weller, C., S. Thieme, P. Härtel, H. Althues, and S. Kaskel, "Intrinsic Shuttle Suppression in Lithium-Sulfur Batteries for Pouch Cell Application", *Journal of the Electrochemical Society*, Vol. 164, No. 14, pp. A3766–A3771, 2017.

36. Nakanishi, A., K. Ueno, D. Watanabe, et al., "Sulfolane-Based Highly Concentrated Electrolytes of Lithium Bis(Trifluoromethanesulfonyl)Amide: Ionic Transport, Li-ion Coordination, and Li-S Battery Performance", *Journal of Physical Chemistry C*, Vol. 123, No. 23, pp. 14229–14238, 2019.

37. Kilic, A., Ç. Odabaşı, R. Yildirim, and D. Eroglu, "Assessment of Critical Materials and Cell Design Factors for High Performance Lithium-Sulfur Batteries Using Machine Learning", *Chemical Engineering Journal*, Vol. 390, No. 124117, 2020.

38. Ghaznavi, M., and P. Chen, "Sensitivity Analysis of a Mathematical Model of Lithium-Sulfur Cells Part I: Applied Discharge Current and Cathode Conductivity", *Journal of Power Sources*, Vol. 257, pp. 394–401, 2014.

39. Newman, J., and K.E. Thomas-Alyea, *Electrochemical Systems*, Third Edition John Wiley & Sons, Berkeley, 2021.

40. He, G., S. Evers, X. Liang, M. Cuisinier, A. Garsuch, and L.F. Nazar, "Tailoring Porosity in Carbon Nanospheres for Lithium-Sulfur Battery Cathodes", *ACS Nano*, Vol. 7, No. 12, pp. 10920–10930, 2013.

41. Kim, H.M., J.Y. Hwang, A. Manthiram, and Y.K. Sun, "High-Performance Lithium-Sulfur Batteries with a Self-Assembled Multiwall Carbon Nanotube Interlayer and a Robust Electrode-Electrolyte Interface", *ACS Applied Materials and interfaces*, Vol. 8, No. 1, pp. 983–987, 2016.

42. Zhang, W., S. Li, A. Zhou, H. Song, Z. Cui, and L. Du, "Recent Advances and Perspectives in Lithium−sulfur Pouch Cells", *Molecules*, Vol. 26, No. 21, p. 6341, 2021.

43. Deng, C., Z. Wang, S. Wang, and J. Yu, "Inhibition of Polysulfide Diffusion in Lithium-Sulfur Batteries: Mechanism and Improvement Strategies", *Journal of Materials Chemistry A*, Vol. 7, No. 20, pp. 12381-12413, 2019.

44. Zech, C., P. Hönicke, Y. Kayser, et al., "Polysulfide Driven Degradation in Lithium-Sulfur Batteries During Cycling - Quantitative and High Time-Resolution Operando X-Ray Absorption Study for Dissolved Polysulfides Probed at Both Electrode Sides", *Journal of Materials Chemistry A*, Vol. 9, No. 16, pp. 10231–10239, 2021.

45. Gu, S., C. Sun, D. Xu, Y. Lu, J. Jin, and Z. Wen, "Recent Progress in Liquid Electrolyte-Based Li–S Batteries: Shuttle Problem and Solutions", *Electrochemical Energy Reviews*, Vol. 1, pp. 599-624, 2018.

46. Zhang, S., K. Ueno, K. Dokko, and M. Watanabe, "Recent Advances in Electrolytes for Lithium-Sulfur Batteries", *Advanced Energy Materials*, Vol. 5, No. 16, 2015.

47. Bhargav, A., J. He, A. Gupta, and A. Manthiram, "Lithium-Sulfur Batteries: Attaining the Critical Metrics", *Joule*, Vol. 4, No. 2, pp. 285-291, 2020.

48. Sun, K., A.K. Matarasso, R.M. Epler, et al., "Effect of Electrolyte on High Sulfur Loading Li-S Batteries", *Journal of the Electrochemical Society*, Vol. 165, No. 2, pp. A416–A423, 2018.

49. Diao, Y., K. Xie, S. Xiong, and X. Hong, “Shuttle Phenomenon - The Irreversible Oxidation Mechanism of Sulfur Active Material in Li-S Battery”, *Journal of Power Sources*, Vol. 235, pp. 181–186, 2013.

50. Song, M.K., E.J. Cairns, and Y. Zhang, “Lithium/Sulfur Batteries with High Specific Energy: Old Challenges and New Opportunities”, *Nanoscale*, Vol. 5, No. 6, pp. 2186–2204, 2013.

51. Donato, G. D., T. Ates, H. Adenusi, A. Varzi, M.A. Navarra, and S. Passerini, “Electrolyte Measures to Prevent Polysulfide Shuttle in Lithium-Sulfur Batteries”, *Batteries & Supercaps,* Vol. 5, No. 7, 2022.

52. Abdulkadiroglu, B., H. Bektas, and D. Eroglu, “How to Model the Cathode Area in Lithium-Sulfur Batteries?”, *ChemElectroChem*, Vol. 9, No. 4, 2022.

53. Yuksel, K., A. Firtin, E. Karaseva, E. Kuzmina, V. Kolosnitsyn, D. Eroglu D., “Effect of the Electrolyte Amount and Type on the Lithium-Sulfur Battery Performance”, under review.

APPENDIX A: FORTRAN CODE OF ZERO-DIMENSIONAL CYCLE MODEL

```
module cycle_common
   IMPLICIT DOUBLE PRECISION(a-h,o-z)
   COMMON A(12,12), B(12,12), Delc(12,903), D(12,25), G(12), X(12,12), Y(12,12)
   COMMON /SMALL/ SMA(13,13) , SMB(13,13), SMD(13,13), SMG(13), SME(13,13),
SMP(13,13), SMF(13)
   COMMON /var/ Cprev(12,903), DCDx(12), D2Cdx2(12)
   COMMON /MISC/ Delt, XX(1001), time, aa, bb, timecalca, timecalcb, timech, timedc
   COMMON /PARS/ TONdischarge, temp, abc, f1, f2, f3, f4, f5, f6, f7, f8, f9, f10, f11, f12,
g1, g2, g3, g4,&
   &g5, g6, g7, g8, g9, g10, g11, g12, stotdc, diff, ara, avg&
   &c1, c2, c3, c4, c5, c6, c7, c8, c9, c10, c11, c12, b1, b2, b3, b4, b5, b6, b7, b8, b9, b10, b11,
b12, var, vartwo
   COMMON/ints/ N, NJ, Numbertimesteps, ki
   END module cycle_common

module cycle_common_dc
   IMPLICIT DOUBLE PRECISION(a-h,o-z)
   PARAMETER (aMS8 = 32, ane=4, ans8=8, ans4=4, ans2=2, ans=1, rhos=2000,
anu=0.0114, fH=0.7296, &
   & fL=0.0665, sstar2=0.0001, akp=100, aks=0.0002, ams = 2.7, F = 96485, R = 8.3145, &
   &T = 298, ar=0.960 , c_rate = 0.5 ,aIcurrent = 1.675*ams*c_rate, aiH0=10, aiL0=5
,EH0=2.35,EL0=2.195)
   END module cycle_common_dc

module cycle_common_ch
   IMPLICIT DOUBLE PRECISION(a-h,o-z)
```

```
    PARAMETER (aMS8 = 32, ane=4, ans8=8, ans4=4, ans2=2, ans=1, rhos=2000,
anu=0.0114, fH=0.7296, &
    & fL=0.0665, sstar2=0.0001, akp=100, aks=0.0002, ams = 2.7, F = 96485, R = 8.3145, &
    &T = 298, ar=0.960 , c_rate = 0.5 ,aIcurrent = -1.675*ams*c_rate, aiH0=10, aiL0=5
,EH0=2.35,EL0=2.195)
    END module cycle_common_ch
program main
    use, intrinsic :: ieee_arithmetic
    use cycle_common
    use cycle_common_dc
    OPEN (71,FILE='cyc.0.5c.dc.cv.txt',STATUS='unknown')
    OPEN (75,FILE='cyc.0.5c.dc.capno.txt',STATUS='unknown')
    OPEN (73,FILE='cyc.0.5c.dc.tv.txt',STATUS='unknown')
    abc = ieee_value( abc, ieee_signaling_nan )
    abc = ieee_value( abc, ieee_quiet_nan )
    !print *, abc
    aa = 0
    bb = 0
    ki=0
    var = 0
    vartwo=0
    timecalca = 0 !discharge time
    timecalcb = 0 !charge time
    timech = 0
    N=12
    NJ=103
    Xmax=1
    H = Xmax/FLOAT(NJ-1)
    DO j = 1 , NJ
       XX(j) = H*FLOAT(j-1)
       if(j.eq.NJ) then
```

```
      XX(j)=Xmax
   end if
ENDDO
time=0.0
Delt=0.0
CALL INTIAL_CONDITION(H)
   DO j = 1 , NJ !to write initial conditions
      if (j.eq.3) then
         WRITE (71,913) (1675.0/(3600.0/c_rate))*(time),Cprev(8,j) !file id=71
         913 FORMAT (2(G12.6,1X)) !6 decimal points
         WRITE(73,912)time,XX(j),Cprev(1,j),Cprev(2,j),Cprev(3,j),&
           &Cprev(4,j),Cprev(5,j),Cprev(6,j),Cprev(7,j), Cprev(8,j),&
           &Cprev(9,j),Cprev(10,j),Cprev(11,j),Cprev(12,j)
           912 FORMAT (14(G12.6,1X))
      end if
   END DO
one: DO  ki=1,2
   Numbertimesteps= 72000
   TONdischarge = 7200
   Delt = TONdischarge/FLOAT(Numbertimesteps)
   two: DO it = 1 , Numbertimesteps
      CALL BOUND_VAL(H)
      time = time + Delt
      three: DO j = 1 , NJ
      if (time .gt. vartwo) then
      if (c8 - cprev(8,j) .gt. 0.01) then
      !stotdc = cprev(1,j) + cprev(2,j) + cprev(3,j) + cprev(4,j) + cprev(5,j)
         time = time - delt
         aa = time
         timecalca = aa-bb
```

```
            print *, 'cycle is', ki, 'timecalca is', timecalca, 'capacity is',
(1675.0/(3600.0/c_rate))*timecalca
            exit two
            end if
          end if

            f1=Cprev(1,j)
            f2=Cprev(2,j)
            f3=Cprev(3,j)
            f4=Cprev(4,j)
            f5=Cprev(5,j)
            f6=Cprev(6,j)
            f7=Cprev(7,j)
            f8=Cprev(8,j)
            f9=Cprev(9,j)
            f10=Cprev(10,j)
            f11=Cprev(11,j)
            f12=Cprev(12,j)

            if (f1.lt.0.0) then
            f1=0.0000000000000001
            cprev(1,j)=f1
            end if
            if (f2.lt.0.0) then
            f2=0.00001
            cprev(2,j)=f2
            end if
            if (f3.lt.0.0) then
            f3=0.00001
            cprev(3,j)=f3
            end if
```

```
if (f4.lt.0.0) then
f4=0.00001
cprev(4,j)=f4
end if
if (f5.lt.0.0) then
f5=0.0000000000000001
cprev(5,j)=f5
end if
if (f6.lt.0.0) then
f6=0.0
cprev(6,j)=f6
end if
if (f7.lt.0.0) then
f7=0.0
cprev(7,j)=f7
end if
if (f9.gt.0.0) then
f9=0.0
cprev(9,j)=f9
end if
if (f10.gt.0.0) then
f10=0.0
cprev(10,j)=f10
end if
if (f8.lt.0.0) then
f8=0.0000000000000001
cprev(8,j)=f8
end if
if (f11.lt.0.0) then
f11=0.0000000000000001
cprev(11,j)=f11
```

```
      end if
      if (f12.lt.0.0) then
      f12=0.0000000000000001
      cprev(12,j)=f12
      end if

      if (j.eq.3) then
         WRITE (71,911) (1675.0/(3600.0/c_rate))*(time-timech),Cprev(8,j)
         911 FORMAT (2(G12.6,1X))
         WRITE(73,910)time,XX(j),Cprev(1,j),Cprev(2,j),Cprev(3,j),&
           &Cprev(4,j),Cprev(5,j),Cprev(6,j),Cprev(7,j), Cprev(8,j),&
           &Cprev(9,j),Cprev(10,j),Cprev(11,j),Cprev(12,j)
           910 FORMAT (14(G12.6,1X))
           if (cprev(8,j) .NE. abc) then
              c1=cprev(1,j)
              c2=cprev(2,j)
              c3=cprev(3,j)
              c4=cprev(4,j)
              c5=cprev(5,j)
              c6=cprev(6,j)
              c7=cprev(7,j)
              c8=cprev(8,j)
              c9=cprev(9,j)
              c10=cprev(10,j)
              c11=cprev(11,j)
              c12=cprev(12,j)
           end if
      end if
   END DO three
END DO two
    DO j = 1 , NJ
```

```
        cprev(1,j) = c1
        cprev(2,j) = c2
        cprev(3,j) = c3
        cprev(4,j) = c4
        cprev(5,j) = c5
        cprev(6,j) = c6
        cprev(7,j) = c7
        cprev(8,j) = c8
        cprev(9,j) = c9
        cprev(10,j) = c10
        cprev(11,j) = c11
        cprev(12,j) = c12

        end do

        timedc = time

        WRITE (75, 915) (1675.0/(3600.0/c_rate))*(timecalca),ki
        915 FORMAT (2(G12.6,1X))
        var = time + 10

    CALL CHARGE
  END DO one
  END program main

SUBROUTINE INTIAL_CONDITION(H)
  use cycle_common
  use cycle_common_dc
  DO j = 1 , NJ
    Cprev(1,j) = ams*0.99
    Cprev(5,j) = 0.000001*ams
```

```
      Cprev(6,j) = aIcurrent
      Cprev(7,j) = aIcurrent - Cprev(6,j) ! or Cprev(7,j) = 0
      Cprev(8,j) = 2.4
      Cprev(9,j) = asinh(-Cprev(6,j)/(2*aiH0*ar))*((2*R*T)/(ane*F))
      Cprev(10,j) = asinh(-Cprev(7,j)/(2*aiL0*ar))/((2*R*T)/(ane*F))
      Cprev(11,j) = Cprev(8,j) - Cprev (9,j)
      Cprev(2,j) = SQRT( (fH*Cprev(1,j)) / exp(((cprev(11,j)-EH0)*4*F) / (R*T)) )
      Cprev(12,j) = Cprev(8,j) - Cprev (10,j)
      Cprev(4, j) = 0.00000001 !initial guess
      var_4: DO kl = 1, 100000 !!
            Cprev(3,j) = Cprev(4,j) + Cprev(5,j)
            temp = Cprev(4,j)
            Cprev(4,j) = SQRT ((fL * Cprev(2, j))  / (exp((Cprev(12, j) - EL0) * (4 * F) / (R *
T)) * Cprev(3, j)))
            if (ABS(temp - Cprev(4, j)) < 0.000000000000001) then
                  exit var_4
              end if
         ENDDO var_4
      Cprev(3,j) = Cprev(4,j)+Cprev(5,j)
      !IF ( j.EQ.1 ) THEN
      !    DO i= 1 , 12
      !       print*, Cprev(i,j)
      !       ENDDO
      !ENDIF
      ENDDO
      RETURN
   END

SUBROUTINE FILLMAT(H,J)
      use cycle_common
      use cycle_common_dc
```

```
!_____Boundary-condition at x=0
   IF ( J.EQ.1 ) THEN
      DO ic = 1 , N
         DCDx(ic) = (-3.0*Cprev(ic,J)+4.0*Cprev(ic,J+1)-Cprev(ic,J+2))/2.0/H
         ENDDO
         SME(1,1)=1+(aks*Delt)
         SME(1,6)=(ans8*aMS8*Delt)/(ane*F)
         SMF(1)=((-aMS8*Delt*ans8*Cprev(6,J))/(ane*F))-(Delt*Cprev(1,J)*aks)

         SME(2,1)=-(Delt*aks)
         SME(2,2)=1
         SME(2,6)=(-ans8*Delt*aMS8)/(ane*F)
         SME(2,7)=(ans4*aMS8*Delt)/(ane*F)
         SMF(2)=-
((Delt*ans4*aMS8*Cprev(7,J))/(ane*F))+((Delt*ans8*aMS8*Cprev(6,J))/(ane*F))+(aks*Delt
*Cprev(1,J))

         SME(3,3)=1
         SME(3,7)=(-Delt*ans2*aMS8)/(F*ane)
         SMF(3)=(1/(ane*F))*(Delt*Cprev(7,J)*ans2*aMS8)

         SME(4,4)=1+(akp*Cprev(5,J)*(Delt/(rhos*anu)))
         SME(4,5)=-((sstar2-Cprev(4,J))*Delt*akp)/(rhos*anu)
         SME(4,7)=-(1/(ane*F))*(2*Delt*ans*aMS8)
         SMF(4)=-(((Cprev(4,J)-
sstar2)*akp*Delt*Cprev(5,J))/(anu*rhos))+((2*Delt*ans*aMS8*Cprev(7,J))/(ane*F))

         SME(5,4)=-(1/(anu*rhos))*(Cprev(5,J)*akp*Delt)
         SME(5,5)=1-((Delt*akp*(Cprev(4,J)-sstar2))*(1/(anu*rhos)))
         SMF(5)=(1/(anu*rhos))*((Cprev(4,J)-sstar2)*Delt*akp*Cprev(5,J))
```

```
SME(6,6)=-1
SME(6,9)=2*(cosh(ane*F*Cprev(9,J)/(2*R*T)))*(-1/(2*R*T))*aiH0*ar*ane*F
SMF(6)=(sinh(ane*Cprev(9,J)/(2*R*T))*2*aiH0*ar*F)+Cprev(6,J)

SME(7,6)=1
SME(7,7)=1
SMF(7)=-Cprev(6,J)+aIcurrent-Cprev(7,J)

SME(8,8)=1
SME(8,10)=-1
SME(8,12)=-1
SMF(8)=+Cprev(10,J)+Cprev(12,J)-Cprev(8,J)

SME(9,8)=-1
SME(9,9)=1
SME(9,11)=1
SMF(9)=+Cprev(8,J)-Cprev(9,J)-Cprev(11,J)

SME(10,7)=-1
SME(10,10)=(-1/(R*T))*(cosh(ane*F*Cprev(10,J)/(2*R*T))*aiL0*ar*ane*F)
SMF(10)=(sinh(ane*F*Cprev(10,J)/(2*R*T))*2*aiL0*ar)+Cprev(7,J)

SME(11,1)=(-1/(4*F*Cprev(1,J)))*R*T
SME(11,2)=(1/(Cprev(2,J)*2*F))*R*T
SME(11,11)=1
SMF(11)=-((R*T*dlog((Cprev(2,J)*Cprev(2,J))/(fH*Cprev(1,J))))/(4*F))+EH0-
Cprev(11,J)

SME(12,2)=(-1/(Cprev(2,J)*4*F))*(R*T)
SME(12,3)=(1/(Cprev(3,J)*4*F))*(R*T)
SME(12,4)=(1/(Cprev(4,J)*2*F))*(R*T)
```

```
            SME(12,12)=1
            SMF(12)=-
Cprev(12,J)+EL0+(R*T*dlog(fL*Cprev(2,J)/((Cprev(4,J)*Cprev(4,J))*Cprev(3,J)))/(4*F))
            RETURN
            ENDIF
      !_____________________Boundary-condition at x=Xmax
         IF ( J.EQ.NJ ) THEN
            DO ic = 1 , N
               DCDx(ic) = (3.0*Cprev(ic,J)-4.0*Cprev(ic,J-1)+Cprev(ic,J-2))/2.0/H
               ENDDO
               SME(1,1)=1+(aks*Delt)
               SME(1,6)=(ans8*aMS8*Delt)/(ane*F)
               SMF(1)=((-aMS8*Delt*ans8*Cprev(6,J))/(ane*F))-(Delt*Cprev(1,J)*aks)

               SME(2,1)=-(Delt*aks)
               SME(2,2)=1
               SME(2,6)=(-ans8*Delt*aMS8)/(ane*F)
               SME(2,7)=(ans4*aMS8*Delt)/(ane*F)
               SMF(2)=-
((Delt*ans4*aMS8*Cprev(7,J))/(ane*F))+((Delt*ans8*aMS8*Cprev(6,J))/(ane*F))+(aks*Delt
*Cprev(1,J))

               SME(3,3)=1
               SME(3,7)=(-Delt*ans2*aMS8)/(F*ane)
               SMF(3)=(1/(ane*F))*(Delt*Cprev(7,J)*ans2*aMS8)

               SME(4,4)=1+(akp*Cprev(5,J)*(Delt/(rhos*anu)))
               SME(4,5)=-((sstar2-Cprev(4,J))*Delt*akp)/(rhos*anu)
               SME(4,7)=-(1/(ane*F))*(2*Delt*ans*aMS8)
               SMF(4)=-(((Cprev(4,J)-
sstar2)*akp*Delt*Cprev(5,J))/(anu*rhos))+((2*Delt*ans*aMS8*Cprev(7,J))/(ane*F))
```

```
SME(5,4)=-(1/(anu*rhos))*(Cprev(5,J)*akp*Delt)
SME(5,5)=1-((Delt*akp*(Cprev(4,J)-sstar2))*(1/(anu*rhos)))
SMF(5)=(1/(anu*rhos))*((Cprev(4,J)-sstar2)*Delt*akp*Cprev(5,J))

SME(6,6)=-1
SME(6,9)=2*(cosh(ane*F*Cprev(9,J)/(2*R*T)))*(-1/(2*R*T))*aiH0*ar*ane*F
SMF(6)=(sinh(ane*Cprev(9,J)/(2*R*T))*2*aiH0*ar*F)+Cprev(6,J)

SME(7,6)=1
SME(7,7)=1
SMF(7)=-Cprev(6,J)+aIcurrent-Cprev(7,J)

SME(8,8)=1
SME(8,10)=-1
SME(8,12)=-1
SMF(8)=+Cprev(10,J)+Cprev(12,J)-Cprev(8,J)

SME(9,8)=-1
SME(9,9)=1
SME(9,11)=1
SMF(9)=+Cprev(8,J)-Cprev(9,J)-Cprev(11,J)

SME(10,7)=-1
SME(10,10)=(-1/(R*T))*(cosh(ane*F*Cprev(10,J)/(2*R*T))*aiL0*ar*ane*F)
SMF(10)=(sinh(ane*F*Cprev(10,J)/(2*R*T))*2*aiL0*ar)+Cprev(7,J)

SME(11,1)=(-1/(4*F*Cprev(1,J)))*R*T
SME(11,2)=(1/(Cprev(2,J)*2*F))*R*T
SME(11,11)=1
```

```
            SMF(11)=-((R*T*dlog((Cprev(2,J)*Cprev(2,J))/(fH*Cprev(1,J))))/(4*F))+EH0-
Cprev(11,J)

            SME(12,2)=(-1/(Cprev(2,J)*4*F))*(R*T)
            SME(12,3)=(1/(Cprev(3,J)*4*F))*(R*T)
            SME(12,4)=(1/(Cprev(4,J)*2*F))*(R*T)
            SME(12,12)=1
            SMF(12)=-
Cprev(12,J)+EL0+(R*T*dlog(fL*Cprev(2,J)/((Cprev(4,J)*Cprev(4,J))*Cprev(3,J)))/(4*F))
            RETURN
            ENDIF
      !_____Governing Equations
         DO ic = 1 , N
            DCDx(ic) = (Cprev(ic,J+1)-Cprev(ic,J-1))/2.D0/H
            D2Cdx2(ic) = (Cprev(ic,J+1)-2.0*Cprev(ic,J)+Cprev(ic,J-1))/H**2
            ENDDO
         SMD(1,1)=1+(aks*Delt)
         SMD(1,6)=(ans8*aMS8*Delt)/(ane*F)
         SMG(1)=((-aMS8*Delt*ans8*Cprev(6,J))/(ane*F))-(Delt*Cprev(1,J)*aks)

         SMD(2,1)=-(Delt*aks)
         SMD(2,2)=1
         SMD(2,6)=(-ans8*Delt*aMS8)/(ane*F)
         SMD(2,7)=(ans4*aMS8*Delt)/(ane*F)
         SMG(2)=-
((Delt*ans4*aMS8*Cprev(7,J))/(ane*F))+((Delt*ans8*aMS8*Cprev(6,J))/(ane*F))+(aks*Delt
*Cprev(1,J))

         SMD(3,3)=1
         SMD(3,7)=(-Delt*ans2*aMS8)/(F*ane)
         SMG(3)=(1/(ane*F))*(Delt*Cprev(7,J)*ans2*aMS8)
```

```
SMD(4,4)=1+(akp*Cprev(5,J)*(Delt/(rhos*anu)))
SMD(4,5)=-((sstar2-Cprev(4,J))*Delt*akp)/(rhos*anu)
SMD(4,7)=-(1/(ane*F))*(2*Delt*ans*aMS8)
SMG(4)=-(((Cprev(4,J)-
sstar2)*akp*Delt*Cprev(5,J))/(anu*rhos))+((2*Delt*ans*aMS8*Cprev(7,J))/(ane*F))

SMD(5,4)=-(1/(anu*rhos))*(Cprev(5,J)*akp*Delt)
SMD(5,5)=1-((Delt*akp*(Cprev(4,J)-sstar2))*(1/(anu*rhos)))
SMG(5)=(1/(anu*rhos))*((Cprev(4,J)-sstar2)*Delt*akp*Cprev(5,J))

SMD(6,6)=-1
SMD(6,9)=2*(cosh(ane*F*Cprev(9,J)/(2*R*T)))*(-1/(2*R*T))*aiH0*ar*ane*F
SMG(6)=(sinh(ane*Cprev(9,J)/(2*R*T))*2*aiH0*ar*F)+Cprev(6,J)

SMD(7,6)=1
SMD(7,7)=1
SMG(7)=-Cprev(6,J)+aIcurrent-Cprev(7,J)

SMD(8,8)=1
SMD(8,10)=-1
SMD(8,12)=-1
SMG(8)=+Cprev(10,J)+Cprev(12,J)-Cprev(8,J)

SMD(9,8)=-1
SMD(9,9)=1
SMD(9,11)=1
SMG(9)=+Cprev(8,J)-Cprev(9,J)-Cprev(11,J)

SMD(10,7)=-1
SMD(10,10)=(-1/(R*T))*(cosh(ane*F*Cprev(10,J)/(2*R*T))*aiL0*ar*ane*F)
```

```
        SMG(10)=(sinh(ane*F*Cprev(10,J)/(2*R*T))*2*aiL0*ar)+Cprev(7,J)

        SMD(11,1)=(-1/(4*F*Cprev(1,J)))*R*T
        SMD(11,2)=(1/(Cprev(2,J)*2*F))*R*T
        SMD(11,11)=1
        SMG(11)=-((R*T*dlog((Cprev(2,J)*Cprev(2,J))/(fH*Cprev(1,J))))/(4*F))+EH0-
Cprev(11,J)

        SMD(12,2)=(-1/(Cprev(2,J)*4*F))*(R*T)
        SMD(12,3)=(1/(Cprev(3,J)*4*F))*(R*T)
        SMD(12,4)=(1/(Cprev(4,J)*2*F))*(R*T)
        SMD(12,12)=1
        SMG(12)=-
Cprev(12,J)+EL0+(R*T*dlog(fL*Cprev(2,J)/((Cprev(4,J)*Cprev(4,J))*Cprev(3,J))))/(4*F)
    END

SUBROUTINE ABDGXY(H,J)
    use cycle_common
    use cycle_common_dc
    IF ( J.EQ.1 ) THEN
      DO ii = 1 , N
        DO kk = 1 , N
          B(ii,kk) = H*SME(ii,kk) - 1.5*SMP(ii,kk)
          D(ii,kk) = 2.0*SMP(ii,kk)
          X(ii,kk) = -0.5*SMP(ii,kk)
          ENDDO
        G(ii) = H*SMF(ii)
        ENDDO
      RETURN
      ENDIF
```

```
    IF ( J.EQ.NJ ) THEN
      DO ii = 1 , N
        DO kk = 1 , N
          B(ii,kk) = H*SME(ii,kk) + 1.5*SMP(ii,kk)
          A(ii,kk) = -2.0*SMP(ii,kk)
          Y(ii,kk) = 0.5*SMP(ii,kk)
          ENDDO
        G(ii) = H*SMF(ii)
        ENDDO
      RETURN
      ENDIF
    DO ii = 1 , N
        DO kk = 1 , N
        A(ii,kk) = SMA(ii,kk) - H/2.0*SMB(ii,kk)
        B(ii,kk) = -2.0*SMA(ii,kk) + H**2*SMD(ii,kk)
        D(ii,kk) = SMA(ii,kk) + H/2.0*SMB(ii,kk)
        ENDDO
      G(ii) = H**2*SMG(ii)
      ENDDO
    RETURN
    END

SUBROUTINE BOUND_VAL(H)
    use cycle_common
    use cycle_common_dc
    DO j = 1 , NJ
        DO ic = 1 , N
        DO kc = 1 , N
          SMA(ic,kc) = 0.0
          SMB(ic,kc) = 0.0
          SMD(ic,kc) = 0.0
```

```
            SMP(ic,kc) = 0.0
            SME(ic,kc) = 0.0
            ENDDO
         ENDDO
      CALL FILLMAT(H,j)
      CALL ABDGXY(H,j)
      CALL BAND(j)
      ENDDO
   ! DO j = 1 , N
   ! print*, Cprev(1,j) , Cprev(2,j) , Cprev(3,j) ,Cprev(4,j)
   ! ENDDO
   DO k = 1 , N
         DO j = 1 , NJ
         Cprev(k,j) = Cprev(k,j) + Delc(k,j)
         ENDDO
      ENDDO
      RETURN !
   END

SUBROUTINE MATINV(N,M,Determ)
      IMPLICIT DOUBLE PRECISION (a-h,o-z)
      INTEGER i , id , irow , j , jc , jcol , k , M , N , nn
      DIMENSION id(12)
      COMMON A(12,12) , B(12,12) , Delc(12,903) , D(12,25)
      Determ = 1.0
      DO i = 1 , N
         id(i) = 0
         ENDDO
      DO nn = 1 , N
         bmax = 1.1
         DO i = 1 , N
```

```
      IF ( id(i).EQ.0 ) THEN
         bnext = 0.0
         btry = 0.0
         DO j = 1 , N
            IF ( id(j).EQ.0 ) THEN
               IF ( DABS(B(i,j)).GT.bnext ) THEN
                  bnext = DABS(B(i,j))
                  IF ( bnext.GT.btry ) THEN
                     bnext = btry
                     btry = DABS(B(i,j))
                     jc = j
                     ENDIF
                  ENDIF
               ENDIF
            ENDDO
         IF ( bnext.LT.bmax*btry ) THEN
            bmax = bnext/btry
            irow = i
            jcol = jc
            ENDIF
         ENDIF
      ENDDO

   IF ( id(jc).EQ.0 ) THEN
      id(jcol) = 1
      IF ( jcol.NE.irow ) THEN
            DO j = 1 , N
               save = B(irow,j)
               B(irow,j) = B(jcol,j)
               B(jcol,j) = save
               ENDDO
```

```
                DO k = 1 , M
                  save = D(irow,k)
                  D(irow,k) = D(jcol,k)
                  D(jcol,k) = save
                  ENDDO
                ENDIF
              f = 1.0/B(jcol,jcol)
              DO j = 1 , N
                B(jcol,j) = B(jcol,j)*f
                ENDDO
              DO k = 1 , M
                D(jcol,k) = D(jcol,k)*f
                ENDDO
              DO i = 1 , N
                IF ( i.NE.jcol ) THEN
                  f = B(i,jcol)
                  DO j = 1 , N
                    B(i,j) = B(i,j) - f*B(jcol,j)
                    ENDDO
                  DO k = 1 , M
                    D(i,k) = D(i,k) - f*D(jcol,k)
                    ENDDO
                  ENDIF
                ENDDO
                ELSE
            Determ = 0.0
            RETURN
            ENDIF
          ENDDO
    END
SUBROUTINE BAND(J)
```

```
IMPLICIT DOUBLE PRECISION (a-h,o-z)
INTEGER i, j, jj, k, l, lpn, m, N, NJ, np1, Numbertimesteps
DIMENSION e(12,13,903)
COMMON A(12,12) , B(12,12) , Delc(12,903) , D(12,25) , G(12) , X(12,12) , &
& Y(12,12)
COMMON/ints/ n, NJ, Numbertimesteps, ki
SAVE e , np1
IF ( j.LT.2 ) THEN
np1 = N + 1
DO i = 1 , N
   D(i,2*N+1) = G(i)
   DO l = 1 , N
      lpn = l + N
      D(i,lpn) = X(i,l)
      ENDDO
   ENDDO
CALL MATINV(N,2*N+1,determ)
IF ( determ.EQ.0 ) PRINT 99001 , J
   DO k = 1 , N
      e(k,np1,1) = D(k,2*N+1)
      DO l = 1 , N
         e(k,l,1) = -D(k,l)
         lpn = l + N
         X(k,l) = -D(k,lpn)
         ENDDO
      ENDDO
   RETURN
   ELSEIF ( j.EQ.2 ) THEN
      DO i = 1 , N
         DO k = 1 , N
            DO l = 1 , N
```

```
                D(i,k) = D(i,k) + A(i,l)*X(l,k)
                ENDDO
              ENDDO
            ENDDO
   ENDIF
IF ( j.GE.NJ ) THEN
   DO i = 1 , N
      DO l = 1 , N
         G(i) = G(i) - Y(i,l)*e(l,np1,J-2)
         DO m = 1 , N
            A(i,l) = A(i,l) + Y(i,m)*e(m,l,J-2)
         ENDDO
         ENDDO
      ENDDO
   ENDIF
DO i = 1 , N
   D(i,np1) = -G(i)
   DO l = 1 , N
      D(i,np1) = D(i,np1) + A(i,l)*e(l,np1,J-1)
      DO k = 1 , N
         B(i,k) = B(i,k) + A(i,l)*e(l,k,J-1)
         ENDDO
      ENDDO
   ENDDO
CALL MATINV(N,np1,determ)
IF ( determ.EQ.0 ) PRINT 99001 , J
DO k = 1 , N
   DO m = 1 , np1
      e(k,m,J) = -D(k,m)
      ENDDO
   ENDDO
```

```
      IF ( j.GE.NJ ) THEN
        DO k = 1 , N
          Delc(k,J) = e(k,np1,J)
          ENDDO
        DO jj = 2 , NJ
          m = NJ - jj + 1
          DO k = 1 , N
          Delc(k,m) = e(k,np1,m)
            DO l = 1 , N
              Delc(k,m) = Delc(k,m) + e(k,l,m)*Delc(l,m+1)
              ENDDO
            ENDDO
          ENDDO
        DO l = 1 , N
          DO k = 1 , N
            Delc(k,1) = Delc(k,1) + X(k,l)*Delc(l,3)
            ENDDO
          ENDDO
        ENDIF
      99001 FORMAT (' DETERM=0 AT J=',I4)
      END
    SUBROUTINE CHARGE
          use, intrinsic :: ieee_arithmetic
          use cycle_common
          use cycle_common_ch
        OPEN (58,FILE='cyc.0.5c.ch.cv.txt',STATUS='unknown')
        OPEN (60,FILE='cyc.0.5c.ch.capno.txt',STATUS='unknown')
        !OPEN (59,FILE='cyc.0.5c.ch.tv.txt',STATUS='unknown')
        abc = ieee_value( abc, ieee_signaling_nan )
        abc = ieee_value( abc, ieee_quiet_nan )
        N=12
```

```
      NJ=103
      Numbertimesteps = 72000
      Xmax=1
      TONcharge= 7200
      Delt = TONcharge/Numbertimesteps
      H = Xmax/FLOAT(NJ-1)
      DO j = 1 , NJ
         XX(j) = H*FLOAT(j-1)
         if(j.eq.NJ) then
            XX(j)=Xmax
         end if
      ENDDO

      four: DO it = 1 , Numbertimesteps
         CALL BOUND_VAL_CHARGE(H)
         time = time + Delt
         five: DO j = 1 , NJ
               if (time .gt. var) then
               if (cprev(8,j) - b8 .gt. 0.01) then
                  time = time - delt
                  bb = time
                  timecalcb = bb-aa
                  print *,'timecalcb is', timecalcb, 'capacity is',
(1675.0/(3600.0/c_rate))*timecalcb
                  exit four
                  end if
               end if
               g1=Cprev(1,j)
               g2=Cprev(2,j)
               g3=Cprev(3,j)
               g4=Cprev(4,j)
```

```
g5=Cprev(5,j)
g6=Cprev(6,j)
g7=Cprev(7,j)
g8=Cprev(8,j)
g9=Cprev(9,j)
g10=Cprev(10,j)
g11=Cprev(11,j)
g12=Cprev(12,j)
if (g1.lt.0.0) then
g1=0.0000000000000001
cprev(1,j)=g1
end if
if (g2.lt.0.0) then
g2=0.00001
cprev(2,j)=g2
end if
if (g3.lt.0.0) then
g3=0.00001
cprev(3,j)=g3
end if
if (g4.lt.0.0) then
g4=0.00001
cprev(4,j)=g4
end if
if (g5.lt.0.0) then
g5=0.0000000000000001
cprev(5,j)=g5
end if
if (g6.gt.0.0) then !ih, il
g6=0.0
cprev(6,j)=g6
```

```
      end if
      if (g7.gt.0.0) then
      g7=0.0
      cprev(7,j)=g7
      end if
      if (g9.lt.0.0) then !etah, etal
      g9=0.0
      cprev(9,j)=g9
      end if
      if (g10.lt.0.0) then
      g10=0.0
      cprev(10,j)=g10
      end if
      if (g8.lt.0.0) then
      g8=0.0000000000000001
      cprev(8,j)=g8
      end if
      if (g11.lt.0.0) then
      g11=0.0000000000000001
      cprev(11,j)=g11
      end if
      if (g12.lt.0.0) then
      g12=0.0000000000000001
      cprev(12,j)=g12
      end if

   if (j.eq.3) then
      WRITE (58,911) (1675.0/(3600.0/c_rate))*(time-timedc),Cprev(8,j)
         911 FORMAT (2(G12.6,1X))
      WRITE(73,910)time,XX(j),Cprev(1,j),Cprev(2,j),Cprev(3,j),&
         &Cprev(4,j),Cprev(5,j),Cprev(6,j),Cprev(7,j), Cprev(8,j),&
```

```
            &Cprev(9,j),Cprev(10,j),Cprev(11,j),Cprev(12,j)
            910 FORMAT (14(G12.6,1X))
            if (cprev(8,j) .NE. abc) then
               b1=cprev(1,j)
               b2=cprev(2,j)
               b3=cprev(3,j)
               b4=cprev(4,j)
               b5=cprev(5,j)
               b6=cprev(6,j)
               b7=cprev(7,j)
               b8=cprev(8,j)
               b9=cprev(9,j)
               b10=cprev(10,j)
               b11=cprev(11,j)
               b12=cprev(12,j)
            end if
         end if
      END DO five
   END DO four
      DO j = 1 , NJ
         cprev(1,j) = b1
         cprev(2,j) = b2
         cprev(3,j) = b3
         cprev(4,j) = b4
         cprev(5,j) = b5
         cprev(6,j) = b6
         cprev(7,j) = b7
         cprev(8,j) = b8
         cprev(9,j) = b9
         cprev(10,j) = b10
         cprev(11,j) = b11
```

```
            cprev(12,j) = b12
            end do

            WRITE (60, 915) (1675.0/(3600.0/c_rate))*(timecalcb),ki
            915 FORMAT (2(G12.6,1X))
            timech = time
            vartwo = time + 10
   RETURN
   END

SUBROUTINE FILLMAT_CHARGE(H,J)
         use cycle_common
         use cycle_common_ch
      !_____________________Boundary-condition at x=0
         IF ( J.EQ.1 ) THEN
            DO ic = 1 , N
               DCDx(ic) = (-3.0*Cprev(ic,J)+4.0*Cprev(ic,J+1)-Cprev(ic,J+2))/2.0/H
               ENDDO
               SME(1,1)=1+(aks*Delt)
               SME(1,6)=(ans8*aMS8*Delt)/(ane*F)
               SMF(1)=((-aMS8*Delt*ans8*Cprev(6,J))/(ane*F))-(Delt*Cprev(1,J)*aks)

               SME(2,1)=-(Delt*aks)
               SME(2,2)=1
               SME(2,6)=(-ans8*Delt*aMS8)/(ane*F)
               SME(2,7)=(ans4*aMS8*Delt)/(ane*F)
               SMF(2)=-
((Delt*ans4*aMS8*Cprev(7,J))/(ane*F))+((Delt*ans8*aMS8*Cprev(6,J))/(ane*F))+(aks*Delt
*Cprev(1,J))

               SME(3,3)=1
```

```
SME(3,7)=(-Delt*ans2*aMS8)/(F*ane)
SMF(3)=(1/(ane*F))*(Delt*Cprev(7,J)*ans2*aMS8)

SME(4,4)=1+(akp*Cprev(5,J)*(Delt/(rhos*anu)))
SME(4,5)=-((sstar2-Cprev(4,J))*Delt*akp)/(rhos*anu)
SME(4,7)=-(1/(ane*F))*(2*Delt*ans*aMS8)
SMF(4)=-(((Cprev(4,J)-
sstar2)*akp*Delt*Cprev(5,J))/(anu*rhos))+((2*Delt*ans*aMS8*Cprev(7,J))/(ane*F))

SME(5,4)=-(1/(anu*rhos))*(Cprev(5,J)*akp*Delt)
SME(5,5)=1-((Delt*akp*(Cprev(4,J)-sstar2))*(1/(anu*rhos)))
SMF(5)=(1/(anu*rhos))*((Cprev(4,J)-sstar2)*Delt*akp*Cprev(5,J))

SME(6,6)=-1
SME(6,9)=2*(cosh(ane*F*Cprev(9,J)/(2*R*T)))*(-1/(2*R*T))*aiH0*ar*ane*F
SMF(6)=(sinh(ane*Cprev(9,J)/(2*R*T))*2*aiH0*ar*F)+Cprev(6,J)

SME(7,6)=1
SME(7,7)=1
SMF(7)=-Cprev(6,J)+aIcurrent-Cprev(7,J)

SME(8,8)=1
SME(8,10)=-1
SME(8,12)=-1
SMF(8)=+Cprev(10,J)+Cprev(12,J)-Cprev(8,J)

SME(9,8)=-1
SME(9,9)=1
SME(9,11)=1
SMF(9)=+Cprev(8,J)-Cprev(9,J)-Cprev(11,J)
```

```
            SME(10,7)=-1
            SME(10,10)=(-1/(R*T))*(cosh(ane*F*Cprev(10,J)/(2*R*T))*aiL0*ar*ane*F)
            SMF(10)=(sinh(ane*F*Cprev(10,J)/(2*R*T))*2*aiL0*ar)+Cprev(7,J)

            SME(11,1)=(-1/(4*F*Cprev(1,J)))*R*T
            SME(11,2)=(1/(Cprev(2,J)*2*F))*R*T
            SME(11,11)=1
            SMF(11)=-((R*T*dlog((Cprev(2,J)*Cprev(2,J))/(fH*Cprev(1,J))))/(4*F))+EH0-
Cprev(11,J)

            SME(12,2)=(-1/(Cprev(2,J)*4*F))*(R*T)
            SME(12,3)=(1/(Cprev(3,J)*4*F))*(R*T)
            SME(12,4)=(1/(Cprev(4,J)*2*F))*(R*T)
            SME(12,12)=1
            SMF(12)=-
Cprev(12,J)+EL0+(R*T*dlog(fL*Cprev(2,J)/((Cprev(4,J)*Cprev(4,J))*Cprev(3,J)))/(4*F))
          RETURN
          ENDIF
    !_____________________Boundary-condition at x=Xmax
      IF ( J.EQ.NJ ) THEN
        DO ic = 1 , N
          DCDx(ic) = (3.0*Cprev(ic,J)-4.0*Cprev(ic,J-1)+Cprev(ic,J-2))/2.0/H
          ENDDO
          SME(1,1)=1+(aks*Delt)
          SME(1,6)=(ans8*aMS8*Delt)/(ane*F)
          SMF(1)=((-aMS8*Delt*ans8*Cprev(6,J))/(ane*F))-(Delt*Cprev(1,J)*aks)

          SME(2,1)=-(Delt*aks)
          SME(2,2)=1
          SME(2,6)=(-ans8*Delt*aMS8)/(ane*F)
          SME(2,7)=(ans4*aMS8*Delt)/(ane*F)
```

```
SMF(2)=-
((Delt*ans4*aMS8*Cprev(7,J))/(ane*F))+((Delt*ans8*aMS8*Cprev(6,J))/(ane*F))+(aks*Delt
*Cprev(1,J))

SME(3,3)=1
SME(3,7)=(-Delt*ans2*aMS8)/(F*ane)
SMF(3)=(1/(ane*F))*(Delt*Cprev(7,J)*ans2*aMS8)

SME(4,4)=1+(akp*Cprev(5,J)*(Delt/(rhos*anu)))
SME(4,5)=-((sstar2-Cprev(4,J))*Delt*akp)/(rhos*anu)
SME(4,7)=-(1/(ane*F))*(2*Delt*ans*aMS8)
SMF(4)=-(((Cprev(4,J)-
sstar2)*akp*Delt*Cprev(5,J))/(anu*rhos))+((2*Delt*ans*aMS8*Cprev(7,J))/(ane*F))

SME(5,4)=-(1/(anu*rhos))*(Cprev(5,J)*akp*Delt)
SME(5,5)=1-((Delt*akp*(Cprev(4,J)-sstar2))*(1/(anu*rhos)))
SMF(5)=(1/(anu*rhos))*((Cprev(4,J)-sstar2)*Delt*akp*Cprev(5,J))

SME(6,6)=-1
SME(6,9)=2*(cosh(ane*F*Cprev(9,J)/(2*R*T)))*(-1/(2*R*T))*aiH0*ar*ane*F
SMF(6)=(sinh(ane*Cprev(9,J)/(2*R*T))*2*aiH0*ar*F)+Cprev(6,J)

SME(7,6)=1
SME(7,7)=1
SMF(7)=-Cprev(6,J)+aIcurrent-Cprev(7,J)

SME(8,8)=1
SME(8,10)=-1
SME(8,12)=-1
SMF(8)=+Cprev(10,J)+Cprev(12,J)-Cprev(8,J)
```

```
            SME(9,8)=-1
            SME(9,9)=1
            SME(9,11)=1
            SMF(9)=+Cprev(8,J)-Cprev(9,J)-Cprev(11,J)

            SME(10,7)=-1
            SME(10,10)=(-1/(R*T))*(cosh(ane*F*Cprev(10,J)/(2*R*T))*aiL0*ar*ane*F)
            SMF(10)=(sinh(ane*F*Cprev(10,J)/(2*R*T))*2*aiL0*ar)+Cprev(7,J)

            SME(11,1)=(-1/(4*F*Cprev(1,J)))*R*T
            SME(11,2)=(1/(Cprev(2,J)*2*F))*R*T
            SME(11,11)=1
            SMF(11)=-((R*T*dlog((Cprev(2,J)*Cprev(2,J))/(fH*Cprev(1,J))))/(4*F))+EH0-
Cprev(11,J)

            SME(12,2)=(-1/(Cprev(2,J)*4*F))*(R*T)
            SME(12,3)=(1/(Cprev(3,J)*4*F))*(R*T)
            SME(12,4)=(1/(Cprev(4,J)*2*F))*(R*T)
            SME(12,12)=1
            SMF(12)=-
Cprev(12,J)+EL0+(R*T*dlog(fL*Cprev(2,J)/((Cprev(4,J)*Cprev(4,J))*Cprev(3,J)))/(4*F))
            RETURN
            ENDIF
      !_____________________Governing Equations
         DO ic = 1 , N
            DCDx(ic) = (Cprev(ic,J+1)-Cprev(ic,J-1))/2.D0/H
            D2Cdx2(ic) = (Cprev(ic,J+1)-2.0*Cprev(ic,J)+Cprev(ic,J-1))/H**2
            ENDDO
            SMD(1,1)=1+(aks*Delt)
            SMD(1,6)=(ans8*aMS8*Delt)/(ane*F)
            SMG(1)=((-aMS8*Delt*ans8*Cprev(6,J))/(ane*F))-(Delt*Cprev(1,J)*aks)
```

```
SMD(2,1)=-(Delt*aks)
SMD(2,2)=1
SMD(2,6)=(-ans8*Delt*aMS8)/(ane*F)
SMD(2,7)=(ans4*aMS8*Delt)/(ane*F)
SMG(2)=-
((Delt*ans4*aMS8*Cprev(7,J))/(ane*F))+((Delt*ans8*aMS8*Cprev(6,J))/(ane*F))+(aks*Delt
*Cprev(1,J))

SMD(3,3)=1
SMD(3,7)=(-Delt*ans2*aMS8)/(F*ane)
SMG(3)=(1/(ane*F))*(Delt*Cprev(7,J)*ans2*aMS8)

SMD(4,4)=1+(akp*Cprev(5,J)*(Delt/(rhos*anu)))
SMD(4,5)=-((sstar2-Cprev(4,J))*Delt*akp)/(rhos*anu)
SMD(4,7)=-(1/(ane*F))*(2*Delt*ans*aMS8)
SMG(4)=-(((Cprev(4,J)-
sstar2)*akp*Delt*Cprev(5,J))/(anu*rhos))+((2*Delt*ans*aMS8*Cprev(7,J))/(ane*F))

SMD(5,4)=-(1/(anu*rhos))*(Cprev(5,J)*akp*Delt)
SMD(5,5)=1-((Delt*akp*(Cprev(4,J)-sstar2))*(1/(anu*rhos)))
SMG(5)=(1/(anu*rhos))*((Cprev(4,J)-sstar2)*Delt*akp*Cprev(5,J))

SMD(6,6)=-1
SMD(6,9)=2*(cosh(ane*F*Cprev(9,J)/(2*R*T)))*(-1/(2*R*T))*aiH0*ar*ane*F
SMG(6)=(sinh(ane*Cprev(9,J)/(2*R*T))*2*aiH0*ar*F)+Cprev(6,J)

SMD(7,6)=1
SMD(7,7)=1
SMG(7)=-Cprev(6,J)+aIcurrent-Cprev(7,J)
```

```
            SMD(8,8)=1
            SMD(8,10)=-1
            SMD(8,12)=-1
            SMG(8)=+Cprev(10,J)+Cprev(12,J)-Cprev(8,J)

            SMD(9,8)=-1
            SMD(9,9)=1
            SMD(9,11)=1
            SMG(9)=+Cprev(8,J)-Cprev(9,J)-Cprev(11,J)

            SMD(10,7)=-1
            SMD(10,10)=(-1/(R*T))*(cosh(ane*F*Cprev(10,J)/(2*R*T))*aiL0*ar*ane*F)
            SMG(10)=(sinh(ane*F*Cprev(10,J)/(2*R*T))*2*aiL0*ar)+Cprev(7,J)

            SMD(11,1)=(-1/(4*F*Cprev(1,J)))*R*T
            SMD(11,2)=(1/(Cprev(2,J)*2*F))*R*T
            SMD(11,11)=1
            SMG(11)=-((R*T*dlog((Cprev(2,J)*Cprev(2,J))/(fH*Cprev(1,J))))/(4*F))+EH0-
Cprev(11,J)

            SMD(12,2)=(-1/(Cprev(2,J)*4*F))*(R*T)
            SMD(12,3)=(1/(Cprev(3,J)*4*F))*(R*T)
            SMD(12,4)=(1/(Cprev(4,J)*2*F))*(R*T)
            SMD(12,12)=1
            SMG(12)=-
Cprev(12,J)+EL0+(R*T*dlog(fL*Cprev(2,J)/((Cprev(4,J)*Cprev(4,J))*Cprev(3,J))))/(4*F)
          RETURN
    END

SUBROUTINE ABDGXY_CHARGE(H,J)
       use cycle_common
```

```
    use cycle_common_ch

IF ( J.EQ.1 ) THEN
    DO ii = 1 , N
        DO kk = 1 , N
            B(ii,kk) = H*SME(ii,kk) - 1.5*SMP(ii,kk)
            D(ii,kk) = 2.0*SMP(ii,kk)
            X(ii,kk) = -0.5*SMP(ii,kk)
            ENDDO
        G(ii) = H*SMF(ii)
        ENDDO
    RETURN
    ENDIF

IF ( J.EQ.NJ ) THEN
    DO ii = 1 , N
        DO kk = 1 , N
            B(ii,kk) = H*SME(ii,kk) + 1.5*SMP(ii,kk)
            A(ii,kk) = -2.0*SMP(ii,kk)
            Y(ii,kk) = 0.5*SMP(ii,kk)
            ENDDO
        G(ii) = H*SMF(ii)
        ENDDO
    RETURN
    ENDIF
DO ii = 1 , N
        DO kk = 1 , N
        A(ii,kk) = SMA(ii,kk) - H/2.0*SMB(ii,kk)
        B(ii,kk) = -2.0*SMA(ii,kk) + H**2*SMD(ii,kk)
        D(ii,kk) = SMA(ii,kk) + H/2.0*SMB(ii,kk)
        ENDDO
```

```
      G(ii) = H**2*SMG(ii)
      ENDDO
      RETURN
    END

SUBROUTINE BOUND_VAL_CHARGE(H)
    use cycle_common
    use cycle_common_ch

    DO j = 1 , NJ
          DO ic = 1 , N
          DO kc = 1 , N
             SMA(ic,kc) = 0.0
             SMB(ic,kc) = 0.0
             SMD(ic,kc) = 0.0
             SMP(ic,kc) = 0.0
             SME(ic,kc) = 0.0
             ENDDO
          ENDDO
       CALL FILLMAT_CHARGE(H,j)
       CALL ABDGXY_CHARGE(H,j)
       CALL BAND_CHARGE(j)
       ENDDO
    ! DO j = 1 , N
    ! print*, Cprev(1,j) , Cprev(2,j) , Cprev(3,j) ,Cprev(4,j)
    ! ENDDO
    DO k = 1 , N
          DO j = 1 , NJ
          Cprev(k,j) = Cprev(k,j) + Delc(k,j)
          ENDDO
       ENDDO
```

```
      RETURN
    END

SUBROUTINE MATINV_CHARGE(N,M,Determ)
      IMPLICIT NONE
      DOUBLE PRECISION A , B , bmax , bnext , btry , D , Delc , Determ ,&
      & f , save
      INTEGER i , id , irow , j , jc , jcol , k , M , N , nn
      DIMENSION id(12)
      COMMON A(12,12) , B(12,12) , Delc(12,903) , D(12,25)
      Determ = 1.0
      DO i = 1 , N
         id(i) = 0
         ENDDO
      DO nn = 1 , N
         bmax = 1.1
         DO i = 1 , N
            IF ( id(i).EQ.0 ) THEN
               bnext = 0.0
               btry = 0.0
               DO j = 1 , N
                  IF ( id(j).EQ.0 ) THEN
                     IF ( DABS(B(i,j)).GT.bnext ) THEN
                        bnext = DABS(B(i,j))
                        IF ( bnext.GT.btry ) THEN
                           bnext = btry
                           btry = DABS(B(i,j))
                           jc = j
                           ENDIF
                        ENDIF
                     ENDIF
```

```
            ENDDO
          IF ( bnext.LT.bmax*btry ) THEN
            bmax = bnext/btry
            irow = i
            jcol = jc
            ENDIF
          ENDIF
        ENDDO

      IF ( id(jc).EQ.0 ) THEN
        id(jcol) = 1
        IF ( jcol.NE.irow ) THEN
            DO j = 1 , N
              save = B(irow,j)
              B(irow,j) = B(jcol,j)
              B(jcol,j) = save
              ENDDO
            DO k = 1 , M
              save = D(irow,k)
              D(irow,k) = D(jcol,k)
              D(jcol,k) = save
              ENDDO
            ENDIF
          f = 1.0/B(jcol,jcol)
          DO j = 1 , N
            B(jcol,j) = B(jcol,j)*f
            ENDDO
          DO k = 1 , M
            D(jcol,k) = D(jcol,k)*f
            ENDDO
          DO i = 1 , N
```

```
                IF ( i.NE.jcol ) THEN
                  f = B(i,jcol)
                  DO j = 1 , N
                    B(i,j) = B(i,j) - f*B(jcol,j)
                    ENDDO
                  DO k = 1 , M
                    D(i,k) = D(i,k) - f*D(jcol,k)
                    ENDDO
                  ENDIF
              ENDDO
              ELSE
            Determ = 0.0
            RETURN
            ENDIF
          ENDDO
    END
SUBROUTINE BAND_CHARGE(J)
    IMPLICIT NONE
    DOUBLE PRECISION A, B, D, Delc, determ, e, G, X, Y
    INTEGER i, j, jj, k, l, lpn, m, N, NJ, np1, Numbertimesteps, ki
    DIMENSION e(12,13,903)
    COMMON A(12,12) , B(12,12) , Delc(12,903) , D(12,25) , G(12) , X(12,12) , &
    & Y(12,12)
    COMMON/ints/ n, NJ, Numbertimesteps, ki
    SAVE e , np1
    IF ( j.LT.2 ) THEN
    np1 = N + 1
    DO i = 1 , N
      D(i,2*N+1) = G(i)
      DO l = 1 , N
        lpn = l + N
```

```
      D(i,lpn) = X(i,l)
      ENDDO
   ENDDO
CALL MATINV_CHARGE(N,2*N+1,determ)
IF ( determ.EQ.0 ) PRINT 99001 , J
   DO k = 1 , N
      e(k,np1,1) = D(k,2*N+1)
      DO l = 1 , N
         e(k,l,1) = -D(k,l)
         lpn = l + N
         X(k,l) = -D(k,lpn)
         ENDDO
      ENDDO
   RETURN
   ELSEIF ( j.EQ.2 ) THEN
      DO i = 1 , N
         DO k = 1 , N
            DO l = 1 , N
               D(i,k) = D(i,k) + A(i,l)*X(l,k)
               ENDDO
            ENDDO
         ENDDO
   ENDIF
IF ( j.GE.NJ ) THEN
   DO i = 1 , N
      DO l = 1 , N
         G(i) = G(i) - Y(i,l)*e(l,np1,J-2)
         DO m = 1 , N
            A(i,l) = A(i,l) + Y(i,m)*e(m,l,J-2)
            ENDDO
         ENDDO
```

```
      ENDDO
   ENDIF
DO i = 1 , N
   D(i,np1) = -G(i)
   DO l = 1 , N
      D(i,np1) = D(i,np1) + A(i,l)*e(l,np1,J-1)
      DO k = 1 , N
         B(i,k) = B(i,k) + A(i,l)*e(l,k,J-1)
         ENDDO
      ENDDO
   ENDDO
CALL MATINV_CHARGE(N,np1,determ)
IF ( determ.EQ.0 ) PRINT 99001 , J
DO k = 1 , N
   DO m = 1 , np1
      e(k,m,J) = -D(k,m)
      ENDDO
   ENDDO
IF ( j.GE.NJ ) THEN
   DO k = 1 , N
      Delc(k,J) = e(k,np1,J)
      ENDDO
   DO jj = 2 , NJ
      m = NJ - jj + 1
      DO k = 1 , N
      Delc(k,m) = e(k,np1,m)
         DO l = 1 , N
            Delc(k,m) = Delc(k,m) + e(k,l,m)*Delc(l,m+1)
            ENDDO
         ENDDO
      ENDDO
```

```
    DO l = 1 , N
      DO k = 1 , N
        Delc(k,1) = Delc(k,1) + X(k,l)*Delc(l,3)
        ENDDO
      ENDDO
    ENDIF
99001 FORMAT (' DETERM=0 AT J=',I4)
RETURN
END
```

APPENDIX B: FORTRAN CODE OF ZERO-DIMENSIONAL DISCHARGE MODEL

```
module cycle_common
   IMPLICIT DOUBLE PRECISION(a-h,o-z)
   COMMON A(12,12), B(12,12), Delc(12,903), D(12,25), G(12), X(12,12), Y(12,12)
   COMMON /SMALL/ SMA(13,13) , SMB(13,13), SMD(13,13), SMG(13), SME(13,13),
SMP(13,13), SMF(13)
   COMMON /var/ Cprev(12,903), DCDx(12), D2Cdx2(12)
   COMMON /MISC/ Delt, XX(1001), time, aa, bb, timecalca, timecalcb, timech, timedc
   COMMON /PARS/ TONdischarge, temp, abc, f1, f2, f3, f4, f5, f6, f7, f8, f9, f10, f11, f12,
g1, g2, g3, g4,&
   &g5, g6, g7, g8, g9, g10, g11, g12, stotdc, diff, ara, avg&
   &c1, c2, c3, c4, c5, c6, c7, c8, c9, c10, c11, c12, b1, b2, b3, b4, b5, b6, b7, b8, b9, b10, b11,
b12, var, vartwo
   COMMON/ints/ N, NJ, Numbertimesteps, ki
   END module cycle_common
!962.89
module cycle_common_dc
   IMPLICIT DOUBLE PRECISION(a-h,o-z)
   PARAMETER (aMS8 = 32, ane=4, ans8=8, ans4=4, ans2=2, ans=1, rhos=2000,
anu=0.0243, fH=0.7296, &
   & fL=0.0665, sstar2=0.0001, akp=100, aks=5, ams = 2.7, F = 96485, R = 8.3145, &
   &T = 298, ar=0.960 , c_rate = 0.5 ,aIcurrent = 1.675*ams*c_rate, aiH0=10, aiL0=5
,EH0=2.35,EL0=2.195)
   END module cycle_common_dc


program main
```

```
use, intrinsic :: ieee_arithmetic
use cycle_common
use cycle_common_dc
OPEN (71,FILE='ES9.0.5c.dc.cv.txt',STATUS='unknown')
OPEN (75,FILE='ES9.0.5c.dc.capno.txt',STATUS='unknown')
OPEN (73,FILE='ES9.0.5c.dc.tv.txt',STATUS='unknown')
abc = ieee_value( abc, ieee_signaling_nan )
abc = ieee_value( abc, ieee_quiet_nan )
!print *, abc
aa = 0
bb = 0
ki=0
var = 0
vartwo=0
timecalca = 0 !discharge time
timecalcb = 0 !charge time
timech = 0
N=12
NJ=103
Xmax=1
H = Xmax/FLOAT(NJ-1)
DO j = 1 , NJ
   XX(j) = H*FLOAT(j-1)
   if(j.eq.NJ) then
      XX(j)=Xmax
   end if
ENDDO
time=0.0
Delt=0.0
CALL INTIAL_CONDITION(H)
   DO j = 1 , NJ !to write initial conditions
```

```
      if (j.eq.3) then
         WRITE (71,913) (1675.0/(3600.0/c_rate))*(time),Cprev(8,j) !file id=71
         913 FORMAT (2(G12.6,1X)) !6 decimal points
         WRITE(73,912)time,XX(j),Cprev(1,j),Cprev(2,j),Cprev(3,j),&
           &Cprev(4,j),Cprev(5,j),Cprev(6,j),Cprev(7,j), Cprev(8,j),&
           &Cprev(9,j),Cprev(10,j),Cprev(11,j),Cprev(12,j)
           912 FORMAT (14(G12.6,1X))
      end if
   END DO
one: DO  ki=1,1
   Numbertimesteps= 72000
   TONdischarge = 7200
   Delt = TONdischarge/FLOAT(Numbertimesteps)
   two: DO it = 1 , Numbertimesteps
      CALL BOUND_VAL(H)
      time = time + Delt
      three: DO j = 1 , NJ
      if (time .gt. vartwo) then
      if (c8 - cprev(8,j) .gt. 0.01) then
      !stotdc = cprev(1,j) + cprev(2,j) + cprev(3,j) + cprev(4,j) + cprev(5,j)
      !if (stotdc .gt. 2.69832000000) then
         !if (cprev(8,j) .lt. 2.22222222) then
         !if(cprev(1,j) .lt. 0.0 .or. cprev(2,j) .lt. 0.0 .or. cprev(3,j) .lt. 0.0 &
         !&.or. cprev(4,j) .lt. 0.0 )  then
         time = time - delt
         aa = time
         timecalca = aa-bb
         print *,  'ks is', aks,'capacity is', (1675.0/(3600.0/c_rate))*timecalca, 'timecalca is',&
         & timecalca, 'voltage', cprev(8,j)
         exit two
         end if
```

```
end if

   f1=Cprev(1,j)
   f2=Cprev(2,j)
   f3=Cprev(3,j)
   f4=Cprev(4,j)
   f5=Cprev(5,j)
   f6=Cprev(6,j)
   f7=Cprev(7,j)
   f8=Cprev(8,j)
   f9=Cprev(9,j)
   f10=Cprev(10,j)
   f11=Cprev(11,j)
   f12=Cprev(12,j)

   if (f1.lt.0.0) then
   f1=0.0000000000000001
   cprev(1,j)=f1
   end if
   if (f2.lt.0.0) then
   f2=0.00001
   cprev(2,j)=f2
   end if
   if (f3.lt.0.0) then
   f3=0.00001
   cprev(3,j)=f3
   end if
   if (f4.lt.0.0) then
   f4=0.00001
   cprev(4,j)=f4
   end if
```

```
if (f5.lt.0.0) then
f5=0.0000000000000001
cprev(5,j)=f5
end if
if (f6.lt.0.0) then
f6=0.0
cprev(6,j)=f6
end if
if (f7.lt.0.0) then
f7=0.0
cprev(7,j)=f7
end if
if (f9.gt.0.0) then
f9=0.0
cprev(9,j)=f9
end if
if (f10.gt.0.0) then
f10=0.0
cprev(10,j)=f10
end if
if (f8.lt.0.0) then
f8=0.0000000000000001
cprev(8,j)=f8
end if
if (f11.lt.0.0) then
f11=0.0000000000000001
cprev(11,j)=f11
end if
if (f12.lt.0.0) then
f12=0.0000000000000001
cprev(12,j)=f12
```

```
        end if

        if (j.eq.3) then
           WRITE (71,911) (1675.0/(3600.0/c_rate))*(time-timech),Cprev(8,j)
           911 FORMAT (2(G12.6,1X))
           WRITE(73,910)time,XX(j),Cprev(1,j),Cprev(2,j),Cprev(3,j),&
              &Cprev(4,j),Cprev(5,j),Cprev(6,j),Cprev(7,j), Cprev(8,j),&
              &Cprev(9,j),Cprev(10,j),Cprev(11,j),Cprev(12,j)
              910 FORMAT (14(G12.6,1X))
              if (cprev(8,j) .NE. abc) then
                 c1=cprev(1,j)
                 c2=cprev(2,j)
                 c3=cprev(3,j)
                 c4=cprev(4,j)
                 c5=cprev(5,j)
                 c6=cprev(6,j)
                 c7=cprev(7,j)
                 c8=cprev(8,j)
                 c9=cprev(9,j)
                 c10=cprev(10,j)
                 c11=cprev(11,j)
                 c12=cprev(12,j)
              end if
        end if
     END DO three
  END DO two
     DO j = 1 , NJ
     cprev(1,j) = c1
     cprev(2,j) = c2
     cprev(3,j) = c3
     cprev(4,j) = c4
```

```
        cprev(5,j) = c5
        cprev(6,j) = c6
        cprev(7,j) = c7
        cprev(8,j) = c8
        cprev(9,j) = c9
        cprev(10,j) = c10
        cprev(11,j) = c11
        cprev(12,j) = c12

        end do

        timedc = time

        WRITE (75, 915) (1675.0/(3600.0/c_rate))*(timecalca),ki
        915 FORMAT (2(G12.6,1X))

    END DO one
    END program main

SUBROUTINE INTIAL_CONDITION(H)
    use cycle_common
    use cycle_common_dc
    DO j = 1 , NJ
      Cprev(1,j) = ams*0.99
      Cprev(5,j) = 0.000001*ams
      Cprev(6,j) = aIcurrent
      Cprev(7,j) = aIcurrent - Cprev(6,j) ! or Cprev(7,j) = 0
      Cprev(8,j) = 2.4
      Cprev(9,j) = asinh(-Cprev(6,j)/(2*aiH0*ar))*((2*R*T)/(ane*F))
      Cprev(10,j) = asinh(-Cprev(7,j)/(2*aiL0*ar))/((2*R*T)/(ane*F))
      Cprev(11,j) = Cprev(8,j) - Cprev (9,j)
```

```
      Cprev(2,j) = SQRT( (fH*Cprev(1,j)) / exp(((cprev(11,j)-EH0)*4*F) / (R*T)) )
      Cprev(12,j) = Cprev(8,j) - Cprev (10,j)
      Cprev(4, j) = 0.00000001 !initial guess
      var_4: DO kl = 1, 100000 !!
            Cprev(3,j) = Cprev(4,j) + Cprev(5,j)
            temp = Cprev(4,j)
            Cprev(4,j) = SQRT ((fL * Cprev(2, j))  / (exp((Cprev(12, j) - EL0) * (4 * F) / (R *
T)) * Cprev(3, j)))
            if (ABS(temp - Cprev(4, j)) < 0.000000000000001) then
                  exit var_4
              end if
         ENDDO var_4
      Cprev(3,j) = Cprev(4,j)+Cprev(5,j)
      !IF ( j.EQ.1 ) THEN
      !    DO i= 1 , 12
      !       print*, Cprev(i,j)
      !       ENDDO
      !ENDIF
      ENDDO
      RETURN
   END

SUBROUTINE FILLMAT(H,J)
      use cycle_common
      use cycle_common_dc
      !_____________________Boundary-condition at x=0
        IF ( J.EQ.1 ) THEN
          DO ic = 1 , N
            DCDx(ic) = (-3.0*Cprev(ic,J)+4.0*Cprev(ic,J+1)-Cprev(ic,J+2))/2.0/H
            ENDDO
            SME(1,1)=1+(aks*Delt)
```

```
SME(1,6)=(ans8*aMS8*Delt)/(ane*F)
SMF(1)=((-aMS8*Delt*ans8*Cprev(6,J))/(ane*F))-(Delt*Cprev(1,J)*aks)

SME(2,1)=-(Delt*aks)
SME(2,2)=1
SME(2,6)=(-ans8*Delt*aMS8)/(ane*F)
SME(2,7)=(ans4*aMS8*Delt)/(ane*F)
SMF(2)=-
((Delt*ans4*aMS8*Cprev(7,J))/(ane*F))+((Delt*ans8*aMS8*Cprev(6,J))/(ane*F))+(aks*Delt
*Cprev(1,J))

SME(3,3)=1
SME(3,7)=(-Delt*ans2*aMS8)/(F*ane)
SMF(3)=(1/(ane*F))*(Delt*Cprev(7,J)*ans2*aMS8)

SME(4,4)=1+(akp*Cprev(5,J)*(Delt/(rhos*anu)))
SME(4,5)=-((sstar2-Cprev(4,J))*Delt*akp)/(rhos*anu)
SME(4,7)=-(1/(ane*F))*(2*Delt*ans*aMS8)
SMF(4)=-(((Cprev(4,J)-
sstar2)*akp*Delt*Cprev(5,J))/(anu*rhos))+((2*Delt*ans*aMS8*Cprev(7,J))/(ane*F))

SME(5,4)=-(1/(anu*rhos))*(Cprev(5,J)*akp*Delt)
SME(5,5)=1-((Delt*akp*(Cprev(4,J)-sstar2))*(1/(anu*rhos)))
SMF(5)=(1/(anu*rhos))*((Cprev(4,J)-sstar2)*Delt*akp*Cprev(5,J))

SME(6,6)=-1
SME(6,9)=2*(cosh(ane*F*Cprev(9,J)/(2*R*T)))*(-1/(2*R*T))*aiH0*ar*ane*F
SMF(6)=(sinh(ane*Cprev(9,J)/(2*R*T))*2*aiH0*ar*F)+Cprev(6,J)

SME(7,6)=1
SME(7,7)=1
```

```
            SMF(7)=-Cprev(6,J)+aIcurrent-Cprev(7,J)

            SME(8,8)=1
            SME(8,10)=-1
            SME(8,12)=-1
            SMF(8)=+Cprev(10,J)+Cprev(12,J)-Cprev(8,J)

            SME(9,8)=-1
            SME(9,9)=1
            SME(9,11)=1
            SMF(9)=+Cprev(8,J)-Cprev(9,J)-Cprev(11,J)

            SME(10,7)=-1
            SME(10,10)=(-1/(R*T))*(cosh(ane*F*Cprev(10,J)/(2*R*T))*aiL0*ar*ane*F)
            SMF(10)=(sinh(ane*F*Cprev(10,J)/(2*R*T))*2*aiL0*ar)+Cprev(7,J)

            SME(11,1)=(-1/(4*F*Cprev(1,J)))*R*T
            SME(11,2)=(1/(Cprev(2,J)*2*F))*R*T
            SME(11,11)=1
            SMF(11)=-((R*T*dlog((Cprev(2,J)*Cprev(2,J))/(fH*Cprev(1,J))))/(4*F))+EH0-
Cprev(11,J)

            SME(12,2)=(-1/(Cprev(2,J)*4*F))*(R*T)
            SME(12,3)=(1/(Cprev(3,J)*4*F))*(R*T)
            SME(12,4)=(1/(Cprev(4,J)*2*F))*(R*T)
            SME(12,12)=1
            SMF(12)=-
Cprev(12,J)+EL0+(R*T*dlog(fL*Cprev(2,J)/((Cprev(4,J)*Cprev(4,J))*Cprev(3,J)))/(4*F))
          RETURN
          ENDIF
     !_____Boundary-condition at x=Xmax
```

```
IF ( J.EQ.NJ ) THEN
   DO ic = 1 , N
      DCDx(ic) = (3.0*Cprev(ic,J)-4.0*Cprev(ic,J-1)+Cprev(ic,J-2))/2.0/H
      ENDDO
      SME(1,1)=1+(aks*Delt)
      SME(1,6)=(ans8*aMS8*Delt)/(ane*F)
      SMF(1)=((-aMS8*Delt*ans8*Cprev(6,J))/(ane*F))-(Delt*Cprev(1,J)*aks)

      SME(2,1)=-(Delt*aks)
      SME(2,2)=1
      SME(2,6)=(-ans8*Delt*aMS8)/(ane*F)
      SME(2,7)=(ans4*aMS8*Delt)/(ane*F)
      SMF(2)=-
((Delt*ans4*aMS8*Cprev(7,J))/(ane*F))+((Delt*ans8*aMS8*Cprev(6,J))/(ane*F))+(aks*Delt
*Cprev(1,J))

      SME(3,3)=1
      SME(3,7)=(-Delt*ans2*aMS8)/(F*ane)
      SMF(3)=(1/(ane*F))*(Delt*Cprev(7,J)*ans2*aMS8)

      SME(4,4)=1+(akp*Cprev(5,J)*(Delt/(rhos*anu)))
      SME(4,5)=-((sstar2-Cprev(4,J))*Delt*akp)/(rhos*anu)
      SME(4,7)=-(1/(ane*F))*(2*Delt*ans*aMS8)
      SMF(4)=-(((Cprev(4,J)-
sstar2)*akp*Delt*Cprev(5,J))/(anu*rhos))+((2*Delt*ans*aMS8*Cprev(7,J))/(ane*F))

      SME(5,4)=-(1/(anu*rhos))*(Cprev(5,J)*akp*Delt)
      SME(5,5)=1-((Delt*akp*(Cprev(4,J)-sstar2))*(1/(anu*rhos)))
      SMF(5)=(1/(anu*rhos))*((Cprev(4,J)-sstar2)*Delt*akp*Cprev(5,J))

      SME(6,6)=-1
```

SME(6,9)=2*(cosh(ane*F*Cprev(9,J)/(2*R*T)))*(-1/(2*R*T))*aiH0*ar*ane*F
SMF(6)=(sinh(ane*Cprev(9,J)/(2*R*T))*2*aiH0*ar*F)+Cprev(6,J)

SME(7,6)=1
SME(7,7)=1
SMF(7)=-Cprev(6,J)+aIcurrent-Cprev(7,J)

SME(8,8)=1
SME(8,10)=-1
SME(8,12)=-1
SMF(8)=+Cprev(10,J)+Cprev(12,J)-Cprev(8,J)

SME(9,8)=-1
SME(9,9)=1
SME(9,11)=1
SMF(9)=+Cprev(8,J)-Cprev(9,J)-Cprev(11,J)

SME(10,7)=-1
SME(10,10)=(-1/(R*T))*(cosh(ane*F*Cprev(10,J)/(2*R*T))*aiL0*ar*ane*F)
SMF(10)=(sinh(ane*F*Cprev(10,J)/(2*R*T))*2*aiL0*ar)+Cprev(7,J)

SME(11,1)=(-1/(4*F*Cprev(1,J)))*R*T
SME(11,2)=(1/(Cprev(2,J)*2*F))*R*T
SME(11,11)=1
SMF(11)=-((R*T*dlog((Cprev(2,J)*Cprev(2,J))/(fH*Cprev(1,J))))/(4*F))+EH0-Cprev(11,J)

SME(12,2)=(-1/(Cprev(2,J)*4*F))*(R*T)
SME(12,3)=(1/(Cprev(3,J)*4*F))*(R*T)
SME(12,4)=(1/(Cprev(4,J)*2*F))*(R*T)
SME(12,12)=1

```
            SMF(12)=-
Cprev(12,J)+EL0+(R*T*dlog(fL*Cprev(2,J)/((Cprev(4,J)*Cprev(4,J))*Cprev(3,J)))/(4*F))
            RETURN
            ENDIF
      !_____Governing Equations
            DO ic = 1 , N
            DCDx(ic) = (Cprev(ic,J+1)-Cprev(ic,J-1))/2.D0/H
            D2Cdx2(ic) = (Cprev(ic,J+1)-2.0*Cprev(ic,J)+Cprev(ic,J-1))/H**2
            ENDDO
            SMD(1,1)=1+(aks*Delt)
            SMD(1,6)=(ans8*aMS8*Delt)/(ane*F)
            SMG(1)=((-aMS8*Delt*ans8*Cprev(6,J))/(ane*F))-(Delt*Cprev(1,J)*aks)

            SMD(2,1)=-(Delt*aks)
            SMD(2,2)=1
            SMD(2,6)=(-ans8*Delt*aMS8)/(ane*F)
            SMD(2,7)=(ans4*aMS8*Delt)/(ane*F)
            SMG(2)=-
((Delt*ans4*aMS8*Cprev(7,J))/(ane*F))+((Delt*ans8*aMS8*Cprev(6,J))/(ane*F))+(aks*Delt
*Cprev(1,J))

            SMD(3,3)=1
            SMD(3,7)=(-Delt*ans2*aMS8)/(F*ane)
            SMG(3)=(1/(ane*F))*(Delt*Cprev(7,J)*ans2*aMS8)

            SMD(4,4)=1+(akp*Cprev(5,J)*(Delt/(rhos*anu)))
            SMD(4,5)=-((sstar2-Cprev(4,J))*Delt*akp)/(rhos*anu)
            SMD(4,7)=-(1/(ane*F))*(2*Delt*ans*aMS8)
            SMG(4)=-(((Cprev(4,J)-
sstar2)*akp*Delt*Cprev(5,J))/(anu*rhos))+((2*Delt*ans*aMS8*Cprev(7,J))/(ane*F))
```

```
SMD(5,4)=-(1/(anu*rhos))*(Cprev(5,J)*akp*Delt)
SMD(5,5)=1-((Delt*akp*(Cprev(4,J)-sstar2))*(1/(anu*rhos)))
SMG(5)=(1/(anu*rhos))*((Cprev(4,J)-sstar2)*Delt*akp*Cprev(5,J))

SMD(6,6)=-1
SMD(6,9)=2*(cosh(ane*F*Cprev(9,J)/(2*R*T)))*(-1/(2*R*T))*aiH0*ar*ane*F
SMG(6)=(sinh(ane*Cprev(9,J)/(2*R*T))*2*aiH0*ar*F)+Cprev(6,J)

SMD(7,6)=1
SMD(7,7)=1
SMG(7)=-Cprev(6,J)+aIcurrent-Cprev(7,J)

SMD(8,8)=1
SMD(8,10)=-1
SMD(8,12)=-1
SMG(8)=+Cprev(10,J)+Cprev(12,J)-Cprev(8,J)

SMD(9,8)=-1
SMD(9,9)=1
SMD(9,11)=1
SMG(9)=+Cprev(8,J)-Cprev(9,J)-Cprev(11,J)

SMD(10,7)=-1
SMD(10,10)=(-1/(R*T))*(cosh(ane*F*Cprev(10,J)/(2*R*T))*aiL0*ar*ane*F)
SMG(10)=(sinh(ane*F*Cprev(10,J)/(2*R*T))*2*aiL0*ar)+Cprev(7,J)

SMD(11,1)=(-1/(4*F*Cprev(1,J)))*R*T
SMD(11,2)=(1/(Cprev(2,J)*2*F))*R*T
SMD(11,11)=1
SMG(11)=-((R*T*dlog((Cprev(2,J)*Cprev(2,J))/(fH*Cprev(1,J))))/(4*F))+EH0-
Cprev(11,J)
```

```
        SMD(12,2)=(-1/(Cprev(2,J)*4*F))*(R*T)
        SMD(12,3)=(1/(Cprev(3,J)*4*F))*(R*T)
        SMD(12,4)=(1/(Cprev(4,J)*2*F))*(R*T)
        SMD(12,12)=1
        SMG(12)=-
Cprev(12,J)+EL0+(R*T*dlog(fL*Cprev(2,J)/((Cprev(4,J)*Cprev(4,J))*Cprev(3,J))))/(4*F)
   END

SUBROUTINE ABDGXY(H,J)
   use cycle_common
   use cycle_common_dc
   IF ( J.EQ.1 ) THEN
      DO ii = 1 , N
         DO kk = 1 , N
            B(ii,kk) = H*SME(ii,kk) - 1.5*SMP(ii,kk)
            D(ii,kk) = 2.0*SMP(ii,kk)
            X(ii,kk) = -0.5*SMP(ii,kk)
            ENDDO
         G(ii) = H*SMF(ii)
         ENDDO
      RETURN
      ENDIF

   IF ( J.EQ.NJ ) THEN
      DO ii = 1 , N
         DO kk = 1 , N
            B(ii,kk) = H*SME(ii,kk) + 1.5*SMP(ii,kk)
            A(ii,kk) = -2.0*SMP(ii,kk)
            Y(ii,kk) = 0.5*SMP(ii,kk)
            ENDDO
```

```
        G(ii) = H*SMF(ii)
        ENDDO
      RETURN
      ENDIF
    DO ii = 1 , N
        DO kk = 1 , N
        A(ii,kk) = SMA(ii,kk) - H/2.0*SMB(ii,kk)
        B(ii,kk) = -2.0*SMA(ii,kk) + H**2*SMD(ii,kk)
        D(ii,kk) = SMA(ii,kk) + H/2.0*SMB(ii,kk)
        ENDDO
      G(ii) = H**2*SMG(ii)
      ENDDO
    RETURN
    END

SUBROUTINE BOUND_VAL(H)
    use cycle_common
    use cycle_common_dc
    DO j = 1 , NJ
        DO ic = 1 , N
        DO kc = 1 , N
          SMA(ic,kc) = 0.0
          SMB(ic,kc) = 0.0
          SMD(ic,kc) = 0.0
          SMP(ic,kc) = 0.0
          SME(ic,kc) = 0.0
          ENDDO
        ENDDO
      CALL FILLMAT(H,j)
      CALL ABDGXY(H,j)
      CALL BAND(j)
```

```
      ENDDO
   ! DO j = 1 , N
   ! print*, Cprev(1,j) , Cprev(2,j) , Cprev(3,j) ,Cprev(4,j)
   ! ENDDO
   DO k = 1 , N
        DO j = 1 , NJ
        Cprev(k,j) = Cprev(k,j) + Delc(k,j)
        ENDDO
      ENDDO
      RETURN !
   END

SUBROUTINE MATINV(N,M,Determ)
      IMPLICIT DOUBLE PRECISION (a-h,o-z)
      INTEGER i , id , irow , j , jc , jcol , k , M , N , nn
      DIMENSION id(12)
      COMMON A(12,12) , B(12,12) , Delc(12,903) , D(12,25)
      Determ = 1.0
      DO i = 1 , N
        id(i) = 0
        ENDDO
      DO nn = 1 , N
        bmax = 1.1
        DO i = 1 , N
          IF ( id(i).EQ.0 ) THEN
            bnext = 0.0
            btry = 0.0
            DO j = 1 , N
              IF ( id(j).EQ.0 ) THEN
                IF ( DABS(B(i,j)).GT.bnext ) THEN
                  bnext = DABS(B(i,j))
```

```
                IF ( bnext.GT.btry ) THEN
                   bnext = btry
                   btry = DABS(B(i,j))
                   jc = j
                   ENDIF
                ENDIF
             ENDIF
          ENDDO
       IF ( bnext.LT.bmax*btry ) THEN
          bmax = bnext/btry
          irow = i
          jcol = jc
          ENDIF
       ENDIF
    ENDDO

IF ( id(jc).EQ.0 ) THEN
   id(jcol) = 1
   IF ( jcol.NE.irow ) THEN
         DO j = 1 , N
            save = B(irow,j)
            B(irow,j) = B(jcol,j)
            B(jcol,j) = save
            ENDDO
         DO k = 1 , M
            save = D(irow,k)
            D(irow,k) = D(jcol,k)
            D(jcol,k) = save
            ENDDO
         ENDIF
      f = 1.0/B(jcol,jcol)
```

```
            DO j = 1 , N
               B(jcol,j) = B(jcol,j)*f
               ENDDO
            DO k = 1 , M
               D(jcol,k) = D(jcol,k)*f
               ENDDO
            DO i = 1 , N
               IF ( i.NE.jcol ) THEN
                  f = B(i,jcol)
                  DO j = 1 , N
                     B(i,j) = B(i,j) - f*B(jcol,j)
                     ENDDO
                  DO k = 1 , M
                     D(i,k) = D(i,k) - f*D(jcol,k)
                     ENDDO
                  ENDIF
               ENDDO
               ELSE
            Determ = 0.0
            RETURN
            ENDIF
         ENDDO
   END
SUBROUTINE BAND(J)
   IMPLICIT DOUBLE PRECISION (a-h,o-z)
   INTEGER i, j, jj, k, l, lpn, m, N, NJ, np1, Numbertimesteps
   DIMENSION e(12,13,903)
   COMMON A(12,12) , B(12,12) , Delc(12,903) , D(12,25) , G(12) , X(12,12) , &
   & Y(12,12)
   COMMON/ints/ n, NJ, Numbertimesteps, ki
   SAVE e , np1
```

```
IF ( j.LT.2 ) THEN
np1 = N + 1
DO i = 1 , N
   D(i,2*N+1) = G(i)
   DO l = 1 , N
      lpn = l + N
      D(i,lpn) = X(i,l)
      ENDDO
   ENDDO
CALL MATINV(N,2*N+1,determ)
IF ( determ.EQ.0 ) PRINT 99001 , J
   DO k = 1 , N
      e(k,np1,1) = D(k,2*N+1)
      DO l = 1 , N
         e(k,l,1) = -D(k,l)
         lpn = l + N
         X(k,l) = -D(k,lpn)
         ENDDO
      ENDDO
   RETURN
   ELSEIF ( j.EQ.2 ) THEN
      DO i = 1 , N
         DO k = 1 , N
            DO l = 1 , N
               D(i,k) = D(i,k) + A(i,l)*X(l,k)
               ENDDO
            ENDDO
         ENDDO
   ENDIF
IF ( j.GE.NJ ) THEN
   DO i = 1 , N
```

```
      DO l = 1 , N
        G(i) = G(i) - Y(i,l)*e(l,np1,J-2)
        DO m = 1 , N
          A(i,l) = A(i,l) + Y(i,m)*e(m,l,J-2)
          ENDDO
        ENDDO
      ENDDO
    ENDIF
  DO i = 1 , N
    D(i,np1) = -G(i)
    DO l = 1 , N
      D(i,np1) = D(i,np1) + A(i,l)*e(l,np1,J-1)
      DO k = 1 , N
        B(i,k) = B(i,k) + A(i,l)*e(l,k,J-1)
        ENDDO
      ENDDO
    ENDDO
  CALL MATINV(N,np1,determ)
  IF ( determ.EQ.0 ) PRINT 99001 , J
  DO k = 1 , N
    DO m = 1 , np1
      e(k,m,J) = -D(k,m)
      ENDDO
    ENDDO
  IF ( j.GE.NJ ) THEN
    DO k = 1 , N
      Delc(k,J) = e(k,np1,J)
      ENDDO
    DO jj = 2 , NJ
      m = NJ - jj + 1
      DO k = 1 , N
```

```
      Delc(k,m) = e(k,np1,m)
         DO l = 1 , N
            Delc(k,m) = Delc(k,m) + e(k,l,m)*Delc(l,m+1)
            ENDDO
         ENDDO
      ENDDO
   DO l = 1 , N
      DO k = 1 , N
         Delc(k,1) = Delc(k,1) + X(k,l)*Delc(l,3)
         ENDDO
      ENDDO
   ENDIF
99001 FORMAT (' DETERM=0 AT J=',I4)
END
```

APPENDIX C: PERMISSION FOR FIGURES

Permissions for Figure 1.1 and Figure 1.2 is shown below.

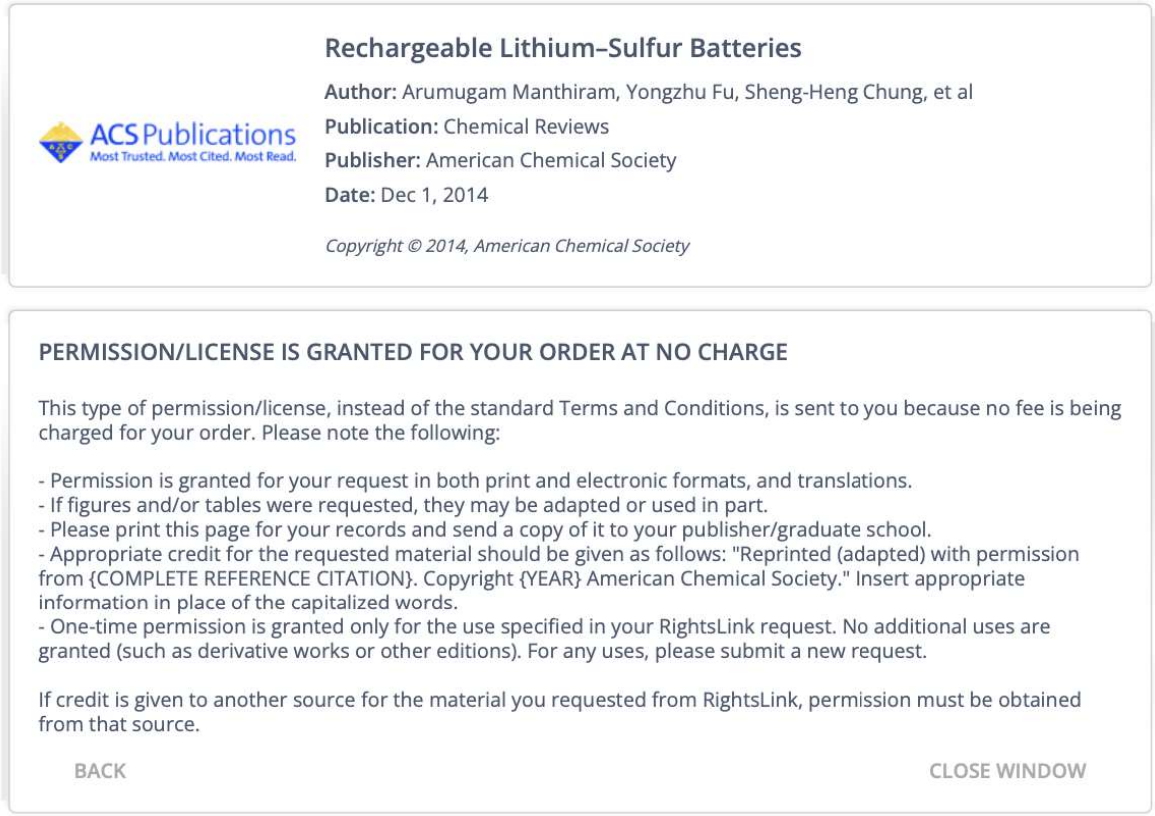

ACS Publications
Most Trusted. Most Cited. Most Read.

Rechargeable Lithium–Sulfur Batteries

Author: Arumugam Manthiram, Yongzhu Fu, Sheng-Heng Chung, et al
Publication: Chemical Reviews
Publisher: American Chemical Society
Date: Dec 1, 2014

Copyright © 2014, American Chemical Society

PERMISSION/LICENSE IS GRANTED FOR YOUR ORDER AT NO CHARGE

This type of permission/license, instead of the standard Terms and Conditions, is sent to you because no fee is being charged for your order. Please note the following:

- Permission is granted for your request in both print and electronic formats, and translations.
- If figures and/or tables were requested, they may be adapted or used in part.
- Please print this page for your records and send a copy of it to your publisher/graduate school.
- Appropriate credit for the requested material should be given as follows: "Reprinted (adapted) with permission from {COMPLETE REFERENCE CITATION}. Copyright {YEAR} American Chemical Society." Insert appropriate information in place of the capitalized words.
- One-time permission is granted only for the use specified in your RightsLink request. No additional uses are granted (such as derivative works or other editions). For any uses, please submit a new request.

If credit is given to another source for the material you requested from RightsLink, permission must be obtained from that source.

BACK CLOSE WINDOW

Figure Appendix.1. Permissions for Figure 1.1 and Figure 1.2